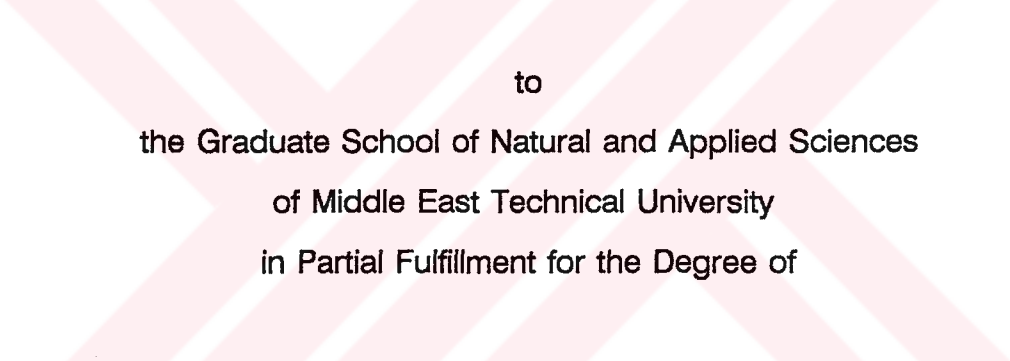


**A COMPARATIVE STUDY OF FINITE ELASTOSTATICS OF  
COMPRESSIBLE HYPERELASTIC MATERIALS**

**A Master's Thesis  
Presented by  
Uğurhan Akyüz**



**to  
the Graduate School of Natural and Applied Sciences  
of Middle East Technical University  
in Partial Fulfillment for the Degree of**

**MASTER OF SCIENCE**

**in**

**CIVIL ENGINEERING**

**MIDDLE EAST TECHNICAL UNIVERSITY**

**ANKARA**

**June, 1992**


Approval of the Graduate School of Natural and Applied Sciences.

  
Prof. Dr. Alpay ANKARA  

---

Director


I certify that this thesis satisfies all the requirements as a thesis for the degree of Master of Science.

  
Prof. Dr. Doğan ALTINBILEK  

---

Chairman of the Department

We certify that we have read this thesis and that in our opinion it is fully adequate, in scope and quality, as a thesis for the degree of Master of Science in Civil Engineering.

  
Prof. Dr. Aybar ERTEPINAR  

---

Supervisor

Examining Committee in Charge :

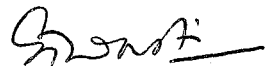



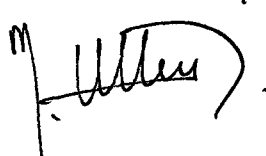
Prof. Dr. S. Tanvir WASTI

Prof. Dr. Aybar ERTEPINAR

Prof. Dr. Fuat ERBATUR

Assoc. Prof. Dr. Engin KEYDER

Assoc. Prof. Dr. Mehmet UTKU

## ABSTRACT

# A COMPARATIVE STUDY OF FINITE ELASTOSTATICS OF COMPRESSIBLE HYPERELASTIC MATERIALS

AKYÜZ, Uğurhan

M.S. in Civil Engineering

Supervisor : Prof. Dr. Aybar ERTEPINAR

June, 1992, 110 pages

In this work, the behavior of hollow, circular cylindrical shells made of compressible, hyperelastic materials and undergoing large elastic deformations is investigated. The responses of three material models, namely, Blatz, Blatz-Ko, and Levinson-Burgess models are compared when the shells are subjected to:

- a. anti-plane shear,
- b. constant spin and circumferential shear,
- c. uniform circumferential shear,

The theory of finite elasticity is used in the formulation of the problems. The method of adjoints is used to solve the highly non-linear governing differential equations numerically. The stress and the displacement fields are obtained for various values of material constants. The validity of existing models is discussed.

Key words: Finite elastic deformation, compressible hyperelastic materials

Science Code: 625.01.01

ÖZ

SIKIŞTIRILABİLİR HİPERELASTİK MALZEMELERİN  
ELASTOSTATİK DAVRANIŞLARININ KARŞILAŞTIRILMASI

AKYÜZ, Uğurhan

Yüksek Lisans tezi, İnşaat Mühendisliği Anabilim Dalı

Tez Yöneticisi: Prof.Dr. Aybar ERTEPINAR

Haziran, 1992, 110 sayfa

Bu çalışmada, sıkıştırılabilir, hiperelastik malzemelerden yapılan içi boş, dairesel silindirik kabukların büyük elastik şekil değiştirmeler altındaki davranışları incelenmiştir. Düzlem dışı kesme, sabit dönme ve çevresel kesme, düzgün yayılı çevresel kesme kuvvetlerine maruz kalan kabuklar Blatz, Blatz-Ko ve Levinson-Burgess modelleri kullanılarak karşılaştırılmıştır. Problemin formülasyonunda sonlu elastisite teorisi kullanılmıştır. Lineer olmayan diferansiyel denklemler adjointler metoduyla nümerik olarak çözülmüştür. Gerilme ve şekil değiştirme bileşenleri malzeme sabitlerinin değişik değerleri için elde edilmiştir. Mevcut modellerin geçerliliği

tartıřılmıřtır.

**Anahtar Kelimeler:** Sonlu Őekil deęiřtirme, sıkıřtırılabilir hiperelastik malzemeler

**Bilim Kodu:** 625.01.01



## ACKNOWLEDGEMENTS

This study was conducted under the supervision of Prof. Dr. Aybar Ertepinar. His guidance for this study has transcended the bounds of thesis supervision. My appreciation for all his help is beyond expression. I am deeply grateful to him for his invaluable suggestions, criticism and encouragement in the preparation of this thesis.

I also wish to express sincere thanks to my Research Assistant Colleagues for their friendly help and support.

## TABLE OF CONTENTS

	Page
ABSTRACT.....	iii
ÖZ.....	v
ACKNOWLEDGEMENTS.....	vii
LIST OF TABLES.....	xii
LIST OF FIGURES.....	xiii
LIST OF SYMBOLS.....	xvii
CHAPTER I : INTRODUCTION.....	1
CHAPTER II : THEORETICAL FOUNDATIONS.....	11
2.1 Field Equations of Finite Elastic Deformations.....	11
2.2 Forms of Strain Energy Density Function.....	16
CHAPTER III : FORMULATION OF THE PROBLEM.....	27
3.1 Governing Equations.....	27



3.1.1 Finite Anti-Plane Shear of Compressible Hyperelastic Tube	
Subjected to External Axial Shear.....	27
3.1.2 Compressible Hyperelastic Spinning Tubes Subjected to	
Circumferential Shear.....	37
3.1.3 Finite Circumferential Shearing of Compressible Hyperelastic	
Tube.....	45
3.2 Non-Dimensionalization.....	46
3.3 Non-Dimensional Governing Equations.....	47
3.3.1 Finite Anti-Plane Shear of Compressible Hyperelastic Tube	
Subjected to External Axial Shear.....	48
3.3.2 Compressible Hyperelastic Spinning Tubes Subjected to	
Circumferential Shear.....	54
3.3.3 Finite Circumferential Shearing of Compressible Hyperelastic	
Tube.....	61

#### CHAPTER IV : METHOD OF ADJOINTS AND THE NUMERICAL

SOLUTION OF THE PROBLEMS.....	63
4.1 Method of Adjoint.....	63
4.2 Numerical Solution of the Problems.....	71
4.2.1 Implicit Boundary Conditions.....	71

4.2.1.1 Anti-Plane Shear.....	72
4.2.1.2 Constant Spin and Circumferential Shear.....	73
4.2.1.3 Circumferential Shear.....	74
4.3 Computational Procedure.....	76
CHAPTER V : DISCUSSION.....	77
5.1 Finite Anti-Plane Shear of Compressible Hyperelastic Tube.....	78
5.2 Compressible Hyperelastic Spinning Tubes Subjected to Circumferential Shear.....	81
5.3 Finite Circumferential Shearing of Compressible Hyperelastic Tube.....	84
CHAPTER VI : CONCLUSIONS.....	108
REFERENCES.....	111

APPENDICES

APPENDIX A. TRANSFORMATION FORMULAS.....	115
A.1 Transformation Formulas for Defining Variables in Terms of $R$ .....	115

A.2 Formulas for the Dimensionless Terms..... 117

APPENDIX B. COMPUTER PROGRAM USER'S MANUAL..... 120



## LIST OF TABLES

	Page
Table 2.1 Results of Blatz Ko Studies.....	20



## LIST OF FIGURES

	Page
Figure 2.1 Simple Uniaxial Stress.....	25
Figure 2.2 Equal Biaxial Plane Stress.....	25
Figure 2.3 Hydrostatic Stress.....	26
Figure 5.1 Dimensionless Radial Position vs. Dimensionless Radial Displacement.....	87
Figure 5.2 Dimensionless Radial Position vs. $\bar{r}^{-13}$ .....	87
Figure 5.3 Dimensionless Radial Position vs. $\bar{r}^{-22}$ .....	88
Figure 5.4 Dimensionless Radial Position vs. $\bar{r}^{-33}$ .....	88
Figure 5.5 f vs. Dimensionless Radial Displacement at the Outer Boundary.....	89
Figure 5.6 f vs. Dimensionless Axial Displacement at the Outer Boundary.....	89
Figure 5.7 f vs. $\bar{r}^{-11}$ at the Inner Boundary.....	90
Figure 5.8 f vs. $\bar{r}^{-22}$ at the Inner Boundary.....	90
Figure 5.9 f vs. $\bar{r}^{-33}$ at the Inner Boundary.....	91

Figure 5.10 $v$ vs. Dimensionless Radial Displacement at the Outer Boundary.....	91
Figure 5.11 $v$ vs. $\bar{r}^{-13}$ at the Inner Boundary.....	92
Figure 5.12 $v$ vs. $\bar{r}^{-33}$ at the Inner Boundary.....	92
Figure 5.13 $\lambda$ vs. Dimensionless Radial Displacement at the Outer Boundary.....	93
Figure 5.14 $\lambda$ vs. $\bar{r}^{-13}$ at the Inner Boundary.....	93
Figure 5.15 $\lambda$ vs. $\bar{r}^{-22}$ at the Inner Boundary.....	94
Figure 5.16 $\lambda$ vs. $\bar{r}^{-33}$ at the Inner Boundary.....	94
Figure 5.17 Dimensionless Radial Position vs. Dimensionless Radial Displacement.....	95
Figure 5.18 Dimensionless Radial Position vs. Dimensionless Angular Displacement.....	95
Figure 5.19 Dimensionless Radial Position vs. $\bar{r}^{-11}$ .....	96
Figure 5.20 Dimensionless Radial Position vs. $\bar{r}^{-22}$ .....	96
Figure 5.21 $f$ vs. Dimensionless Radial Displacement at the Outer Boundary.....	97
Figure 5.22 $f$ vs. $\bar{r}^{-11}$ at the Inner Boundary.....	97
Figure 5.23 $f$ vs. $\bar{r}^{-22}$ at the Inner Boundary.....	98
Figure 5.24 $v$ vs. Dimensionless Radial Displacement at the Outer Boundary.....	98

Figure 5.25 $v$ vs. $\bar{r}^{12}$ at the Inner Boundary.....	99
Figure 5.26 $v$ vs. $\bar{r}^{22}$ at the Inner Boundary.....	99
Figure 5.27 Dimensionless Spin vs. Dimensionless Radial & Angular Displacements at the Outer Boundary.....	100
Figure 5.28 Dimensionless Spin vs. $\bar{r}^{12}$ & $\bar{r}^{22}$ at the Inner Boundary.....	100
Figure 5.29 Dimensionless Radial Position vs. Dimensionless Radial Displacement.....	101
Figure 5.30 Dimensionless Radial Position vs. Dimensionless Angular Displacement.....	101
Figure 5.31 Dimensionless Radial Position vs. $\bar{r}^{-11}$ .....	102
Figure 5.32 Dimensionless Radial Position vs. $\bar{r}^{-12}$ .....	102
Figure 5.33 Dimensionless Radial Position vs. $\bar{r}^{-22}$ .....	103
Figure 5.34 $f$ vs. Dimensionless Radial Displacement at the Outer Boundary.....	103
Figure 5.35 $f$ vs. $\bar{r}^{12}$ at the Inner Boundary.....	104
Figure 5.36 $f$ vs. $\bar{r}^{22}$ at the Inner Boundary.....	104
Figure 5.37 $v$ vs. Dimensionless Radial Displacement at the Outer Boundary.....	105
Figure 5.38 $v$ vs. $\bar{r}^{12}$ at the Inner Boundary.....	105
Figure 5.39 $v$ vs. $\bar{r}^{22}$ at the Inner Boundary.....	106

Figure 5.40 Dimensionless Surface Traction vs. Dimensionless Radial  
& Angular Displacements at the Outer Boundary..... 106

Figure 5.41 Dimensionless Surface Traction vs.  $\bar{r}^{11}$  &  $\bar{r}^{33}$  at the Inner  
Boundary..... 107

Figure 5.42 Dimensionless Surface Traction vs.  $\bar{r}^{12}$  &  $\bar{r}^{22}$  at the Inner  
Boundary..... 107





## LIST OF SYMBOLS

$f$	A material constant
$\underline{g}_i$	Covariant base vectors of $\theta^j$ in the deformed state
$\underline{g}^i$	Contravariant base vectors of $\theta^j$ in the deformed state
$g_{ij}$	Covariant metric tensor of the deformed body B
$g^{ij}$	Contravariant metric tensor of the deformed body B
$g$	Determinant of $g_{ij}$
$p$	Coefficient defined in equation (2.12)
$r$	Radius of a material point in B
$r_1, r_2$	Inner and outer radii in B respectively
$u$	Radial displacement
$\bar{u}$	Dimensionless radial displacement defined as $u/R_1$
$w$	Axial displacement
$\bar{w}$	Dimensionless axial displacement defined as $w/R_1$
$x$	Dimensionless radial position defined as $R/R_1$
$x_i$	Fixed rectangular cartesian coordinates in $B_0$

$z$	Convected coordinate in a cylindrical coordinate system in $B$
$B$	An elastic body in its finitely strained state
$B_0$	An elastic body in its unstrained state
$B^{ij}$	A second order tensor defined in (2.12)
$\underline{G}_i$	Covariant base vectors of $\theta^j$ in the undeformed state
$\underline{G}^i$	Contravariant base vectors of $\theta^j$ in the undeformed state
$G_{ij}$	Covariant metric tensor of the undeformed body $B_0$
$G^{ij}$	Contravariant metric tensor of the undeformed body $B_0$
$G$	Determinant of $G_{ij}$
$I_1, I_2, I_3$	Strain invariants defined in (2.10)
$R$	Radius of a material point in $B_0$
$R_1, R_2$	Inner and outer radii in $B_0$ respectively
$W(I_1, I_2, I_3)$	Strain energy density function
$X_i$	Fixed rectangular coordinates in $B$
$Z$	Convected coordinate in a cylindrical coordinate system in $B_0$
$\Upsilon_{ij}$	Covariant strain tensor defined in (2.8)
$\lambda$	A constant defined as $R_2/R_1$
$\mu$	Shear modulus
$\nu$	Poisson's ratio
$\rho$	Mass density in state $B$
$\rho_0$	Mass density in state $B_0$

$\theta$	A material angular coordinates in B
$\theta_j$	A set of curvilinear coordinates which deforms with the body
$\sigma_{ij}$	Physical components of stress
$\Phi$	Coefficient defined in (2.12)
$\Psi$	Coefficient defined in (2.12)
$\Gamma_{ij}^r$	Christoffel symbols of the second kind defined in (2.16)
$\theta$	A material angular coordinate in $B_0$
$\tau_0$	External axial shear
$\bar{\tau}_0$	Dimensionless external axial shear defined as $\tau_0/\mu$
$\tau^{ij}$	Contravariant stress tensor defined in (2.11)
$\bar{\tau}^{ij}$	Dimensionless stress components defined as $\sigma_{ij}/\rho$
$\phi$	Angular displacement
$\bar{\phi}$	Dimensionless angular displacement defined as $\phi$
$\Omega$	Spin speed
$\bar{\Omega}$	Dimensionless spin speed defined in (3.63)

## CHAPTER I

### INTRODUCTION

The research in finite elasticity began in 1940's with the increasing importance of rubber and rubber-like materials in industrial applications. During the last fifty years, several researchers investigated the mechanical properties of this type of materials. The early researchers assumed the materials to be ideally elastic, isotropic, homogeneous, and incompressible. The works on the compressible materials have begun in 1970's. These works can be classified as

- theoretical and experimental studies performed for determining a suitable strain energy density function for such materials,
- works which investigate deformations, stresses, and surface tractions in materials of different geometry which undergo finite elastic deformations for various boundary conditions.

It has been shown that qualitative differences exist between the bodies made of incompressible and compressible elastic materials for the same boundary value problems. The incompressible material models are considerably easier than their compressible counterparts, and give an idea about the behaviour of the body under a large variety of static and dynamic loading. These models, however, cannot fully explain the behaviour of hyperelastic materials, and hence the compressibility of the material must be taken into account for a closer approximation to the real behaviour. But, with the compressible material models, only equilibrium type of problems have so far been solved, except some relatively easy problems. Stability and propagation type problems are yet to be investigated with compressible material models due to their mathematical complexity.

Before proceeding with a detailed description of the contents of this study, it is suitable to give a brief review of the historical developments relevant to the subject.

M. Mooney [1] was the first scientist to investigate the expression for the strain energy function of a hyperelastic body subjected to a finite homogeneous strain field. If the body is isotropic and the strains are small, it is known that the energy can be expressed in terms of strains and two

material constants, the compression modulus and the rigidity modulus. However, the deformations which rubber and similar substances undergo are too large to be included in the classical theory of small strains, even when the theory is extended to the second and higher approximations. Mooney proposed a strain energy density function for rubber-like materials. He assumed that, besides being homogeneous and free from hysteresis, the material is isotropic, the deformations are isochoric (i.e. without change in volume), shear is proportional to the traction in simple shear in any isotropic plane for linear case, and the traction in simple shear is an analytic function of the shear for non-linear traction-shear relation. He calculated the forces necessary to produce isochoric simple stretch in a tensile test specimen. Calculated forces agreed closely with experimental data on soft rubber from 400 percent elongation to 50 percent compression.

Then, in late 1940's, R. S. Rivlin [2,3,4] considered the problem of determining the strain energy density function for rubber-like materials from both theoretical and experimental points of view. He wrote a series of papers about large elastic deformations of isotropic materials. First, he gave the stress-strain relations, equations of motion and boundary conditions for an incompressible material, the so-called "neo-Hookean" material which has the simplest strain energy density function with one constant and depending on

only the first strain invariant. Then, he calculated the surface tractions necessary to produce simple deformation field in a right-circular cylinder and in a tube of circular cross-section of the same material. Next, the stress-strain relations, equations of motion and boundary conditions for an incompressible material which is isotropic in its undeformed state and for which the strain energy density function is a function of two strain invariants, were derived in a form suitable for the calculation of the forces necessary to produce a specified deformation, without any explicit form for the strain energy density function being assumed. Then, these equations were applied to calculate the forces necessary to produce simple torsion in a cylinder. It was found that, apart from an arbitrary hydrostatic pressure applied over the whole surface of the cylinder, azimuthal and normal surface tractions must be applied to the ends of the cylinder. In 1949, he expressed the forces necessary to produce simple deformation field in a tube of incompressible, highly elastic, isotropic material by using the so-called Mooney strain energy density function which is a linear equation with two constants, and depends on the first two strain invariants [4]. In this study, he first considered three types of simple deformation fields individually. These were

- a uniform simple extension,
- a uniform simple inflation of the tube, in which its length remains

constant,

- a uniform simple torsion, in which planes perpendicular to the axis of the tube are rotated in their own plane.

Then, he examined the first two deformations followed successively by simple shears about the axis of the tube and parallel to it.

The neo-Hookean, and the Mooney strain energy densities may be viewed as the simplest such representations of  $W$  for incompressible materials.

Rivlin's theory was later generalized by Green and Zerna [5] using a curvilinear coordinate system moving with the body. The problems of small twist superposed upon a finite extension, upon a hydrostatic pressure, or upon a combined hydrostatic pressure and tension were solved by Green and Shield [6].

Treloar [7] approached the problem both from a molecular and a phenomenological point of view. His molecular theory is based on the conception of vulcanized rubber as an assembly of long chain molecules, linked together at a relatively small number of points. He supplemented his theory by experimental examination, and gave the photo-elastic, mechanical,



and dynamic properties of rubbers.

In 1968, H. Alexander [8] proposed a new constitutive relation based on previous works and experiments performed on neoprene film. In this study, Alexander considered a new model to represent incompressible materials. The goal of his work was to obtain a constitutive relation for rubber and rubber-like materials which experience large deformations under loading with a non-linear stress-strain characteristic. He claimed all of the previous theories to be inadequate, and he proposed a new relation to represent the response throughout the entire range of deformations more accurately. In fact, this was a generalization of earlier theories.

As mentioned before, there exist qualitative differences between the bodies made of incompressible and compressible elastic materials for the same boundary value problem. Specific forms of strain energy density functions of some slightly compressible hyperelastic materials were first proposed by Blatz<sup>1</sup> and then by Blatz-Ko[9]. Later Levinson-Burgess[10] introduced the polynomial compressible material model. These models, in the limiting cases of incompressible behaviour or infinitesimal deformations,

---

<sup>1</sup> Reference is made by Levinson and Burgess [10]

reduce, respectively, to Mooney or classical Hooke materials.

In the same context, Shahinpoor [11] obtained the governing equations of a class of finite screw-dislocations for a general strain energy function. The solutions of these governing equations were then obtained for some slightly compressible materials such as the Blatz, Blatz-Ko, Levinson-Burgess and Murnaghan [12] material which has a strain energy density function with five elastic constants, and depends on all three strain invariants.

Finite telescopic shear of a compressible hyperelastic tube was considered by Mioduchowski and Haddow [13]. They showed that solutions with isochoric deformation fields exist for a class of strain energy functions. A numerical method was proposed for the analysis of the problem when a solution with an isochoric deformation field does not exist.

Knowles [14,15] was the first scientist who considered the problem of anti-plane shear in finite elasticity for a homogeneous, isotropic, compressible elastic body which is unstressed in its undeformed state. Agarwal [16] used Knowles theorem for anti-plane shear of compressible, homogeneous, isotropic, elastic materials to determine some restrictions on a strain energy density function.

The stability and the small vibrations of rectangular, layered columns undergoing finite axial deformations were investigated by Tokdemir and Ertepinar [17], and Ertepinar and Akkas [18]. The layers of the column were assumed to be made of compressible, hyperelastic materials. Some numerical results of the closed form solutions were provided to study the effect of material and geometric properties.

One of the most important recent contributions to finite elasticity of compressible hyperelastic materials is due to Carroll [19] who introduced three classes of compressible isotropic elastic solids for each of which strain energy, expressed as a function of the three principal invariants, is linear in two of its arguments and non-linear in the third argument. He examined several deformation fields for which the governing equations reduce to a set of non-linear ordinary differential equations.

In late 80's and 90's, anti-plane shear, constant spin and circumferential shear, and circumferential shear problems which are the subject of this study, are worked by Ertepinar [20,21,22], by using Levinson-Burgess model only.

The objective of this work is to investigate the deformation fields

and stresses of these three types of problems using three existing models, namely, Blatz, Blatz-Ko, and Levinson-Burgess models. In all of the problems a long, circular cylindrical tube whose inner surface is bonded to a rigid cylinder is considered. The deformation fields are

**A. Anti-Plane Shear:**

Outer surface is subjected to a uniformly distributed shear stress applied in the axial direction.

**B. Constant Spin and Circumferential Shear:**

Inner surface spin with a constant angular speed while the tube is subjected to uniformly distributed circumferential shearing tractions on its outer surface.

**C. Circumferential Shear:**

Outer surface is subjected to a uniformly distributed circumferential shearing tractions.

The general theory of finite elastic deformations is briefly reviewed in Chapter 2, the contents of which are essentially extracted from the text of Green and Zerna [5]. In Chapter 3, the general theory is applied to circular cylindrical tube which is made of a compressible material. The governing equations of the three types of problem for three models are obtained, and these governing equations are put in a form suitable for numerical solution. In Chapter 4, the shooting method, namely the method of adjoints, is briefly discussed, the contents of which are essentially extracted from the text of Robert and Shipmann [23]. The numerical solution of the problems are given in the same chapter. Finally, a discussion pertaining to the numerical results of these investigations, and conclusions are presented in Chapter 5, and Chapter 6.

## CHAPTER II

### THEORETICAL FOUNDATIONS

In this chapter, a brief summary of the general theory of finite elasticity is given. The derivations are essentially based on the text of Green and Zerna [5].

#### 2.1 Field Equations of Finite Elastic Deformations

Let a body  $B_0$  in the unstrained state be defined by a fixed rectangular cartesian system of axes  $x_i$ . Suppose that the positions of the points of the body  $B_0$  change so that a typical material point  $P_0$  moves to  $P$  in the deformed state. The point  $P$  is referred to a new fixed rectangular cartesian system of axes  $X_i$  in the deformed state  $B$ . The material points of the body can also be described by a set of curvilinear coordinates  $\theta^j$  which deform with the body. Then the unique functional relations  $x_i(\theta^j)$  and  $X_i(\theta^j)$  define the deformation of the body from  $B_0$  to  $B$ .

The covariant and contravariant base vectors  $\underline{g}_i$ , reciprocal base vectors  $\underline{g}^i$  and the corresponding metric tensors  $g_{ij}$  and  $g^{ij}$  of the material coordinates  $\theta^j$  in the undeformed body  $B_0$  are given by

$$\underline{g}_i = \frac{\partial x^k}{\partial \theta^i} \underline{i}_k \quad , \quad \underline{g}^i = \frac{\partial \theta^i}{\partial x^k} \underline{i}^k \quad (2.1)$$

$$g_{ij} = \underline{g}_i \cdot \underline{g}_j = \frac{\partial x^k}{\partial \theta^i} \frac{\partial x^k}{\partial \theta^j} \quad (2.2)$$

$$g^{ij} = \underline{g}^i \cdot \underline{g}^j = \frac{\partial \theta^i}{\partial x^k} \frac{\partial \theta^j}{\partial x^k} \quad (2.3)$$

where  $\underline{i}_k$  and  $\underline{i}^k$  are the unit vectors along a fixed cartesian coordinate axis. The range of free indices is three, and a repeated index indicates summation over the range.

Similarly, the base and the reciprocal base vectors, and the metric tensors in the deformed body B are given by

$$\underline{G}_i = \frac{\partial X^k}{\partial \theta^i} \underline{i}_k \quad , \quad \underline{G}^i = \frac{\partial \theta^i}{\partial X^k} \underline{i}^k \quad (2.4)$$

$$G_{ij} = \underline{G}_i \cdot \underline{G}_j = \frac{\partial X^k}{\partial \theta^i} \frac{\partial X^k}{\partial \theta^j} \quad (2.5)$$

$$G^{ij} = \underline{G^i} \cdot \underline{G^j} = \frac{\partial \theta^i}{\partial X^k} \frac{\partial \theta^j}{\partial X^k} \quad (2.6)$$

In other words, consider a deformation in which a point of an isotropic elastic body initially having cartesian coordinates  $P_0 (x^i)$  is displaced to a new cartesian position  $P (X^i)$ . The deformation tensor which characterizes this mapping is denoted by

$$G_{ij} = \frac{\partial X^k}{\partial x^i} \frac{\partial X^k}{\partial x^j} \quad (2.7)$$

For conciseness, and without loss of generality, it is assumed in the subsequent formulations that  $x_i$  and  $X_i$  coincide.

The state of strain at a point of the body is determined by the covariant strain tensor

$$\gamma_{ij} = \frac{1}{2} (G_{ij} - g_{ij}) \quad (2.8)$$

For bodies made of perfectly homogeneous, isotropic, and elastic materials, it is assumed that the strain energy density function, (strain energy per unit mass of the deformed body), has the form



$$W = W(I_1, I_2, I_3) \quad (2.9)$$

where the three strain invariants  $I_1$ ,  $I_2$ , and  $I_3$  are given by

$$\begin{aligned} I_1 &= g^{ij} G_{ij} \\ I_2 &= g_{ij} G^{ij} I_3 \\ I_3 &= \frac{G}{g} \end{aligned} \quad (2.10)$$

in which  $g$  and  $G$  denote, respectively, the determinants of the covariant metric tensors  $g_{ij}$  and  $G_{ij}$ .

The components of the stress tensor, which are derivable from the strain energy density function are given by

$$\tau^{ij} = \Phi g^{ij} + \psi B^{ij} + p G^{ij} \quad (2.11)$$

where

$$\begin{aligned} \Phi &= \frac{2}{\sqrt{I_3}} \frac{\partial W}{\partial I_1} \\ \psi &= \frac{2}{\sqrt{I_3}} \frac{\partial W}{\partial I_2} \\ p &= 2\sqrt{I_3} \frac{\partial W}{\partial I_3} \end{aligned} \quad (2.12)$$

$$B^{ij} = I_1 g^{ij} - g^{ir} g^{js} G_{rs} \quad (2.13)$$

The equations of the motion are given by

$$\tau^{ij}{}_{\parallel i} + \rho F^j = \rho f^j \quad (2.14)$$

where a double line denotes covariant differentiation with respect to the strained body B ( $\theta^i$  variable),  $\rho$  is the mass density of the deformed body,  $F^j$ , and  $f^j$  denote the contravariant components of the body force and the acceleration vectors, respectively.

The covariant differentiation in the equation of motion can be expressed as

$$\tau^{ij}{}_{\parallel i} = \tau^{ij}{}_{,i} + \Gamma_{ir}^j \tau^{ir} + \Gamma_{ir}^r \tau^{ij} \quad (2.15)$$

where  $\Gamma_{ij}^r$  are called the Christoffel symbols of the second kind, and they are derived from

$$\Gamma_{ij}^r = \frac{1}{2} g^{rs} (g_{is,j} + g_{js,i} - g_{ij,s}) \quad (2.16)$$

By introducing equation (2.15) in equation (2.14), the equation of motion becomes

$$\tau^{ij}{}_{,i} + \Gamma_{ir}^j \tau^{ir} + \Gamma_{ir}^r \tau^{ij} = \rho f^j \quad (2.17)$$

For the static case, righthand side of the equation vanishes.

The physical components of stress can be written as

$$\sigma_{ij} = \sqrt{\frac{G_{ij}}{G^{ii}}} \tau^{ij} \quad (ij \text{ not summed}) \quad (2.18)$$

Note that  $\sigma_{ij}$  is not a tensor.

## 2.2 Forms of Strain Energy Density Function

A hyperelastic material is a material for which the stresses are derivable from a potential  $W$ , called the strain energy density function. The strain energy  $W$  per unit volume of the undeformed state for a homogeneous, isotropic, compressible hyperelastic material may be expressed as a function of the three strain invariants (see equation (2.9))

If the material is incompressible, then  $I_3 = 1$ . The most general form of strain energy function for a homogeneous, isotropic, incompressible elastic material may be expressed as the sum of series of terms involving powers of  $(I_1-3)$  and  $(I_2-3)$

$$W = \sum_{i=0, j=0}^{\infty} C_{ij} (I_1 - 3)^i (I_2 - 3)^j \quad (2.19)$$

where  $I_1 = I_2 = 3$  for zero strain and  $C_{00} = 0$  to insure that  $W = 0$  at zero strain, [7].

Besides its mathematical simplicity, it is reasonable to assume that a small number of terms, corresponding to the linear terms of the series, would predominate [7]. Therefore the strain energy density function can be approximated as

$$W = C_1 (I_1 - 3) + C_2 (I_2 - 3) \quad (2.20)$$

which represents the most general first order relationship in  $I_1$  and  $I_2$ , and which was derived by Mooney [1].

Treloar [7] found, by applying Gaussian statistics to a simple model of a network of long chain molecules, that  $W$  could be expressed as

$$W = C_1 (I_1 - 3) \quad (2.21)$$

This form was used by Rivlin [2,3,4] to characterize the so called Neo-Hookean solid. Treloar [7], Blatz-Ko [9], and Alexander [8] show that Neo-Hookean form gives a reasonable description of the behaviour of continuum rubber-like materials for  $0.6 < \lambda < 2.0$  where  $\lambda$  denotes the stretch ratio.

The Mooney-Rivlin [8] material is defined by the strain energy density

$$W = \frac{\mu}{2} [f(I_1 - 3) + (1 - f)(I_2 - 3)] \quad (2.22)$$

where  $\mu$  is the shear modulus of the material for vanishingly small strains, and  $f$  is the material constant whose value lies between zero and unity. It was found that for a highly elastic rubber  $f = 0$  and for a solid rubber  $f = 1$  [11].

It is seen that when  $f$  is unity the Mooney-Rivlin material reduces to the Neo-Hookean material. Neo-Hookean, and Mooney-Rivlin strain energy density functions may be viewed as the simplest representations of  $W$  for incompressible materials.

It is known that for the same boundary conditions, there exist qualitative differences between the behaviour of compressible elastic materials, and incompressible elastic materials.

Specific forms of strain energy density functions of some slightly compressible hyperelastic materials were first introduced by Blatz, and Blatz-Ko [9]. Blatz proposed a material whose strain energy density is given by

$$W_B = \frac{\mu}{2} [(J_1 - 3) - (\frac{2}{1-2\nu}) \ln J_3 + (\frac{4\nu}{1-2\nu})(J_3 - 1)] \quad (2.23)$$

where

$$\begin{aligned} J_1 &= I_1 \\ J_2 &= \frac{I_2}{I_3} \\ J_3 &= \sqrt{I_3} \end{aligned} \quad (2.24)$$

and  $\nu$  is Poisson's ratio for the material as the deformations become vanishingly small.

Blatz and Ko introduced the following strain energy density [9]

$$\begin{aligned} W_{BK} &= \frac{\mu}{2} [f(J_1 - 3) + (1-f)(J_2 - 3) \\ &+ (\frac{1-2\nu}{\nu})(f(J_3^{\frac{-2\nu}{1-2\nu}} - 1) + (1-f)(J_3^{\frac{2\nu}{1-2\nu}} - 1))] \end{aligned} \quad (2.25)$$

Blatz and Ko [9] found, experimentally, that for the polyurethane rubber  $(\partial W/\partial J_2)$  is nearly zero. For the foam rubber as opposed to the continuum rubber,  $(\partial W/\partial J_1)$  is approximately zero, while  $(\partial W/\partial J_2)$  is large and positive. These results indicate that, all the shear behaviour arises from the second Mooney-Rivlin type constant. The results of foam rubber can be summarized as

Table 2.1 Results of Blatz-Ko studies

Test type	$\mu$ (MPa)	f	$\nu$
Simple tension	0.262	0.13	0.25
Strip-biaxial tension	0.200	0.07	0.25
Homogeneous-biaxial tension	0.186	-0.19	0.25
Average value	0.220	0.00	0.25

For the continuum rubber, they observed that f is nearly equal to unity up to very high compressive stresses, and the finite strain value of Poisson's ratio is 0.463. They concluded that under all the stress fields they considered, both foam rubber and continuum rubber soften as the tensile stress increases.

Poisson's ratio of 0.463 given by Blatz and Ko for a particular polyurethane rubber seems to be the smallest experimental value found for this parameter by workers in rubber elasticity [10].

Levinson and Burgess [10] introduced the polynomial representation of the strain energy density function for a compressible hyperelastic material which reduces to the Mooney-Rivlin material as  $\nu \rightarrow 0.5$

$$W_{LB} = \frac{\mu}{2} [f(J_1 - 3) + (1 - f)(J_2 - 3) + 2(1 - 2f)(J_3 - 1) + (2f + \frac{4\nu - 1}{1 - 2\nu})(J_3 - 1)^2] \quad (2.26)$$

The strain energy density functions  $W_B$ ,  $W_{BK}$ , and  $W_{LB}$  reduce to the classical Hooke's material for small strains which indicates that  $W_B$ ,  $W_{BK}$  and  $W_{LB}$  do not differ in quadratic terms of  $e_i$  which is defined as the principal extension. On the other hand, each of these strain energy densities is different from the others in all third and higher order terms of  $e_i$ 's. In other words, their non-linear, finite strain behaviours are different.

Levinson-Burgess considered five stress fields in [10] to investigate the deformation behaviour of bodies having these three strain energy density functions. The five stress fields are

- a. uniaxial tension
- b. equal biaxial tension
- c. hydrostatic stress
- d. equal biaxial plane strain
- e. uniaxial strain



To derive the equations describing these relations they used the constitutive relation

$$s_i = \frac{2}{\lambda_i} \left( \lambda_i^2 \frac{\partial W}{\partial J_1} - \frac{1}{\lambda_i^2} \frac{\partial W}{\partial J_2} \right) + \frac{J_3}{\lambda_i} \frac{\partial W}{\partial J_3} \quad (2.27)$$

where  $s_i$  is the so-called nominal stress on the undeformed cross-section,  $J_1$ ,  $J_2$ , and  $J_3$  can be expressed in terms of principal stretch ratios  $\lambda_i$

$$\begin{aligned} J_1 &= \lambda_1^2 + \lambda_2^2 + \lambda_3^2 \\ J_2 &= \frac{1}{\lambda_1^2} + \frac{1}{\lambda_2^2} + \frac{1}{\lambda_3^2} \\ J_3 &= \lambda_1 \lambda_2 \lambda_3 \end{aligned} \quad (2.28)$$

The true stress on the deformed cross-section is given by

$$\tau_i = \frac{\lambda_i}{J_3} s_i \quad (2.29)$$

The conclusions arrived at the end of their study can be summarized as follows

#### a. Uniaxial Tension

For  $\nu > 0.40$  all materials behave reasonably in tension and compression, and the results are close to the Neo-Hookean material in the

range  $0.6 < \lambda < 2.0$  (Figure [2.1]).

#### b. Equal Biaxial Plane Stress

For  $\nu > 0.46$  all materials behave reasonably in tension and compression, and the results are similar in behaviour to the incompressible Neo-Hookean material in the range  $0.6 < \lambda < 2.0$ . For  $\nu = 0.40$  the Blatz, and Blatz-Ko materials still behave reasonably over the whole range of  $\lambda$  considered, however the compressible polynomial material behaves somewhat unreasonably in compression in that it softens for  $\lambda < 0.8$  (Figure [2.2]).

#### c. Hydrostatic Stress

The behaviours of Blatz, Blatz-Ko, and compressible polynomial material are quite different. The Blatz-Ko material stiffens under compression, and dramatically softens under tension. The Blatz material behaves, perhaps, in the most intuitively reasonable manner in that it shows moderate stiffening under compression and tension (Figure [2.3])

#### d. Equal Biaxial Plane Strain

The behaviours of all three types are similar to those in case c, except that the Blatz material softens slightly in tension.

#### e. Uniaxial Strain

All of the materials behave as in case d, but here the polynomial material gives a completely linear characteristic.

Reasonable means that a stiffening under compression and tension.

This paper leads to the conclusion that the Blatz, Blatz-Ko, and compressible polynomial materials may be used to study the qualitative effects of slight compressibility on the finite strain behaviour of rubber-like materials. These simple relations provide models for analysis of the theoretical aspect, and not models for the design of rubber-like components. The term "slightly compressible" is taken to mean that  $\nu$  is close to 0.5, and the smallest  $\nu$  one need consider is 0.46.

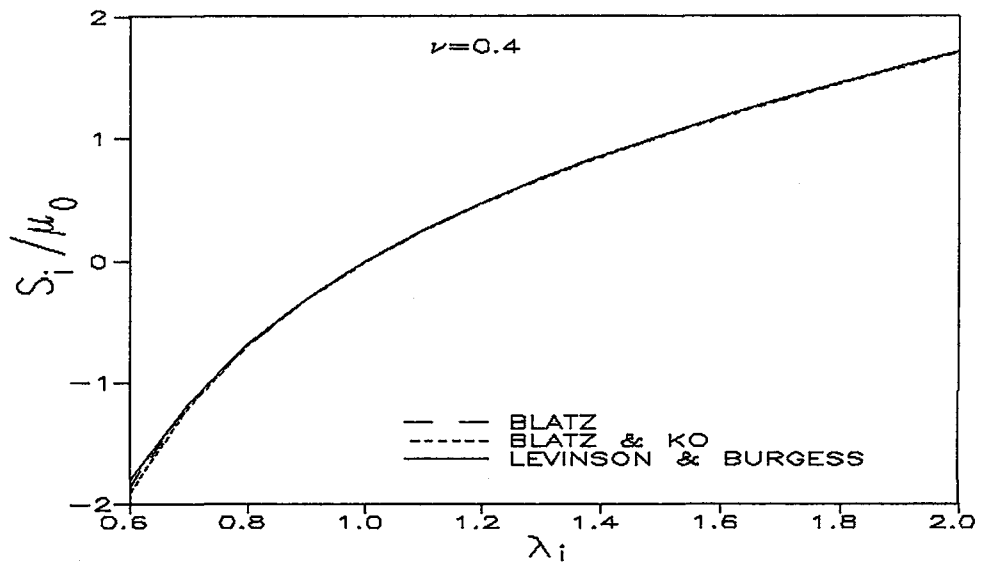


Figure 2.1 Simple Uniaxial Stress (taken from [10])

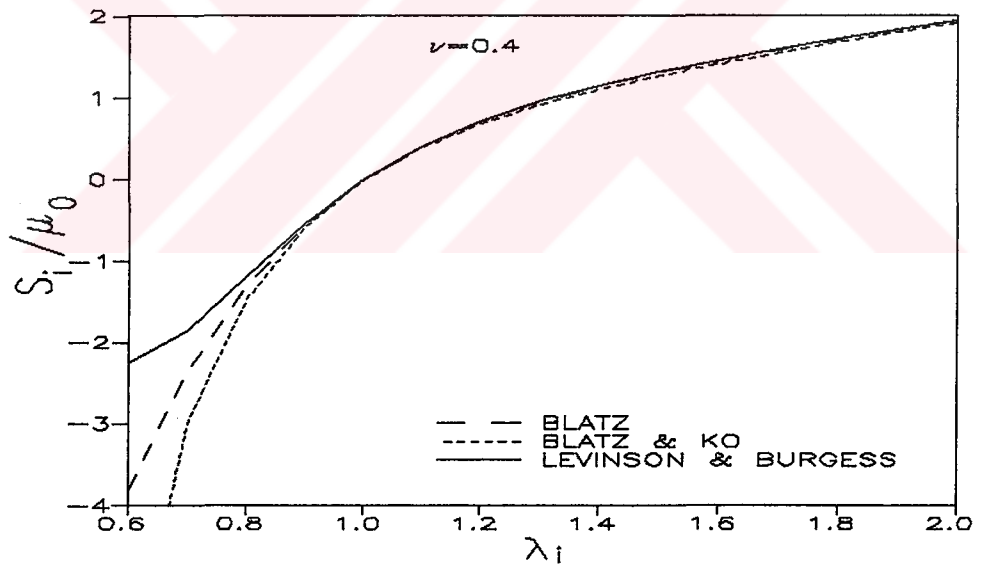


Figure 2.2 Equal Biaxial Plane Stress (taken from [10])

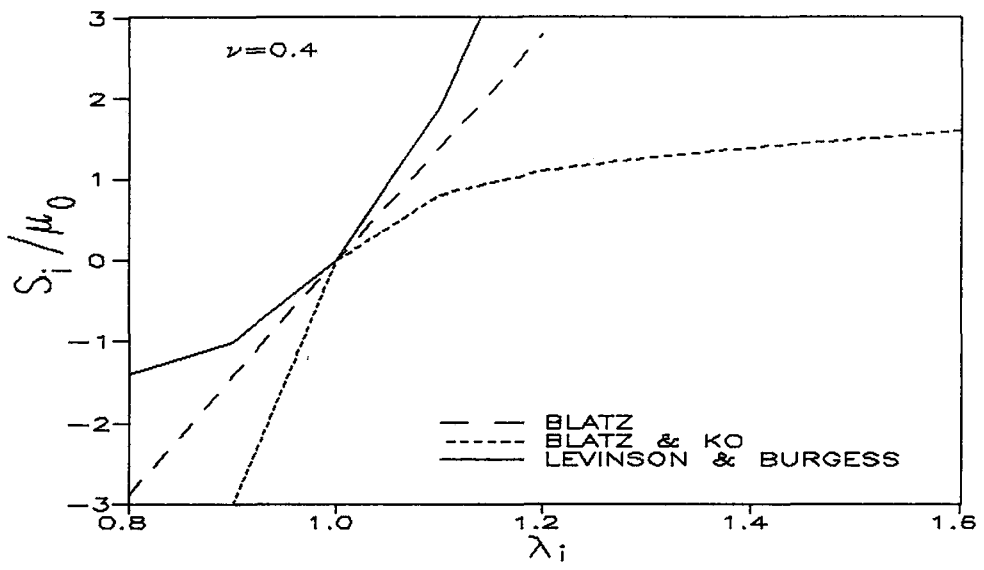


Figure 2.3 Hydrostatic Stress (taken from [10])



## CHAPTER III

### FORMULATION OF THE PROBLEM

In this chapter the general theory outlined in the previous chapter will be applied to the problems of anti-plane shear, constant spin and circumferential shear, and pure circumferential shear. In all the problems, the material is assumed to be hyperelastic, isotropic, homogeneous, and compressible. Three specific types of compressible materials are investigated.

#### 3.1 Governing Equations

##### 3.1.1 Finite Anti-Plane Shear of Compressible Hyperelastic Tube Subjected To External Axial Shear

Consider a long, circular, cylindrical tube whose inner surface is assumed to be perfectly bonded to a rigid shaft. The outer surface of the tube is subjected to a uniformly distributed shear stress applied in the axial direction. The inner and the outer radii in the undeformed and the deformed

configurations are respectively denoted by  $R_1, R_2$  and  $r_1, r_2$ . Identifying the cylindrical coordinates  $(r, \theta, z)$  in the deformed state by  $\theta^i$ , and referring this configuration to the fixed cartesian coordinates  $\{X_i\}$ , one has

$$\begin{aligned} X_1 &= r \cos \theta \\ X_2 &= r \sin \theta \\ X_3 &= z \end{aligned} \quad (3.1)$$

In an anti-plane shear deformation, a material point undergoes an axial displacement  $w$ , and a radial displacement  $u$  which are both assumed to be functions of radial coordinate  $r$  only. Hence, a material point whose coordinates are  $(r, \theta, z)$  in the deformed state is originally at  $R=r-u(r)$ ,  $\theta=\theta$ , and  $Z=z-w(r)$  such that

$$\begin{aligned} x_1 &= [r - u(r)] \cos \theta \\ x_2 &= [r - u(r)] \sin \theta \\ x_3 &= z - w(r) \end{aligned} \quad (3.2)$$

From equations (2.2), (2.3), (2.5), and (2.6), the metric tensors  $g_{ij}$ ,  $g^{ij}$ , and  $G_{ij}$ ,  $G^{ij}$  of the undeformed and deformed geometries are obtained as

$$g_{ij} = \begin{bmatrix} (1-u')^2 + (w')^2 & 0 & -w' \\ 0 & (r-u)^2 & 0 \\ -w' & 0 & 1 \end{bmatrix} \quad (3.3)$$

$$g^{ij} = \begin{bmatrix} \frac{1}{(1-u')^2} & 0 & \frac{w'}{(1-u')^2} \\ 0 & \frac{1}{(r-u)^2} & 0 \\ \frac{w'}{(1-u')^2} & 0 & 1 + \frac{(w')^2}{(1-u')^2} \end{bmatrix} \quad (3.4)$$

$$G_{ij} = \begin{bmatrix} 1 & 0 & 0 \\ 0 & r^2 & 0 \\ 0 & 0 & 1 \end{bmatrix} \quad (3.5)$$

$$G^{ij} = \begin{bmatrix} 1 & 0 & 0 \\ 0 & \frac{1}{r^2} & 0 \\ 0 & 0 & 1 \end{bmatrix} \quad (3.6)$$

$$g = \det\{g_{ij}\} = (r-u)^2(1-u')^2 \quad (3.7)$$

$$G = \det\{G_{ij}\} = r^2 \quad (3.8)$$

In equations (3.3), and (3.4) a prime denotes differentiation with respect to  $r$ .

Three strain invariants  $I_1$ ,  $I_2$ , and  $I_3$  of the deformation field are



computed from (2.10). They are

$$\begin{aligned}
 I_1 &= 1 + \frac{r^2}{(r-u)^2} + \frac{1+(w')^2}{(1-u')^2} \\
 I_2 &= \frac{r^2}{(r-u)^2} \left[ 1 + \frac{1+(w')^2}{(1-u')^2} \right] + \frac{1}{(1-u')^2} \\
 I_3 &= \frac{r^2}{(r-u)^2(1+u')^2}
 \end{aligned} \tag{3.9}$$

The contravariant components of the tensor  $B^{ij}$  are obtained as

$$\begin{aligned}
 B^{11} &= \frac{1}{(1-u')^2} \left[ 1 + \frac{r^2}{(r-u)^2} \right] \\
 B^{13} &= B^{31} = \frac{r^2 w'}{(r-u)^2(1-u')^2} \\
 B^{22} &= \frac{1}{(r-u)} \left[ 1 + \frac{1+(w')^2}{(1-u')^2} \right] \\
 B^{33} &= \frac{1}{(1-u')^2} + \frac{r^2}{(r-u)^2} \left[ 1 + \frac{(w')^2}{(1-u')^2} \right] \\
 B^{12} &= B^{21} = B^{23} = B^{32} = 0
 \end{aligned} \tag{3.10}$$

Substituting equations (3.5), and (3.6) into equation (2.16), the Christoffel symbols of the second kind are obtained for the cylindrical system  $(r, \theta, z)$ . The non-zero components are

$$\Gamma_{12}^2 = \Gamma_{21}^2 = \frac{1}{r}, \quad \Gamma_{22}^1 = -r \quad (3.11)$$

The equations of equilibrium in terms of stress components, can be written by inserting Christoffel symbols defined in equation (3.11) into equation (2.17) as

$$\begin{aligned} \frac{\partial \tau^{11}}{\partial r} + \frac{\tau^{11} - r^2 \tau^{22}}{r} + \frac{\partial \tau^{21}}{\partial \theta} &= 0 \\ \frac{\partial \tau^{21}}{\partial r} + \frac{3\tau^{12}}{r} + \frac{\partial \tau^{22}}{\partial \theta} &= 0 \\ \frac{\partial \tau^{13}}{\partial r} + \frac{\partial \tau^{23}}{\partial r} + \frac{\tau^{13}}{r} &= 0 \end{aligned} \quad (3.12)$$

From equations (2.11), and (2.12) the stresses can be written as

$$\tau^{\dot{y}} = \frac{2}{\sqrt{I_3}} \frac{\partial W}{\partial I_1} g^{\dot{y}} + \frac{2}{\sqrt{I_3}} \frac{\partial W}{\partial I_2} B^{\dot{y}} + 2\sqrt{I_3} \frac{\partial W}{\partial I_3} G^{\dot{y}} \quad (3.13)$$

At this point, specific forms of the strain energy density functions are introduced.

## A. Polynomial Material

As mentioned before, this model is proposed by Levinson and Burgess [10], and the strain energy density function in terms of strain invariants  $I_1$ ,  $I_2$ , and  $I_3$  is given by

$$\begin{aligned}
 W_{LB} = & \frac{\mu}{2} [f(I_1 - 3) + (1-f)\left(\frac{I_2}{I_3} - 3\right) \\
 & + 2(1-2f)(\sqrt{I_3} - 1) + \left(2f + \frac{4\nu - 1}{1-2\nu}\right)(\sqrt{I_3} - 1)^2]
 \end{aligned} \tag{3.14}$$

The non-zero components of the stress tensor are obtained by inserting equation (3.14) into equation (3.13) as

$$\begin{aligned}
 \tau^{11} = & \mu \left[ f \frac{(r-u)}{r(1-u')} + (f-1) \frac{(r-u)(1-u')}{r} ((1-u')^2 + (w')^2) + \right. \\
 & \left. \left( \frac{r}{(r-u)(1-u')} \right) \left( 2f + \frac{4\nu-1}{1-2\nu} \right) + \left( 1 - 4f - \frac{4\nu-1}{1-2\nu} \right) \right] \\
 \tau^{13} = & \mu \left[ f \frac{(r-u)}{r(1-u')} w' + (f-1) \frac{(r-u)(1-u')}{r} w' \right] \\
 \tau^{22} = & \mu \left[ f \frac{(1-u')}{r(r-u)} + (f-1) \frac{(r-u)^3(1-u')}{r^5} + \right. \\
 & \left. \left( \frac{1}{r(r-u)(1-u')} \right) \left( 2f + \frac{4\nu-1}{1-2\nu} \right) + \frac{1}{r^2} \left( 1 - 4f - \frac{4\nu-1}{1-2\nu} \right) \right] \\
 \tau^{33} = & \mu \left[ (2f-1) \frac{(r-u)(1-u')}{r} + f \frac{(r-u)}{r(1-u')} (w')^2 + \right. \\
 & \left. \left( \frac{r}{(r-u)(1-u')} \right) \left( 2f + \frac{4\nu-1}{1-2\nu} \right) + \left( 1 - 4f - \frac{4\nu-1}{1-2\nu} \right) \right]
 \end{aligned} \tag{3.15}$$

Since the stress components are independent of  $\theta$ , and  $\tau^{12}=\tau^{21}=0$ , the equation of equilibrium, (3.12), in the tangential direction is automatically satisfied. Taking the derivatives of  $\tau^{11}$ , and  $\tau^{13}$  with respect to  $r$ , and inserting them together with the stress components into equation (3.12), equilibrium equations in the radial and the axial directions, are expressed in terms of displacements  $u$ ,  $w$ , and their derivatives with respect to  $r$ :

$$\begin{aligned} & \mu \left[ f \left( \frac{1}{r} + \frac{(r-u)}{(1-u')} u'' - \frac{(1-u')}{(r-u)} \right) + \right. \\ & (f-1) \left( \frac{(1-u')^4}{r} - \frac{3(r-u)(1-u')^2}{r} u'' + \frac{(1-u')^2 (w')^2}{r} - \right. \\ & \left. \left( \frac{(r-u)(w')^2}{r} \right) u'' + \frac{2(r-u)(1-u') w'}{r} w'' - \frac{(r-u)^3 (1-u')}{r^4} \right) + \\ & \left. \left( 2f + \frac{4\nu-1}{1-2\nu} \right) \left( \frac{1}{(r-u)(1-u')} - \frac{r}{(r-u)^2} + \frac{r}{(r-u)(1-u')} u'' \right) \right] = 0 \end{aligned} \quad (3.16)$$

$$\begin{aligned} & \mu \left[ f \left( \frac{w'}{r} + \frac{(r-u)w'}{r(1-u')^2} u'' + \frac{(r-u)}{r(1-u')} w'' \right) + \right. \\ & \left. (1-f) \left( \frac{(1-u')^2 w'}{r} - \frac{(r-u)w'}{r} u'' + \frac{(r-u)(1-u')}{r} w'' \right) \right] = 0 \end{aligned} \quad (3.17)$$

## B. Blatz-Ko Material

The strain energy density function which is proposed by Blatz and

Ko [9] can be written in terms of strain invariants  $I_1, I_2,$  and  $I_3$  as follows

$$W_{BK} = \frac{\mu}{2} [f(I_1 - 3) + (1-f) \left( \frac{I_2}{I_3} - 3 \right) + \left( \frac{1-2\nu}{\nu} \right) \{ f(I_3^{\frac{1-\nu}{1-2\nu}} - 1) + (1-f) (I_3^{\frac{\nu}{1-2\nu}} - 1) \}] \quad (3.18)$$

The non-zero components of the stress tensor are obtained by substituting equation (3.18) into equation (3.13) as

$$\begin{aligned} \tau^{11} &= \mu \left[ f \frac{(r-u)}{r(1-u')} + (f-1) \frac{(r-u)(1-u')^3}{r} \left( 1 + \frac{(w')^2}{(1-u')^2} \right) \right. \\ &\quad \left. - f \left\{ \frac{(r-u)(1-u')}{r} \right\}^{\frac{1}{1-2\nu}} + (1-f) \left\{ \frac{(r-u)(1-u')}{r} \right\}^{\frac{1-4\nu}{1-2\nu}} \right] \\ \tau^{13} &= \mu \left[ f \frac{(r-u)}{r(1-u')} w' + (1-f) \frac{(r-u)(1-u')}{r} w' \right] \\ \tau^{22} &= \mu \left[ f \frac{(1-u')}{r(r-u)} + (f-1) \frac{(r-u)^3(1-u')}{r^5} \right. \\ &\quad \left. - \frac{f}{r^2} \left\{ \frac{(r-u)(1-u')}{r} \right\}^{\frac{1}{1-2\nu}} + \frac{(1-f)}{r^2} \left\{ \frac{(r-u)(1-u')}{r} \right\}^{\frac{1-4\nu}{1-2\nu}} \right] \\ \tau^{33} &= \mu \left[ (2f-1) \frac{(r-u)(1-u')}{r} + f \frac{(r-u)}{r(1-u')} (w')^2 \right. \\ &\quad \left. - f \left\{ \frac{(r-u)(1-u')}{r} \right\}^{\frac{1}{1-2\nu}} + (1-f) \left\{ \frac{(r-u)(1-u')}{r} \right\}^{\frac{1-4\nu}{1-2\nu}} \right] \end{aligned} \quad (3.19)$$

By using equations (3.12), the equilibrium equation in the radial direction is expressed as

$$\begin{aligned}
& f \left[ \frac{1}{r} + \frac{(r-u)}{r(1-u')^2} u'' - \frac{(1-u')}{(r-u)} \right] + \\
& (f-1) \left[ \frac{(1-u')^4}{r} - \frac{3(r-u)(1-u')^2}{r} u'' + \frac{(1-u')^2 (w')^2}{r} - \right. \\
& \left. \frac{(r-u)(w')^2}{r} u'' + \frac{2(r-u)(1-u')(w')}{r} w'' - \frac{(r-u)^3 (1-u')}{r^4} \right] + \\
& \left\{ \frac{(1-u')^2}{r} - \frac{(r-u)}{r} u'' - \frac{(r-u)(1-u')}{r^2} \right\} \\
& \left\{ -f \frac{1}{1-2\nu} \left[ \frac{(r-u)(1-u')}{r} \right]^{\frac{2\nu}{1-2\nu}} + (1-f) \frac{1-4\nu}{1-2\nu} \left[ \frac{(r-u)(1-u')}{r} \right]^{\frac{-2\nu}{1-2\nu}} \right\} = 0
\end{aligned} \tag{3.20}$$

and the equilibrium equation in the axial direction is identical with the equation (3.17), since  $\tau^{13}$  is the same for both models.

### C. Blatz Material

The strain energy density function proposed by Blatz [10] is written in terms of strain invariant  $I_1$ ,  $I_2$ , and  $I_3$  as

$$W_B = \frac{\mu}{2} \left[ (I_1 - 3) - \left( \frac{2}{1-2\nu} \right) \ln \sqrt{I_3} + \frac{4\nu}{1-2\nu} (\sqrt{I_3} - 1) \right] \tag{3.21}$$

The non-zero components of stresses are obtained by substituting equation (3.21) into equation (3.13)

$$\begin{aligned}
 \tau^{11} &= \mu \left[ \frac{(r-u)}{r(1-u')} + 2 \frac{v}{1-2v} - \frac{1}{1-2v} \frac{(r-u)(1-u')}{r} \right] \\
 \tau^{13} &= \mu \frac{(r-u)}{r(1-u')} w' \\
 \tau^{22} &= \mu \left[ \frac{(1-u')}{r(r-u)} + \frac{2}{r^2} \frac{v}{1-2v} - \frac{1}{1-2v} \frac{(r-u)(1-u')}{r^3} \right] \\
 \tau^{33} &= \mu \left[ \frac{(r-u)(1-u')}{r} + \frac{(r-u)(w')^2}{r(1-u')} + 2 \frac{v}{1-2v} - \frac{1}{1-2v} \frac{(r-u)(1-u')}{r} \right]
 \end{aligned} \tag{3.22}$$

By using equations (3.12), the equilibrium equations in the radial, and the axial directions are obtained as

$$\begin{aligned}
 &\left( \frac{1}{r} \right) + \frac{(r-u)}{r(1-u')^2} u'' - \frac{(1-u')}{(r-u)} + \\
 &\left( \frac{1}{1-2v} \right) \left[ \frac{(r-u)}{r} u'' + \frac{(r-u)(1-u')}{r^2} - \frac{(1-u')^2}{r} \right] = 0
 \end{aligned} \tag{3.23}$$

$$\frac{1}{r} w' + \frac{(r-u)}{r(1-u')} w'' + \frac{(r-u)w'}{r(1-u')^2} u'' = 0 \tag{3.24}$$

### 3.1.2 Compressible, Hyperelastic Spinning Tubes Subjected to Circumferential Shear

Consider a long, circular, cylindrical tube of arbitrary, uniform wall thickness with an inner radius  $R_1$ , and outer radius  $R_2$ . Let the tube be perfectly bonded to a rigid shaft along its inner curved surface. The shaft is assumed to spin with a constant angular speed  $\Omega$  while the tube is subjected to uniformly distributed circumferential shearing tractions  $\tau_0$  on its outer curved surface. Denoting the positions of a material point in the undeformed, and deformed states by cylindrical coordinates  $(R, \Theta, Z)$ , and  $(r, \theta, z)$ , respectively, one has

$$r = R + u \quad \theta = \Theta + \phi + \Omega t \quad z = Z \quad (3.25)$$

where the radial displacement  $u$ , and the angular displacement  $\phi$  depend on the radial location only, and  $t$  denotes the time.

From equations (2.2), (2.3), (2.5), and (2.6), the metric tensors  $g_{ij}$ ,  $g^{ij}$ , and  $G_{ij}$ ,  $G^{ij}$  of the undeformed and deformed geometries, respectively, are obtained as



$$g_{ij} = \begin{bmatrix} \frac{1 + \phi'^2 R^2}{(1 + u')^2} & -\frac{\phi' R^2}{1 + u'} & 0 \\ -\frac{\phi' R^2}{1 + u'} & R^2 & 0 \\ 0 & 0 & 1 \end{bmatrix} \quad (3.26)$$

$$g^{ij} = \begin{bmatrix} (1 + u')^2 & (1 + u')\phi' & 0 \\ (1 + u')\phi' & \frac{1}{R^2} & 0 \\ 0 & 0 & 1 \end{bmatrix} \quad (3.27)$$

$$G_{ij} = \begin{bmatrix} 1 & 0 & 0 \\ 0 & (R + u)^2 & 0 \\ 0 & 0 & 1 \end{bmatrix} \quad (3.28)$$

$$G^{ij} = \begin{bmatrix} 1 & 0 & 0 \\ 0 & \frac{1}{(R + u)^2} & 0 \\ 0 & 0 & 1 \end{bmatrix} \quad (3.29)$$

$$g = \det \{g_{ij}\} = \frac{R^2}{(1 + u')^2} \quad (3.30)$$

$$G = \det \{G_{ij}\} = (R + u)^2 \quad (3.31)$$

In equations (3.26), and (3.27) a prime denotes differentiation with respect to

R.

The three strain invariants associated with this deformation field are given from equation (2.10)

$$\begin{aligned}
 I_1 &= 1 + \frac{(R+u)^2}{R^2} + (1+u')^2 + (R+u)^2 \phi'^2 \\
 I_2 &= \frac{(R+u)^2}{R^2} + (1+u')^2 + \frac{(R+u)^2(1+u')^2}{R^2} + (R+u)^2 \phi'^2 + \\
 &\quad (1+u')^2(R+u)^2 \phi'^2 \\
 I_3 &= \frac{(R+u)^2(1+u')^2}{R^2}
 \end{aligned} \tag{3.32}$$

By using equation (2.13) the components of the tensor  $B^{ij}$  are obtained as

$$\begin{aligned}
 B^{11} &= (1+u')^2 + \frac{(R+u)^2(1+u')^2}{R^2} + (R+u)^2(1+u')^2 \phi'^2 \\
 B^{12} &= B^{21} = (1+u') \phi' \\
 B^{22} &= \frac{1}{R^2} + \frac{(1+u')^2}{R^2} + \phi'^2 + (1+u')^2 \phi'^2 \\
 B^{33} &= \frac{(R+u)^2}{R^2} + (1+u')^2 + (R+u)^2 \phi'^2 \\
 B^{13} &= B^{31} = B^{23} = B^{32} = 0
 \end{aligned} \tag{3.33}$$

Substituting equations (3.28), and (3.29) into equation (2.16), the Christoffel symbols of the second kind are obtained for the cylindrical system  $(r, \theta, z)$ . The non-zero components are

$$\Gamma_{12}^2 = \Gamma_{21}^2 = \frac{1}{(R+u)} \quad \Gamma_{22}^1 = -(R+u) \quad (3.34)$$

The equations of equilibrium in terms of stress components can be written by substituting the Christoffel symbols defined in equation (3.34) into equation (2.17). The equation of equilibrium in the axial direction is trivially satisfied. Those in the radial, and the tangential directions are given by, respectively,

$$\begin{aligned} \frac{\partial \tau^{11}}{\partial R} + \frac{(1+u')}{(R+u)} [\tau^{11} + (R+u)^2 \tau^{22}] + \rho \Omega^2 (R+u) (1+u') &= 0 \\ \frac{\partial \tau^{12}}{\partial R} + \frac{3(1+u')}{(R+u)} \tau^{12} &= 0 \end{aligned} \quad (3.35)$$

where  $\rho$  denotes the current mass density which is related to the mass density  $\rho_0$  in the undeformed state by

$$\rho = \frac{\rho_0 R}{(R+u)(1+u')} \quad (3.36)$$

At this point, specific forms of the strain energy density functions are introduced. For the stress components, equation (3.13) is used.

## A. Polynomial Material

The strain energy density function is given in equation (3.14). The non-zero components of the stress tensor are obtained by inserting equation (3.14) into equation (3.13) as

$$\begin{aligned}
 \tau^{11} &= \mu \left[ 1 - 2f + f \frac{R(1+u')}{(R+u)} - \frac{(1-f)R}{(R+u)(1+u')^3} (1 + R^2 \phi'^2) + \right. \\
 &\quad \left. \left( 2f + \frac{4\nu-1}{1-2\nu} \right) \left( \frac{(R+u)(1+u')}{R} - 1 \right) \right] \\
 \tau^{12} &= \mu \left[ f \frac{R}{(R+u)} \phi' + (1-f) \frac{R^3 \phi'}{(R+u)^3 (1+u')^2} \right] \\
 \tau^{22} &= \frac{\mu}{(R+u)^2} \left[ 1 - 2f + f \frac{(R+u)}{R(1+u')} + f \frac{R(R+u)\phi'^2}{(1+u')} - \right. \\
 &\quad \left. (1-f) \frac{R^3}{(R+u)^3 (1+u')} + \left( 2f + \frac{4\nu-1}{1-2\nu} \right) \left( \frac{(1+u')(R+u)}{R} - 1 \right) \right] \\
 \tau^{33} &= \mu \left[ (1-2f) \left( 1 - \frac{R}{(R+u)(1+u')} \right) - (1-f) \frac{R^3 \phi'^2}{(R+u)(1+u')} + \right. \\
 &\quad \left. \left( 2f + \frac{4\nu-1}{1-2\nu} \right) \left( \frac{(R+u)(1+u')}{R} - 1 \right) \right]
 \end{aligned} \tag{3.37}$$

Substituting equations (3.37) into equations (3.35), equilibrium equations in the radial and tangential directions are expressed as

$$\begin{aligned}
& \left[ f \frac{R}{(R+u)} + \left( 2f + \frac{4\nu-1}{1-2\nu} \right) \frac{(R+u)}{R} + (1-f) \frac{3R(1+R^2\phi'^2)}{(R+u)(1+u')^4} \right] u'' - \\
& (1-f) \frac{2R^3\phi'}{(R+u)(1+u')^3} \phi'' + f \frac{(1+u')}{(R+u)} + (1-f) \left( \frac{R^3}{(R+u)^4} - \frac{1+3R^2\phi'^2}{(R+u)(1+u')^3} \right) - \\
& f \frac{1}{R} - fR\phi'^2 + \left( 2f + \frac{4\nu-1}{1-2\nu} \right) \left( \frac{(1+u')^2}{R} - \frac{(R+u)(1+u')}{R} \right) + \rho_0 \Omega^2 \frac{R}{\mu} = 0
\end{aligned} \tag{3.38}$$

$$\begin{aligned}
& -(1-f) \frac{2R^3\phi'}{(R+u)^3(1+u')^3} u'' + (1-f) \frac{R^3}{(R+u)^3(1+u')^2} \phi'' + \\
& f \frac{R}{(R+u)} \phi'' + f \frac{\phi'}{(R+u)} + f \frac{2R\phi'(1+u')}{(R+u)^2} + (1-f) \frac{3R^2\phi'}{(R+u)^3(1+u')^2} = 0
\end{aligned} \tag{3.39}$$

## B. Blatz-Ko Material

The strain energy density function is given in equation (3.18). The non-zero components of the stress tensor are obtained by substituting equation (3.18) into equation (3.13) as

$$\begin{aligned}
\tau^{11} &= \mu \left[ f \frac{R(1+u')}{(R+u)} - (1-f) \left( \frac{R}{(R+u)(1+u')^3} + \frac{R^3 \phi'^2}{(R+u)(1+u')^3} \right) - \right. \\
&\quad \left. f \left\{ \frac{R}{(R+u)(1+u')} \right\}^{\frac{1}{1-2\nu}} + (1-f) \left\{ \frac{R}{(R+u)(1+u')} \right\}^{\frac{1-4\nu}{1-2\nu}} \right] \\
\tau^{12} &= \mu \left[ f \frac{R\phi'}{(R+u)} + (1-f) \frac{R^3 \phi'}{(R+u)^3 (1+u')^2} \right] \\
\tau^{22} &= \frac{\mu}{(R+u)^2} \left[ f \frac{(R+u)}{R(1+u')} + f \frac{R(R+u)\phi'^2}{(1+u')} - (1-f) \frac{R^3}{(R+u)^3 (1+u')} - \right. \\
&\quad \left. f \left\{ \frac{R}{(R+u)(1+u')} \right\}^{\frac{1}{1-2\nu}} + (1-f) \left\{ \frac{R}{(R+u)(1+u')} \right\}^{\frac{1-4\nu}{1-2\nu}} \right] \\
\tau^{33} &= \mu \left[ f \frac{R}{(R+u)(1+u')} - (1-f) \left( \frac{R}{(R+u)(1+u')} + \frac{R^3 \phi'^2}{(R+u)(1+u')} \right) - \right. \\
&\quad \left. f \left\{ \frac{R}{(R+u)(1+u')} \right\}^{\frac{1}{1-2\nu}} + (1-f) \left\{ \frac{R}{(R+u)(1+u')} \right\}^{\frac{1-4\nu}{1-2\nu}} \right]
\end{aligned} \tag{3.40}$$

By using equation (3.35), the equilibrium equation in the radial direction is obtained as

$$\begin{aligned}
& \left[ f \frac{R}{(R+u)} + (1-f) \frac{3R(1+R^2\phi'^2)}{(R+u)(1+u')^4} + \frac{R}{(R+u)(1+u')^2} \left\{ f \frac{1}{1-2\nu} \left( \frac{R}{(R+u)(1+u')} \right. \right. \right. \\
& \left. \left. \left. (1-f) \frac{1-4\nu}{1-2\nu} \left( \frac{R}{(R+u)(1+u')} \right)^{\frac{-2\nu}{1-2\nu}} \right\} u'' - (1-f) \frac{2R^3\phi'}{(R+u)(1+u')^3} \phi'' + \right. \\
& \left. f \frac{(1+u')}{(R+u)} - f \frac{1}{R} - fR\phi'^2 + (1-f) \left( \frac{R^3}{(R+u)^4} - \frac{1+3R^2\phi'^2}{(R+u)(1+u')^3} \right) + \right. \\
& \left. \left( \frac{1}{(R+u)(1+u')} - \frac{R}{(R+u)^2} \right) \left\{ f \frac{1}{1-2\nu} \left( \frac{R}{(R+u)(1+u')} \right)^{\frac{2\nu}{1-2\nu}} - \right. \right. \\
& \left. \left. (1-f) \frac{1-4\nu}{1-2\nu} \left( \frac{R}{(R+u)(1+u')} \right)^{\frac{-2\nu}{1-2\nu}} \right\} + \rho_0 \Omega^2 \frac{R}{\mu} = 0 \right.
\end{aligned} \tag{3.41}$$

and the equilibrium equation in the tangential direction is identical with the equation (3.39), since  $\tau^{12}$  is same for both models.

### C. Blatz Material

The strain energy density function for Blatz material is given in equation (3.21). The non-zero components of the stresses are obtained by substituting equation (3.21) into equation (3.13) as

$$\begin{aligned}
\tau^{11} &= \mu \left[ \frac{R(1+u')}{(R+u)} + 2 \frac{v}{1-2v} - \frac{1}{1-2v} \frac{R}{(R+u)(1+u')} \right] \\
\tau^{12} &= \mu \frac{R}{(R+u)} \phi' \\
\tau^{22} &= \frac{\mu}{(R+u)^2} \left[ \frac{(R+u)}{R(1+u')} + \frac{R(R+u)^2 \phi'^2}{(1+u')} + \right. \\
&\quad \left. 2 \frac{v}{1-2v} - \frac{1}{1-2v} \frac{R}{(R+u)(1+u')} \right] \\
\tau^{33} &= \mu \left[ \frac{-2v}{1-2v} \frac{R}{(R+u)(1+u')} + 2 \frac{v}{1-2v} \right]
\end{aligned} \tag{3.42}$$

By using equations (3.35) the equilibrium equations in the radial, and the tangential directions are obtained as

$$\begin{aligned}
&\left[ \frac{1}{1-2v} \frac{R}{(R+u)(1+u')^2} + \frac{R}{(R+u)} \right] u'' + \frac{(1+u')}{(R+u)} - \\
&\left( \frac{1}{1-2v} \right) \left( \frac{1}{(R+u)(1+u')} - \frac{R}{(R+u)^2} \right) - \frac{1}{R} - R \phi'^2 + \rho_0 \Omega^2 \frac{R}{\mu} = 0
\end{aligned} \tag{3.43}$$

$$\frac{1}{(1+u')} \frac{R}{(R+u)} \phi'' + \frac{\phi'}{(R+u)(1+u')} + \frac{2R\phi'}{(R+u)^2} = 0 \tag{3.44}$$

### 3.1.3 Finite Circumferential Shearing of Compressible, Hyperelastic

Tube

Consider a long, circular cylindrical tube of arbitrary, uniform wall



thickness with an inner radius  $R_1$ , and outer radius  $R_2$ . Let the tube be perfectly bonded to a rigid shaft along its inner curved surface. It is assumed that the tube is subjected to uniformly distributed circumferential shearing tractions  $\tau_0$  on its outer curved surface. Denoting the positions of a material point in the undeformed and the deformed states by cylindrical coordinates  $(R,\theta,Z)$  and  $(r,\theta,z)$ , respectively, one has

$$r = R + u \quad \theta = \Theta + \phi \quad z = Z \quad (3.45)$$

where the radial displacement  $u$ , and the circumferential displacement  $\phi$  are both assumed to be functions of radial coordinate  $R$  only.

The equations of section 3.1.2 are valid for this problem when the spin speed  $\Omega$  is set equal to zero.

### 3.2 Non-Dimensionalization

For the above type of problems it is desirable to write equilibrium equations, and the stress equations referring to undeformed configuration and in terms of non-dimensional variables. For this purpose, the following relations are used

$$x = \frac{R}{R_1} \quad \bar{u} = \frac{u}{R_1} \quad \bar{w} = \frac{w}{R_1} \quad (3.46)$$

for non-dimensionalization of anti-plane shear problem

$$x = \frac{R}{R_1} \quad \bar{u} = \frac{u}{R_1} \quad \bar{\phi} = \phi \quad (3.47)$$

for non-dimensionalization of circumferential shear problems

The conversions from  $r$  to  $R$ , and the equations for the dimensionless derivative terms are given in Appendix A.

### 3.3 Non-Dimensional Governing Equations

With the above change of variables, the equilibrium equations reduce to two quasi-linear, coupled ordinary differential equations of the form;

$$\begin{aligned} A(x, \bar{u}, \bar{w}, \bar{u}_x, \bar{w}_x) \bar{u}_{xx} + B(x, \bar{u}, \bar{w}, \bar{u}_x, \bar{w}_x) \bar{w}_{xx} &= C(x, \bar{u}, \bar{w}, \bar{u}_x, \bar{w}_x) \\ D(x, \bar{u}, \bar{w}, \bar{u}_x, \bar{w}_x) \bar{u}_{xx} + E(x, \bar{u}, \bar{w}, \bar{u}_x, \bar{w}_x) \bar{w}_{xx} &= F(x, \bar{u}, \bar{w}, \bar{u}_x, \bar{w}_x) \end{aligned} \quad (3.48)$$

for anti-plane shear problem

$$\begin{aligned}
 A(x, \bar{u}, \bar{\phi}, \bar{u}_x, \bar{\phi}_x) \bar{u}_{xx} + B(x, \bar{u}, \bar{\phi}, \bar{u}_x, \bar{\phi}_x) \bar{\phi}_{xx} &= C(x, \bar{u}, \bar{\phi}, \bar{u}_x, \bar{\phi}_x) \\
 D(x, \bar{u}, \bar{\phi}, \bar{u}_x, \bar{\phi}_x) \bar{u}_{xx} + E(x, \bar{u}, \bar{\phi}, \bar{u}_x, \bar{\phi}_x) \bar{\phi}_{xx} &= F(x, \bar{u}, \bar{\phi}, \bar{u}_x, \bar{\phi}_x)
 \end{aligned}
 \tag{3.49}$$

for circumferential shear problems

The stress components are also written in dimensionless form using the transformations mentioned in Appendix A.

### 3.3.1 Finite Anti-Plane Shear of Compressible Hyperelastic Tube

Subjected to External Axial Shear

For this problem the variables of equation (3.48) and the non-dimensional stress components are as follows

### A. Polynomial Material

$$\begin{aligned}
 A &= fx^3(x+\bar{u})^3(1+\bar{u}_x)^4 - 3(f-1)x^3(x+\bar{u})^3 - 3(f-1)x^3(x+\bar{u})^3\bar{w}_x^2 + \\
 &\quad x(x+\bar{u})^5(1+\bar{u}_x)^4\left(2f + \frac{4v-1}{1-2v}\right) \\
 B &= 2(f-1)x^3(x+\bar{u})^3(1+\bar{u}_x)\bar{w}_x \\
 C &= -fx^2(x+\bar{u})^3(1+\bar{u}_x)^5 - (f-1)x^2(x+\bar{u})^3(1+\bar{u}_x) - \\
 &\quad (f-1)x^2(x+\bar{u})^3(1+\bar{u}_x)\bar{w}_x^2 - x(x+\bar{u})^4(1+\bar{u}_x)^6\left(2f + \frac{4v-1}{1-2v}\right) + \quad (3.50) \\
 &\quad (x+\bar{u})^5(1+\bar{u}_x)^5\left(2f + \frac{4v-1}{1-2v}\right) + fx(x+\bar{u})^4(1+\bar{u}_x)^4 + (f-1)x^5(1+\bar{u}_x)^4 \\
 D &= -2(1-f)x\bar{w}_x \\
 E &= fx(1+\bar{u}_x)^3 + (1-f)x(1+\bar{u}_x) \\
 F &= -f(1+\bar{u}_x)^3\bar{w}_x - (1-f)(1+\bar{u}_x)\bar{w}_x
 \end{aligned}$$

$$\begin{aligned}
 \bar{\tau}^{11} &= \frac{\tau^{11}}{\mu} = f\frac{x(1+\bar{u}_x)}{(x+\bar{u})} + (f-1)\frac{x}{(x+\bar{u})(1+\bar{u}_x)^3} + (f-1)\frac{x\bar{w}_x^2}{(x+\bar{u})(1+\bar{u}_x)^3} + \\
 &\quad \left(1-4f - \frac{4v-1}{1-2v}\right) + \frac{(x+\bar{u})(1+\bar{u}_x)}{x}\left(2f + \frac{4v-1}{1-2v}\right) \\
 \bar{\tau}^{13} &= \frac{\tau^{13}}{\mu} = f\frac{x}{(x+\bar{u})}\bar{w}_x + (1-f)\frac{x\bar{w}_x}{(x+\bar{u})(1+\bar{u}_x)^2} \\
 \bar{\tau}^{22} &= r^2\frac{\tau^{22}}{\mu} = \frac{f(x+\bar{u})}{x(1+\bar{u}_x)} + \frac{(f-1)x^3}{(x+\bar{u})^3(1+\bar{u}_x)} + \frac{(x+\bar{u})(1+\bar{u}_x)}{x}\left(2f + \frac{4v-1}{1-2v}\right) + \\
 &\quad \left(1-4f - \frac{4v-1}{1-2v}\right) \\
 \bar{\tau}^{33} &= \frac{\tau^{33}}{\mu} = \frac{(2f-1)x}{(x+\bar{u})(1+\bar{u}_x)} + \frac{fx\bar{w}_x^2}{(x+\bar{u})(1+\bar{u}_x)} + \\
 &\quad \left(\frac{(x+\bar{u})(1+\bar{u}_x)}{x}\right)\left(2f + \frac{4v-1}{1-2v}\right) + \left(1-4f - \frac{4v-1}{1-2v}\right)
 \end{aligned} \tag{3.51}$$

B. Blatz-Ko Material

$$A = fx^3(x+\bar{u})^3(1+\bar{u}_x)^4 - 3(f-1)x^3(x+\bar{u})^3 - 3(f-1)x^3(x+\bar{u})^3\bar{w}_x^2 +$$

$$[x^3(x+\bar{u})^3(1+\bar{u}_x)^2]\left[-\frac{1}{1-2\nu}f\left\{\frac{x}{(x+\bar{u})(1+\bar{u}_x)}\right\}^{\frac{2\nu}{1-2\nu}} +$$

$$\left(\frac{1-4\nu}{1-2\nu}\right)(1-f)\left\{\frac{x}{(x+\bar{u})(1+\bar{u}_x)}\right\}^{\frac{-2\nu}{1-2\nu}}\right]$$

$$B = 2(f-1)x^3(x+\bar{u})^3(1+\bar{u}_x)\bar{w}_x$$

$$C = -fx^2(x+\bar{u})^3(1+\bar{u}_x)^5 - (f-1)x^2(x+\bar{u})^3(1+\bar{u}_x) -$$

$$(f-1)x^2(x+\bar{u})^3(1+\bar{u}_x)\bar{w}_x^2 + fx^2(x+\bar{u})^4(1+\bar{u}_x)^4 + (f-1)x^5(1+\bar{u}_x)^4 +$$

$$[x^2(x+\bar{u})^3(1+\bar{u}_x)^3 - x^3(x+\bar{u})^2(1+\bar{u}_x)^4] *$$

$$\left[-\frac{1}{1-2\nu}f\left\{\frac{x}{(x+\bar{u})(1+\bar{u}_x)}\right\}^{\frac{2\nu}{1-2\nu}} + \frac{1-4\nu}{1-2\nu}(1-f)\left\{\frac{x}{(x+\bar{u})(1+\bar{u}_x)}\right\}^{\frac{-2\nu}{1-2\nu}}\right]$$

$$D = -2(1-f)x\bar{w}_x$$

$$E = fx(1+\bar{u}_x)^3 + (1-f)x(1+\bar{u}_x)$$

$$F = -f(1+\bar{u}_x)^3\bar{w}_x - (1-f)(1+\bar{u}_x)\bar{w}_x$$

(3.52)

$$\begin{aligned}
\bar{\tau}^{11} &= \frac{\tau^{11}}{\mu} = f \frac{x(1+\bar{u}_x)}{(x+\bar{u})} + (f-1) \frac{x}{(x+\bar{u})(1+\bar{u}_x)^3} + (f-1) \frac{x\bar{w}_x^2}{(x+\bar{u})(1+\bar{u}_x)^3} - \\
&\quad f \left\{ \frac{x}{(x+\bar{u})(1+\bar{u}_x)} \right\}^{\frac{1}{1-2\nu}} + (1-f) \left\{ \frac{x}{(x+\bar{u})(1+\bar{u}_x)} \right\}^{\frac{1-4\nu}{1-2\nu}} \\
\bar{\tau}^{13} &= \frac{\tau^{13}}{\mu} = f \frac{x}{(x+\bar{u})} \bar{w}_x + (1-f) \frac{x\bar{w}_x}{(x+\bar{u})(1+\bar{u}_x)^2} \\
\bar{\tau}^{22} &= r^2 \frac{\tau^{22}}{\mu} = \frac{f(x+\bar{u})}{x(1+\bar{u}_x)} + \frac{(f-1)x^3}{(x+\bar{u})^3(1+\bar{u}_x)} - f \left\{ \frac{x}{(x+\bar{u})(1+\bar{u}_x)} \right\}^{\frac{1}{1-2\nu}} + \\
&\quad (1-f) \left\{ \frac{x}{(x+\bar{u})(1+\bar{u}_x)} \right\}^{\frac{1-4\nu}{1-2\nu}} \\
\bar{\tau}^{33} &= \frac{\tau^{33}}{\mu} = \frac{2(f-1)x}{(x+\bar{u})(1+\bar{u}_x)} + \frac{fx\bar{w}_x^2}{(x+\bar{u})(1+\bar{u}_x)} - f \left\{ \frac{x}{(x+\bar{u})(1+\bar{u}_x)} \right\}^{\frac{1}{1-2\nu}} + \\
&\quad (1-f) \left\{ \frac{x}{(x+\bar{u})(1+\bar{u}_x)} \right\}^{\frac{1-4\nu}{1-2\nu}}
\end{aligned} \tag{3.53}$$

### C. Blatz Material

$$\begin{aligned}
A &= x^3(x+\bar{u})^3(1+\bar{u}_x)^4 + \frac{1}{1-2\nu} x^3(x+\bar{u})^3(1+\bar{u}_x)^2 \\
B &= 0 \\
C &= -x^2(x+\bar{u})^3(1+\bar{u}_x)^5 + \frac{1}{1-2\nu} x^2(x+\bar{u})^3(1+\bar{u}_x)^3 - \\
&\quad \left( \frac{1}{1-2\nu} \right) x^3(x+\bar{u})^2(1+\bar{u}_x)^4 + x(x+\bar{u})^4(1+\bar{u}_x)^4 \\
D &= 0 \\
E &= x(1+\bar{u}_x)^3 \\
F &= -(1+\bar{u}_x)^3 \bar{w}_x
\end{aligned} \tag{3.54}$$

$$\begin{aligned}
\bar{\tau}^{11} &= \frac{\tau^{11}}{\mu} = \frac{x(1+\bar{u}_x)}{(x+\bar{u})} + 2 \frac{\nu}{1-2\nu} - \frac{1}{1-2\nu} \frac{x}{(x+\bar{u})(1+\bar{u}_x)} \\
\bar{\tau}^{13} &= \frac{\tau^{13}}{\mu} = \frac{x}{(x+\bar{u})} \bar{w}_x \\
\bar{\tau}^{22} &= r^2 \frac{\tau^{22}}{\mu} = \frac{(x+\bar{u})}{x(1+\bar{u}_x)} + 2 \frac{\nu}{1-2\nu} - \frac{1}{1-2\nu} \frac{x}{(x+\bar{u})(1+\bar{u}_x)} \\
\bar{\tau}^{33} &= \frac{\tau^{33}}{\mu} = \frac{x}{(x+\bar{u})(1+\bar{u}_x)} + \frac{x\bar{w}_x^2}{(x+\bar{u})(1+\bar{u}_x)} + \\
&\quad 2 \frac{\nu}{1-2\nu} - \frac{1}{1-2\nu} \frac{x}{(x+\bar{u})(1+\bar{u}_x)}
\end{aligned} \tag{3.55}$$

The equilibrium equations are linear in the second derivatives but highly non-linear in  $\bar{u}$ ,  $\bar{u}_x$ , and  $\bar{w}_x$ , and no closed form solution of the system seems possible. Using the substitutions

$$\begin{aligned}
\bar{u} &= y_1 & \bar{u}_x &= y_3 & \bar{u}_{xx} &= y_3' \\
\bar{w} &= y_2 & \bar{w}_x &= y_4 & \bar{w}_{xx} &= y_4'
\end{aligned} \tag{3.56}$$

the order of the equations are reduced to one, and the number of the equations is increased to four. These are

$$\begin{aligned}
y_1' &= g_1(y_3) \\
y_2' &= g_2(y_4) \\
y_3' &= g_3(x, y_1, y_3, y_4) \\
y_4' &= g_4(x, y_1, y_3, y_4)
\end{aligned} \tag{3.57}$$

where

$$\begin{aligned}g_1 &= y_3 \\g_2 &= y_4 \\g_3 &= \frac{CE - FB}{AE - BD} \\g_4 &= \frac{CD - AF}{BD - AE}\end{aligned}\tag{3.58}$$

which are in a form suitable for numerical solution.

As for the boundary conditions, the inner surface of the tube is assumed to be bonded to the outer surface of a rigid shaft, therefore displacements in the radial, and in the axial directions are zero at the inner surface of the tube. The outer surface is under uniform axial shear only. These conditions are expressed mathematically as

$$\begin{aligned}u(R_1) &= 0 \\w(R_1) &= 0 \\ \tau^{11}(R_2) &= 0 \\ \tau^{13}(R_2) &= \tau_0\end{aligned}\tag{3.59}$$

If the boundary conditions are non-dimensionalized also using the transformations given in Appendix A, equations (3.59) become



$$\begin{aligned}
\bar{u}(x-1) &= 0 \\
\bar{w}(x-1) &= 0 \\
\bar{\tau}^{11}(x-\lambda) &= 0 \\
\bar{\tau}^{13}(x-\lambda) &= \bar{\tau}_0
\end{aligned}
\tag{3.60}$$

where

$$\lambda = \frac{R_2}{R_1}
\tag{3.61}$$

Dimensionless outer axial shear in equation (3.60) is defined as

$$\bar{\tau}_0 = \frac{\tau_0}{\mu}
\tag{3.62}$$

### 3.3.2. Compressible, Hyperelastic Spinning Tubes Subjected to Circumferential Shear

In this problem the spin term is non-dimensionalized as

$$\bar{\Omega}^2 = \rho_0 \frac{R_1 \Omega^2}{\mu}
\tag{3.63}$$

And the variables of equation (3.49) and the dimensionless stress

equations are obtained as follows

#### A. Polynomial Material

$$\begin{aligned}
 A &= f \frac{x}{(x+\bar{u})} + (2f + \frac{4\nu-1}{1-2\nu}) \frac{(x+\bar{u})}{x} + 3(1-f) \frac{x(1+x^2\bar{\phi}_x^2)}{(x+\bar{u})(1+\bar{u}_x)^4} \\
 B &= -2(1-f) \frac{x^3\bar{\phi}_x}{(x+\bar{u})(1+\bar{u}_x)^3} \\
 C &= (2f + \frac{4\nu-1}{1-2\nu}) (\frac{(1+\bar{u}_x)(x+\bar{u})}{x^2} - \frac{(1+\bar{u}_x)^2}{x}) - f \frac{(1+\bar{u}_x)}{(x+\bar{u})} + \frac{f}{x} + \\
 &\quad fx\bar{\phi}_x^2 + (1-f) (\frac{1+3x^2\bar{\phi}_x^2}{(x+\bar{u})(1+\bar{u}_x)^3} - \frac{x^3}{(x+\bar{u})^4}) - \bar{\Omega}^2 x \\
 D &= -2(1-f) \frac{x^3\bar{\phi}_x}{(x+\bar{u})^3(1+\bar{u}_x)^4} \\
 E &= f \frac{x}{(x+\bar{u})(1+\bar{u}_x)} + (1-f) \frac{x^3}{(x+\bar{u})^3(1+\bar{u}_x)^3} \\
 F &= -f (\frac{\bar{\phi}_x}{(x+\bar{u})(1+\bar{u}_x)} + \frac{2x\bar{\phi}_x}{(x+\bar{u})^2}) - (1-f) \frac{3x^2\bar{\phi}_x}{(x+\bar{u})^3(1+\bar{u}_x)^3}
 \end{aligned} \tag{3.64}$$

$$\begin{aligned}
\bar{\tau}^{11} &= \frac{\tau^{11}}{\mu} = 1 - 2f + f \frac{x(1+\bar{u}_x)}{(x+\bar{u})} + (2f + \frac{4\nu-1}{1-2\nu}) \left( \frac{(x+\bar{u})(1+\bar{u}_x)}{x} - 1 \right) - \\
&\quad (1-f) \frac{x+x^3\bar{\phi}_x^2}{(x+\bar{u})(1+\bar{u}_x)^3} \\
\bar{\tau}^{12} &= \frac{\tau^{12}}{\mu} = fx\bar{\phi}_x + (1-f) \frac{x^3\bar{\phi}_x}{(x+\bar{u})^2(1+\bar{u}_x)^2} \\
\bar{\tau}^{22} &= \tau^{22} \frac{(R+u)^2}{\mu} = 1 - 2f + f \frac{(x+\bar{u})}{x(1+\bar{u}_x)} + f \frac{x(x+\bar{u})\bar{\phi}_x^2}{(1+\bar{u}_x)} - \\
&\quad (1-f) \frac{x^3}{(x+\bar{u})^3(1+\bar{u}_x)} + (2f + \frac{4\nu-1}{1-2\nu}) \left( \frac{(1+\bar{u}_x)(x+\bar{u}_x)}{x} - 1 \right) \\
\bar{\tau}^{33} &= \frac{\tau^{33}}{\mu} = (1-2f) \left( 1 - \frac{x}{(x+\bar{u})(1+\bar{u}_x)} \right) + \\
&\quad \left( 2f + \frac{4\nu-1}{1-2\nu} \right) \left( \frac{(x+\bar{u})(1+\bar{u}_x)}{x} - 1 \right) - (1-f) \frac{x^3\bar{\phi}_x^2}{(x+\bar{u})(1+\bar{u}_x)}
\end{aligned} \tag{3.65}$$

B. Blatz-Ko Material

$$\begin{aligned}
 A &= f \frac{x}{(x+\bar{u})} + 3(1-f) \frac{x(1+x^2\bar{\phi}_x^2)}{(x+\bar{u})(1+\bar{u}_x)^4} + \\
 &\quad \left( \frac{x}{(x+\bar{u})(1+\bar{u}_x)^2} \right) \left[ f \frac{1}{1-2\nu} \left( \frac{x}{(x+\bar{u})(1+\bar{u}_x)} \right)^{\frac{2\nu}{1-2\nu}} - \right. \\
 &\quad \left. (1-f) \frac{1-4\nu}{1-2\nu} \left( \frac{x}{(x+\bar{u})(1+\bar{u}_x)} \right)^{\frac{-2\nu}{1-2\nu}} \right] \\
 B &= -2(1-f) \frac{x^3\bar{\phi}_x}{(x+\bar{u})(1+\bar{u}_x)^3} \\
 C &= -f \frac{(1+\bar{u}_x)}{(x+\bar{u})} + \frac{f}{x} + f x \bar{\phi}_x^2 + (1-f) \left( \frac{1+3x^2\bar{\phi}_x^2}{(x+\bar{u})(1+\bar{u}_x)^3} - \frac{x^3}{(x+\bar{u})^4} \right) - \bar{\Omega}^2 x + \\
 &\quad \left( \frac{1}{(x+\bar{u})(1+\bar{u}_x)} - \frac{x}{(x+\bar{u})^2} \right) \left[ f \frac{1}{1-2\nu} \left( \frac{x}{(x+\bar{u})(1+\bar{u}_x)} \right)^{\frac{2\nu}{1-2\nu}} - \right. \\
 &\quad \left. (1-f) \frac{1-4\nu}{1-2\nu} \left( \frac{x}{(x+\bar{u})(1+\bar{u}_x)} \right)^{\frac{-2\nu}{1-2\nu}} \right] \\
 D &= -2(1-f) \frac{x^3\bar{\phi}_x}{(x+\bar{u})^3(1+\bar{u}_x)^4} \\
 E &= f \frac{x}{(x+\bar{u})(1+\bar{u}_x)} + (1-f) \frac{x^3}{(x+\bar{u})^3(1+\bar{u}_x)^3} \\
 F &= -f \left( \frac{\bar{\phi}_x}{(x+\bar{u})(1+\bar{u}_x)} + \frac{2x\bar{\phi}_x}{(x+\bar{u})^2} \right) - (1-f) \frac{3x^2\bar{\phi}_x}{(x+\bar{u})^3(1+\bar{u}_x)^3}
 \end{aligned}
 \tag{3.66}$$

$$\begin{aligned}
\bar{\tau}^{11} &= \frac{\tau^{11}}{\mu} = f \frac{x(1+\bar{u}_x)}{(x+\bar{u})} - (1-f) \frac{x+x^3\bar{\phi}_x^{-2}}{(x+\bar{u})(1+\bar{u}_x)} - \\
&\quad f \left\{ \frac{x}{(x+\bar{u})(1+\bar{u}_x)} \right\}^{\frac{1}{1-2v}} + (1-f) \left\{ \frac{x}{(x+\bar{u})(1+\bar{u}_x)} \right\}^{\frac{1-4v}{1-2v}} \\
\bar{\tau}^{12} &= \frac{\tau^{12}}{\mu} = fx\bar{\phi}_x + (1-f) \frac{x^3\bar{\phi}_x}{(x+\bar{u})^2(1+\bar{u}_x)^2} \\
\bar{\tau}^{22} &= \tau^{22} \frac{(R+u)^2}{\mu} = f \frac{(x+\bar{u})}{x(1+\bar{u}_x)} + f \frac{x(x+\bar{u})\bar{\phi}_x^{-2}}{(1+\bar{u}_x)} - (1-f) \frac{x^3}{(x+\bar{u})^3(1+\bar{u}_x)} + \\
&\quad f \left\{ \frac{x}{(1+\bar{u}_x)(x+\bar{u}_x)} \right\}^{\frac{1}{1-2v}} + (1-f) \left\{ \frac{x}{(x+\bar{u})(1+\bar{u}_x)} \right\}^{\frac{1-4v}{1-2v}} \\
\bar{\tau}^{33} &= \frac{\tau^{33}}{\mu} = f \frac{x}{(x+\bar{u})(1+\bar{u}_x)} - (1-f) \left( \frac{x}{(x+\bar{u})(1+\bar{u}_x)} + \frac{x^3\bar{\phi}_x^{-2}}{(x+\bar{u})(1+\bar{u}_x)} \right) - \\
&\quad f \left\{ \frac{x}{(x+\bar{u})(1+\bar{u}_x)} \right\}^{\frac{1}{1-2v}} + (1-f) \left\{ \frac{x}{(x+\bar{u})(1+\bar{u}_x)} \right\}^{\frac{1-4v}{1-2v}}
\end{aligned}$$

(3.67)

C. Blatz

$$\begin{aligned}
 A &= \frac{x}{(x+\bar{u})} + \frac{1}{1-2\nu} \frac{x}{(x+\bar{u})(1+\bar{u}_x)^2} \\
 B &= 0 \\
 C &= -\frac{(1+\bar{u}_x)}{(x+\bar{u})} + \frac{1}{x} + x\bar{\phi}_x^2 + \frac{1}{1-2\nu} \left( \frac{1}{(x+\bar{u})(1+\bar{u}_x)} - \frac{x}{(x+\bar{u})^2} \right) - \\
 &\quad x\bar{\Omega}^2 \\
 D &= 0 \\
 E &= \frac{x}{(x+\bar{u})(1+\bar{u}_x)} \\
 F &= -\frac{\bar{\phi}_x}{(x+\bar{u})(1+\bar{u}_x)} + \frac{2x\bar{\phi}_x}{(x+\bar{u})^2}
 \end{aligned} \tag{3.68}$$

$$\begin{aligned}
 \bar{\tau}^{11} &= \frac{\tau^{11}}{\mu} = \frac{x(1+\bar{u}_x)}{(x+\bar{u})} + 2\frac{\nu}{1-2\nu} - \frac{1}{1-2\nu} \frac{x}{(x+\bar{u})(1+\bar{u}_x)} \\
 \bar{\tau}^{12} &= \frac{\tau^{12}}{\mu} = x\bar{\phi}_x \\
 \bar{\tau}^{22} &= \frac{\tau^{22}(R+u)^2}{\mu} = \frac{(x+\bar{u})}{x(1+\bar{u}_x)} + \frac{x(x+\bar{u})\bar{\phi}_x^2}{(1+\bar{u}_x)} + \\
 &\quad 2\frac{\nu}{1-2\nu} - \frac{1}{1-2\nu} \frac{x}{(1+\bar{u}_x)(x+\bar{u})} \\
 \bar{\tau}^{33} &= \frac{\tau^{33}}{\mu} = -2\frac{\nu}{1-2\nu} \frac{x}{(x+\bar{u})(1+\bar{u}_x)} + 2\frac{\nu}{1-2\nu}
 \end{aligned} \tag{3.69}$$

The dimensionless equilibrium equations are linear in the second derivatives, but highly non-linear in  $\bar{u}$ ,  $\bar{u}_x$ , and  $\bar{\theta}_x$ , and no closed form solution

seems possible. Using the substitutions

$$\begin{aligned} \bar{u} &= y_1 & \bar{u}_x &= y_3 & \bar{u}_{xx} &= y_3' \\ \bar{\phi} &= y_2 & \bar{\phi}_x &= y_4 & \bar{\phi}_{xx} &= y_4' \end{aligned} \quad (3.70)$$

the equilibrium equations are converted to four first order, ordinary, non-linear differential equations. These are

$$\begin{aligned} y_1' &= g_1(y_3) \\ y_2' &= g_2(y_4) \\ y_3' &= g_3(x, y_1, y_3, y_4) \\ y_4' &= g_4(x, y_1, y_3, y_4) \end{aligned} \quad (3.71)$$

where

$$\begin{aligned} g_1 &= y_3 \\ g_2 &= y_4 \\ g_3 &= \frac{CE - FB}{AE - BD} \\ g_4 &= \frac{CD - AF}{BD - AE} \end{aligned} \quad (3.72)$$

which are in the suitable form for numerical solution.

As for the boundary conditions the inner surface of the tube is assumed to be perfectly bonded to the outer surface of a rigid shaft, and the outer curved surface is subjected to uniformly distributed circumferential shearing tractions  $\tau_0$ . These conditions are mathematically expressed as

$$\begin{aligned}
u(R_1) &= 0 \\
\phi(R_1) &= 0 \\
\tau^{11}(R_2) &= 0 \\
\tau^{12}(R_2) &= \tau_0
\end{aligned}
\tag{3.73}$$

If the boundary conditions are non-dimensionalized, also, using the transformations given in Appendix A, equation (3.73) become,

$$\begin{aligned}
\bar{u}(x-1) &= 0 \\
\bar{\phi}(x-1) &= 0 \\
\bar{\tau}^{11}(x-\lambda) &= 0 \\
\bar{\tau}^{12}(x-\lambda) &= \bar{\tau}_0
\end{aligned}
\tag{3.74}$$

where the dimensionless outer axial shear is defined as

$$\bar{\tau}_0 = (R_2 + u(R_2)) \frac{\tau_0}{\mu}
\tag{3.75}$$

### 3.3.3 Finite Circumferential Shearing of Compressible Hyperelastic

Tube

For this problem the non-dimensional equilibrium equations, are obtained by taking  $\Omega$  equal to zero in the non-dimensional equilibrium equations of section 3.3.2, and the dimensionless stress equations are equal



to dimensionless stresses given in 3.3.2. Similarly the boundary conditions are the same as given in section 3.3.2.



CHAPTER IV  
METHOD OF ADJOINTS AND THE NUMERICAL SOLUTION  
OF THE PROBLEMS

4.1 Method of Adjoint

In this section, the way how the method of adjoints for linear problems can be applied in an iterative fashion to solve non-linear problems is given. The material of this section is a brief summary of the relevant topic covered in [23].

Boundary value problems are not very suitable for the numerical analysis done by computer. To make it suitable, the boundary value problem is transformed to an initial value problem. The shooting methods are developed for this transformation. Method of adjoints is one of the shooting methods, and is suitable for the solution of boundary value problems.

Now, consider the set of non-linear ordinary differential equations

$$y_i' = g_i(y_1, y_2, \dots, y_n, x) \quad i = 1, 2, \dots, n \quad (4.1)$$

with the initial conditions

$$y_i(x_0) = c_i \quad i = 1, 2, \dots, r \quad (4.2)$$

and the terminal conditions

$$y_{i_m}(x_p) = c_{i_m} \quad m = 1, 2, \dots, n - r \quad (4.3)$$

If  $y_i(x)$ ,  $i=1,2,\dots,n$  ;  $x_0 \leq x \leq x_p$ , is the solution of equation (4.1), let us consider a nearby solution,  $y_i(x) + \delta y_i(x)$ , where  $\delta y_i(x)$  is often called the variation, a first order correction to  $y_i(x)$ .  $y_i(x)$  may be thought of as solutions corresponding to guessed values of the missing initial conditions, and  $\delta y_i(x)$  as corrections necessary to produce the actual solution of the boundary value problem.

If equation (4.1) is subtracted from the differential equations of the nearby equations, it is obtained

$$\delta y_i'(x) - \sum_{j=1}^n \frac{\partial g_i}{\partial y_j} \delta y_j(x) \quad i = 1, 2, \dots, n \quad (4.4)$$

These equations are linear ordinary differential equations with variable coefficients, and are called the variational equations.

The equations which are adjoint to the variational equations can be formed as

$$f'_i(x) = - \sum_{j=1}^n \frac{\partial g_i}{\partial y_j} f_j(x) \quad i = 1, 2, \dots, n \quad (4.5)$$

The matrix of coefficients of the adjoint equations is the negative transpose of the matrix of coefficients in equation (4.4). The adjoint equations are again linear ordinary differential equations in  $f_i$ ,  $i=1, 2, \dots, n$ .

The fundamental identity of the method of adjoints for the linear ordinary differential equations  $\delta y_i'(x)$  in equation (4.4), and the adjoint equations  $f'_i(x)$  in equation (4.5) is reduced to

$$\sum_{i=1}^n f_i(x_p) \delta y_i(x_p) - \sum_{i=1}^n f_i(x_0) \delta y_i(x_0) = 0 \quad (4.6)$$

The variation  $\delta y_i(x)$  is the difference between the true, but unknown profile and the calculated profile; that is

$$\delta y_i(x) = (y_i)_{true}(x) - (y_i)_{calc}(x) \quad i = 1, 2, \dots, n \quad x_0 \leq x \leq x_f \quad (4.7)$$

but, since  $\delta y_i(x)$  are only the approximate systems, the process of finding the true profiles will be an iterative process which terminates when  $\delta y_i(x)$ ,  $i=1, 2, \dots, n$ ;  $x_0 \leq x \leq x_f$ , are sufficiently small.

The fundamental identity given by equation (4.6) can be used to find the corrections  $\delta y_i(x_0)$ ,  $i=r+1, \dots, n$  to the set of missing initial conditions  $y_i(x_0)$ ,  $i=r+1, \dots, n$ . The Kronecker delta is assigned as the terminal conditions for the adjoints variables  $f_i(x_f)$ :

$$f_i^{(m)}(x_f) = \begin{cases} 1 & \text{for } i = i_m \\ 0 & \text{for } i \neq i_m \end{cases} \quad m = 1, 2, \dots, n-r \quad (4.8)$$

where  $f_i^{(m)}(x_f)$  = the terminal conditions for the  $m^{\text{th}}$  backward integration of the adjoint equations,

$i_m$  = the set of indices specified in equation (4.3);

and the adjoint equations are integrated backward.

The fundamental identity for the  $(n-r)$  backward integrations of the adjoint equations provides a set of  $(n-r)$  linear algebraic equations in the  $(n-r)$  unknowns  $\delta y_i^{(k)}(x_0)$ . In order to integrate the adjoint equations the partial derivatives  $\partial g_j / \partial y_j$ ,  $i, j=1, 2, \dots, n$  must be developed analytically. To evaluate

numerically these analytical partial derivatives requires assuming trial values for the missing initial conditions  $y_i(x_0)$ ,  $i=r+1, r+2, \dots, n$ . Once the  $y_i(x)$ ,  $i=1, 2, \dots, n$  profiles are known, the partial derivatives can be evaluated.

For the next iteration through the process the new initial conditions are found from

$$\begin{aligned} y_i^{(k+1)}(x_0) &= y_i(x_0) - c_i & i &= 1, 2, \dots, r \\ y_i^{(k+1)}(x_0) &= y_i^{(k)} + \delta y_i^{(k)}(x_0) & i &= r+1, \dots, n-r \end{aligned} \quad (4.9)$$

If there are explicit boundary conditions at one boundary, and implicit boundary conditions at the other

$$q_i = y_i(x_0) - c_i = 0 \quad i = 1, 2, \dots, r \quad (4.10)$$

$$q_{r+i}(y_1(x_p), y_2(x_p), \dots, y_n(x_p)) = 0 \quad i = 1, 2, \dots, n-r \quad (4.11)$$

Since the first  $r$  initial conditions are specified in equation (4.10), trial values need be assumed only for  $y_{r+i}(x_0)$ ,  $i=1, 2, \dots, n-r$ . The adjoint equations (4.5) are integrated backward once for each  $y_j(x_p)$  that appears in equation (4.11), and the fundamental identity gives

$$\sum_{i=r+1}^n f_i^{(j)}(x_0) \delta y_i(x_0) = \delta y_j(x_p) \quad j = 1, 2, \dots, n \quad (4.12)$$

Since  $\delta y_i(x_0) = 0$ ,  $i = 1, 2, \dots, r$  by virtue of equation (4.10) the summation in equation (4.12) is taken over  $i = r+1, \dots, n$ .

For the terminal conditions the variation is written as

$$\delta q_{r+i} = \sum_{j=1}^n \frac{\partial q_{r+i}}{\partial y_j(x_p)} \delta y_j(x_p) \quad i = 1, 2, \dots, n-r \quad (4.13)$$

Substitution of equation (4.12) in the variation of equation (4.11) which is given by equation (4.13) yields

$$\delta q_{r+i} = \sum_{j=1}^n \frac{\partial q_{r+i}}{\partial y_j(x_p)} \delta y_j(x_p) \left\{ \sum_{p=r+1}^n f_p^{(j)}(x_0) \delta y_p(x_0) \right\} \quad i = 1, 2, \dots, n-r \quad (4.14)$$

$$\text{If } \delta q_i = (q_i)_{\text{true}} - (q_i)_{\text{calc}} \quad i = 1, 2, \dots, n$$

since  $(q_i)_{\text{true}} = 0$  it follows that  $\delta q_i = - (q_i)_{\text{calc}} \quad i = 1, 2, \dots, n$ .

The expression given in equation (4.14) is a set of  $(n-r)$  equations in  $(n-r)$  unknowns  $\delta y_{r+i}(x_0)$ ,  $i = 1, 2, \dots, n-r$ .

To recapitulate, the non-linear two-point boundary value problem with explicit and implicit boundary conditions is solved by the following procedure:

1. Determine analytically the partial derivatives  $\partial q_i / \partial y_j$   $i, j = 1, 2, \dots, n$  from equation (4.1).

2. Determine analytically the partial derivatives  $\partial q_{r+i} / \partial y_j(x_f)$   $i = 1, 2, \dots, n-r$   $j = 1, 2, \dots, n$  from equation (4.11).

3. Initialize the counter on the iterative process. Set  $k=0$ .

4. For  $k=0$  guess the missing initial conditions

$$y_i^{(0)}(x_0) = c_i^{(0)} \quad i = 1, 2, \dots, n$$

5. Integrate equation (4.1) using the specified, and the guessed initial conditions, and store the profiles.

6. Using the calculated terminal values  $y_j^{(k)}(x_f)$   $j = 1, 2, \dots, n$  evaluate  $q_{r+i}(x_f)$   $i = 1, 2, \dots, n-r$ .



7. Set  $\delta q_{r+i} = -q_{r+i}(x_f)$   $i=1,2,\dots,n-r$ .

8. Integrate the adjoint equations backward using the Kronecker delta terminal conditions, equation (4.8). Save  $f_i^{(0)}(x_0)$   $i,j=1,2,\dots,n$

9. On the basis of the item 2, and the profiles in item 5 evaluate numerically the partial derivative  $\partial g_{r+i}/\partial y_j(x_f)$ , and form the matrix of coefficients.

10. Solve  $\delta y_{r+i}(x_0)$   $i=1,2,\dots,n-r$

11. If  $\max(\delta q_{r+i} \ i=1,2,\dots,n-r)$  is less than a specified tolerance terminate the calculation, otherwise go to item 12.

12. Form the next set of trial initial conditions

$$y_{r+i}(x_0) = y_{r+i}^{(k)}(x_0) + \delta y_{r+i}^{(k)}(x_0) \quad i=1,2,\dots,n-r$$

13. Set  $k = k + 1$ . Return item 5.

## 4.2 Numerical Solution of the Problems

In the previous chapter, the governing differential equations, and the associated boundary conditions of three problems were obtained. The governing differential equations are

$$\begin{aligned}y_1' &= g_1(y_3) \\y_2' &= g_2(y_4) \\y_3' &= g_3(x, y_1, y_3, y_4) \\y_4' &= g_4(x, y_1, y_3, y_4)\end{aligned}\tag{4.15}$$

where  $x$  is defined in the interval  $1 \leq x \leq \lambda$ . The boundary conditions can be expressed as

$$\begin{aligned}y_1|_{x=1} &= 0 \\y_2|_{x=1} &= 0 \\q_3|_{x=\lambda} &= 0 \\q_4|_{x=\lambda} &= 0\end{aligned}\tag{4.16}$$

where the boundary conditions at  $x = 1$  are of explicit type, and the ones at  $x = \lambda$  are of implicit type.

### 4.2.1 Implicit Boundary Conditions

#### 4.2.1.1 Anti-Plane Shear

##### A. Polynomial Material

$$q_3 = f \frac{\lambda(1+y_3)}{\lambda+y_1} + (f-1) \frac{\lambda(1+y_4^2)}{(\lambda+y_1)(1+y_3)^3} +$$

$$\left(2f + \frac{4\nu-1}{1-2\nu}\right) \frac{(\lambda+y_1)(1+y_3)}{\lambda} + \left(1-4f - \frac{4\nu-1}{1-2\nu}\right) = 0 \quad (4.17)$$

$$q_4 = f \frac{\lambda}{(\lambda+y_1)} y_4 + (1-f) \frac{\lambda}{(\lambda+y_1)(1+y_3)^2} y_4 - \bar{\tau}_0 = 0$$

##### B. Blatz-Ko Material

$$q_3 = f \frac{\lambda(1+y_3)}{\lambda+y_1} + (f-1) \frac{\lambda(1+y_4^2)}{(\lambda+y_1)(1+y_3)^3} -$$

$$f \left\{ \frac{\lambda}{(\lambda+y_1)(1+y_3)} \right\}^{\frac{1}{1-2\nu}} + (1-f) \left\{ \frac{\lambda}{(\lambda+y_1)(1+y_3)} \right\}^{\frac{1-4\nu}{1-2\nu}} = 0 \quad (4.18)$$

$$q_4 = f \frac{\lambda}{(\lambda+y_1)} y_4 + (1-f) \frac{\lambda}{(\lambda+y_1)(1+y_3)^2} y_4 - \bar{\tau}_0 = 0$$

### C. Blatz Material

$$q_3 = \frac{\lambda(1+y_3)}{\lambda+y_1} + \frac{2\nu}{1-2\nu} - \frac{1}{1-2\nu} \frac{\lambda}{(\lambda+y_1)(1+y_3)} = 0$$

$$q_4 = \frac{\lambda}{(\lambda+y_1)} y_4 - \bar{\tau}_0 = 0 \quad (4.19)$$

#### 4.2.1.2 Constant Spin and Circumferential Shear

##### A. Polynomial Material

$$q_3 = f \frac{\lambda(1+y_3)}{\lambda+y_1} + (f-1) \frac{\lambda(1+\lambda^2 y_4^2)}{(\lambda+y_1)(1+y_3)^3} +$$

$$\left(2f + \frac{4\nu-1}{1-2\nu}\right) \left(\frac{(\lambda+y_1)(1+y_3)}{\lambda} - 1\right) + 1 - 2f = 0 \quad (4.20)$$

$$q_4 = f\lambda y_4 + (1-f) \frac{\lambda^3}{(\lambda+y_1)^2(1+y_3)^2} y_4 - \bar{\tau}_0 = 0$$

### B. Blatz-Ko Material

$$q_3 = f \frac{\lambda(1+y_3)}{\lambda+y_1} + (f-1) \frac{\lambda(1+\lambda^2 y_4^2)}{(\lambda+y_1)(1+y_3)^3} -$$

$$f \left\{ \frac{\lambda}{(\lambda+y_1)(1+y_3)} \right\}^{\frac{1}{1-2\nu}} + (1-f) \left\{ \frac{\lambda}{(\lambda+y_1)(1+y_3)} \right\}^{\frac{1-4\nu}{1-2\nu}} - 0 \quad (4.21)$$

$$q_4 = f\lambda y_4 + (1-f) \frac{\lambda^3}{(\lambda+y_1)^2(1+y_3)^2} y_4 - \bar{\tau}_0 = 0$$

### C. Blatz Material

$$q_3 = \frac{\lambda(1+y_3)}{\lambda+y_1} + \frac{2\nu}{1-2\nu} - \frac{1}{1-2\nu} \frac{\lambda}{(\lambda+y_1)(1+y_3)} = 0 \quad (4.22)$$

$$q_4 = \lambda y_4 - \bar{\tau}_0 = 0$$

#### 4.2.1.3 Circumferential Shear

The boundary conditions of the constant spin and circumferential shear problem are also valid for this problem.

In equations (4.17)-(4.22),  $y_1$ ,  $y_3$ , and  $y_4$  denote the values of these

variables evaluated at  $x = \lambda$ .

Equations (4.15) together with the boundary conditions (4.16) can be solved numerically by the method of adjoints [23] which is briefly discussed in section 4.1. Numerical integrations mentioned in method of adjoints are carried out with fourth order Runge-Kutta integration formulas [24] with equal spacing between pivotal points in the interval  $1 \leq x \leq \lambda$ . For a function  $g(x,y)$ , fourth order Runge-Kutta algorithm is given by

$$y_{i+1} = y_i + \frac{1}{6}(k_1 + 2k_2 + 2k_3 + k_4) \quad (4.23)$$

where

$$\begin{aligned} k_1 &= hg(x_i, y_i) \\ k_2 &= hg\left(x_i + \frac{h}{2}, y_i + \frac{1}{2}k_1\right) \\ k_3 &= hg\left(x_i + \frac{h}{2}, y_i + \frac{1}{2}k_2\right) \\ k_4 &= hg(x_i + h, y_i + k_3) \end{aligned} \quad (4.24)$$

$h$  is the distance between the two pivotal points.

### 4.3 Computational Procedure

In order to solve the system of non-linear equations (4.15) subjected to boundary conditions (4.16), using the method of adjoints, a computer program is developed. All computations reported in this work were carried out on PC's with 16 digits. The typical computer program for one type, and one model problem is given in Appendix B. The general computer program is given in a 5¼ floppy disk with a user manual given in Appendix B.



## CHAPTER V

### DISCUSSION

In this work, the static behaviours of hollow, circular cylindrical shells made of three different compressible, hyperelastic material models under three different types of loading are investigated using the theory of finite elasticity. Explicit results, obtained by applying the method of adjoints to the non-linear differential equations are discussed in this chapter.

The variations of the stress components, and the displacement fields with the surface traction  $\tau_0$ , constant spin speed  $\Omega$ , radii ratio  $\lambda$ , and the material constants  $f$  and  $\nu$  are obtained by considering several examples. In all the examples considered, 21 pivotal points along the radial direction are used to obtain sufficient accuracy in the numerical integration of the first order differential equations. The figure in which no model is indicated is valid for all models. Unless the otherwise stated, the radii ratio  $\lambda$  is taken as 1.25 in the figures.



Figures 5.1 to 5.16 show the results of anti-plane shear problem. The figures 5.17 to 5.28 show the results of constant spin and circumferential shear problem. Figures 5.29 to 5.42 show the results of uniform circumferential shear problem.

### 5.1 Finite Anti-Plane Shear of Compressible Hyperelastic Tubes

Figures 5.1 to 5.4 show the variation of the radial displacement, and the stress components with external axial shear as a function of dimensionless radial position  $x$ .  $\bar{u}$ ,  $\bar{\tau}^{11}$ , and  $\bar{\tau}^{22}$  vanish for Blatz model. For the polynomial material model, all of the stress components have a common trend of decreasing from inner boundary towards outer boundary, whereas the displacements increase linearly in the same direction. This trend is also valid for Blatz-Ko model, except for  $\bar{\tau}^{22}$  which increases from inner boundary towards outer boundary. For the primary components, that is for axial displacement  $\bar{w}$ , shear stress  $\bar{\tau}^{13}$ , and axial stress  $\bar{\tau}^{33}$ , all the models give the same results. On the other hand, there are some differences between polynomial material model and Blatz-Ko model for radial displacement  $\bar{u}$ , radial stress  $\bar{\tau}^{11}$ , and hoop stress  $\bar{\tau}^{22}$ , and this components vanish for Blatz model. The differences in  $\bar{\tau}^{11}$ , and  $\bar{\tau}^{22}$  decrease from inner boundary towards

outer boundary, whereas the difference in  $\bar{u}$  increases in the same direction.

Figures 5.5 to 5.9 display the variation of displacements at the outer boundary ( $x=\lambda$ ), and the stress components at the inner boundary ( $x=1.0$ ) as a function of  $f$ . In these figures Blatz model is not given, since the effect of  $f$  is not considered in his strain energy density function. When  $f$  approaches unity, radial deformation approaches zero. Figures 5.6 and 5.7 indicate that the axial displacement  $\bar{w}$ , and the shearing stress  $\bar{\tau}^{13}$  are not affected by parameter  $f$ . When  $f$  equal to unity, the strain energy density functions do not depend on the second strain invariant. Numerical studies indicate that the radial surface traction at the inner boundary is affected most significantly by changes in parameter  $f$ .  $\bar{\tau}^{11}$ , and  $\bar{\tau}^{22}$  observed to be larger for smaller  $f$  values. This means that second strain invariant is more pronounced for  $\bar{\tau}^{11}$  and  $\bar{\tau}^{22}$ . Whereas for the axial stress  $\bar{\tau}^{33}$  the opposite is observed. For  $f=1.0$  all of the stress components, and the displacements become independent of  $\nu$  and the material model. Although the trends from  $f=0.7$  to  $f=1.0$  are the same for both polynomial material and Blatz-Ko models, there are significant differences for stress components  $\bar{\tau}^{11}$ ,  $\bar{\tau}^{22}$ , and  $\bar{\tau}^{33}$ . The differences decrease as  $f$  increases. For the displacements the differences become smaller as  $\nu$  increases.

In figures 5.10 to 5.12 the effect of  $\nu$  on the radial displacement, and the stress components displayed. Calculations indicate that, when  $f=1.0$  the value of the material constant  $\nu$ , which is a measure of compressibility, does not affect the displacement and the stress components, and the results are the same for the three models. The trends for  $\tau^{11}$  and  $\tau^{22}$  are same as  $\tau^{13}$  and  $\tau^{33}$  respectively. For the polynomial material model, axial displacement  $w$ , and stresses  $\tau^{11}$  and  $\tau^{13}$  are almost constant. For  $f=0.7$  the radial displacement  $u$  at the outer boundary is seen to decrease as  $\nu$  increase. For the polynomial material model  $\tau^{22}$  and  $\tau^{33}$  at the inner boundary increase as  $\nu$  increases. However for Blatz-Ko model all of the stress components decrease until  $\nu$  reaches to 0.4, and then increase as  $\nu$  increases. This behaviour may find its explanation in the fact that, in Blatz-Ko strain energy density function (see equation (3.18)),  $\nu$  affects third strain invariant as a power number. This power is less than unity when  $\nu$  is smaller than 0.33, and greater than unity when  $\nu$  is larger than 0.33. For  $\nu=0.4$  this power is equal to 2.0. On the other hand, in polynomial strain energy density function (see equation (3.14)),  $\nu$  affects the third strain invariant as a multiple. This multiplier is zero for  $\nu=0.25$  and approaches to infinity as  $\nu$  approaches to 0.5.

The effect of tube thickness  $\lambda$  on radial displacement  $u$ , and stress

components  $\bar{r}^{13}$ ,  $\bar{r}^{22}$ , and  $\bar{r}^{33}$  are plotted in figures 5.13 to 5.16.  $\bar{u}$ ,  $\bar{r}^{11}$ , and  $\bar{r}^{22}$  vanish for Blatz model. It is observed that, the displacements and the stress components increase in a linear fashion with increasing  $R_2/R_1$  ratio, except for the radial displacement  $u$  of the Blatz-Ko model which is almost constant. Similarly, for  $\bar{w}$ ,  $\bar{r}^{13}$ , and  $\bar{r}^{33}$  all of the models give essentially the same results. But, there are some differences for  $\bar{u}$ ,  $\bar{r}^{11}$ , and  $\bar{r}^{22}$ . For  $\bar{r}^{22}$ , polynomial material model gives positive results, and Blatz-Ko model give negative results.

## 5.2 Compressible, Hyperelastic Spinning Tubes Subjected to Circumferential Shear

Figure 5.17 to 5.20 show variation of radial and angular displacements, and radial and hoop stress components with constant spin speed as a function of dimensionless radial position  $x$ . For radial displacement  $\bar{u}$ , polynomial material model and Blatz-Ko model behave similarly, but Blatz-Ko model gives higher results as spin speed  $\bar{\omega}$  increases. For all the models, displacements increase from inner boundary towards outer boundary, and stresses decrease in the same direction. Calculations indicate that angular displacement  $\bar{\phi}$  and shear stress  $\bar{r}^{12}$  are independent from spin speed and

same for all the models. For radial stress  $\tau^{11}$ , all the models give the same result. For hoop stress  $\tau^{22}$ , and the axial stress  $\tau^{33}$  polynomial material model and Blatz-Ko model behave similarly, but Blatz-Ko model gives smaller results as spin speed increases. When shear traction  $\tau_0$  and spin speed  $\Omega$  are equal to 1.0,  $\tau^{11}$  and  $\tau^{33}$  are almost equal to zero along the radial position  $x$ .

Figures 5.21 to 5.23 display the variation of radial displacement  $u$  at the outer boundary ( $x=\lambda$ ), and the stress components  $\tau^{11}$  and  $\tau^{22}$  at the inner boundary ( $x=1.0$ ). Since  $f$  effect is not considered in Blatz strain energy density function this model is not given in these figures. For  $\tau_0=1.0$  and  $\Omega=1.0$ , polynomial material model and Blatz-Ko model give essentially the same results for displacements, and stress components. As mentioned in section 5.1, when  $f=1.0$  the strain energy density functions do not depend on the second strain invariant; decreasing  $f$  indicates increasing  $I_2$ -dependence and decreasing  $I_1$ -dependence.  $u$ ,  $\tau^{22}$ , and  $\tau^{33}$  observed to be larger for smaller  $f$  values. This means that second strain invariant is more pronounced for  $u$ ,  $\tau^{22}$ , and  $\tau^{33}$ . The amount of compressibility plays an important role on the radial displacement profile.  $\tau^{22}$  and  $\tau^{33}$  increase as  $v$  increases for smaller  $f$  values, whereas for the region where  $f$  is nearly equal to one the trend is opposite. Calculations indicate that angular displacement  $\phi$ , radial stress  $\tau^{11}$  and shear stress  $\tau^{12}$  are independent from  $f$  and  $v$ .

In figures 5.24 to 5.26 effect of  $\nu$  on the radial displacement, and the stress components displayed. Similar to the anti-plane shear problem, for  $f=1.0$   $\nu$  which is a measure of compressibility, does not affect the stress components and the displacement fields, and the results are same for all the three models. Again polynomial material model and Blatz-Ko model give essentially the same results for the displacements, and stress components. Calculations show that  $\nu$  effect is rather insignificant for angular displacement  $\phi$ , and radial stress  $\tau^{11}$ . The trend for  $u$ ,  $\tau^{12}$ , and  $\tau^{33}$  is decreasing as  $\nu$  increases, whereas  $\tau^{22}$  increases as  $\nu$  increases.

The variations of displacement fields at the outer boundary, and hoop and shear stresses at the inner boundary as a function of spin speed are presented in figures 5.27 and 5.28 for a tube with  $R_2/R_1=1.25$ ,  $\nu=0.458$ ,  $f=0.7$ , and  $\tau_0=1.0$ . It is observed that shear stress  $\tau^{12}$  is independent from spin speed  $\Omega$ . For  $f = 0.7$  Blatz model does not give results far from other two model. This means that  $f$  is rather insignificant. For spin speed less than 3.0, polynomial material model and Blatz-Ko model give same results for displacement fields. For greater spin Blatz-Ko model give smaller results than the polynomial material model. Hoop stress  $\tau^{22}$  increases almost linearly as spin speed increases. Blatz model gives the smallest results, but these are not very different from the results of other two models.

### 5.3 Finite Circumferential Shearing of Compressible Hyperelastic Tubes

Figures 5.29 to 5.33 represent the variation of displacement fields, and stress components with external circumferential shear as a function of dimensionless radial position  $x$ . For the three models, all the stress components have a common trend of decreasing from inner boundary towards outer boundary, whereas the displacements increase in the same direction. For angular displacement  $\bar{\phi}$ , radial stress  $\bar{\tau}^{11}$ , and shearing stress  $\bar{\tau}^{12}$  all the three models give the same results. For the hoop stress  $\bar{\tau}^{22}$ , which is the dominant stress component for this problem, polynomial material model and Blatz-Ko model give the same results. However Blatz model give high results at the inner boundary as external circumferential shear increases. For the radial displacement  $\bar{u}$  the difference between Blatz model and the other two model increases towards the outer boundary.

Figures 5.34 to 5.36 show the variation of radial displacement at the outer boundary ( $x=\lambda$ ), and shearing and hoop stresses at the inner boundary ( $x=1.0$ ) as a function of  $f$ . In these figures Blatz model is not given, because  $f$  effect is not considered in Blatz strain energy density function. Numerical results indicate that angular displacement  $\bar{\phi}$ , radial stress  $\bar{\tau}^{11}$ , and shearing stress  $\bar{\tau}^{12}$  are not significantly affected by the material constant  $f$ .

The only significant effect of material constant  $f$  is on hoop stress  $\tau^{22}$  which decreases with decreasing  $f$ . For  $\tau_0=1.0$ , polynomial material model, and Blatz-Ko model give essentially the same results for the displacements and stress components.

In figures 5.37 to 5.39 effect of  $\nu$  on the radial, and stress components displayed. Calculations show that the angular displacement  $\phi$ , and radial stress  $\tau^{11}$  are not significantly affected by Poisson's ratio  $\nu$ . The radial displacement  $u$  shows a  $\nu$ -dependent behaviour. When  $\nu$  approaches to 0.5, which means that material become more incompressible,  $u$  approaches to zero for all  $f$ . Figure 5.37 together with figure 5.34 show that for a specified value of  $\nu$ ,  $u$  is positive for small  $f$ , it decreases with increasing value of  $f$  and becomes negative for  $f$  greater than 0.91. The circumferential shear stress  $\tau^{12}$  is seen to be little affected by a change in either  $f$  or  $\nu$ . Figure 5.39 shows that for  $f=1.0$  hoop stress  $\tau^{22}$  decreases sharply with increasing  $\nu$ , and for  $f=0.7$  it is less affected by a change in  $\nu$ . Only for  $f=1.0$ , as  $\nu$  decreases there become some differences between the three models in hoop stress  $\tau^{22}$ ; polynomial material model gives the highest values. In other stress components and displacements, for all  $f$  and  $\nu$  values, the results are essentially the same.



Figures 5.40 to 5.42 display the variation of displacements at the outer boundary ( $x=\lambda$ ), and stress components at the inner boundary ( $x=1.0$ ) as a function of applied surface traction. Since in these figures  $f$  is taken as 0.8, Blatz model is not given. Figure 5.40 shows that the radial displacement is very small compared to angular displacement. Angular displacement increases linearly with increasing applied surface traction. Figures 5.41 and 5.42 shows that stress components, also, increase with increasing surface traction. Radial and axial stresses are compressive stresses, and hoop and circumferential shearing stresses are tensile stresses. There is no any significant difference between polynomial material model and Blatz-Ko model.

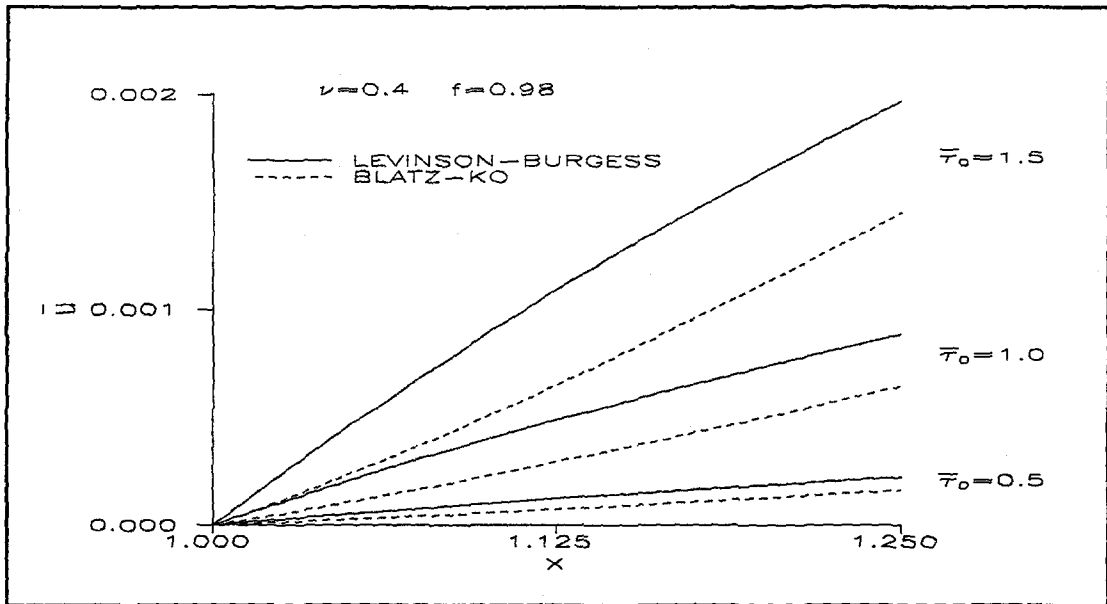


Figure 5.1. Dimensionless Radial Position vs. Dimensionless Radial

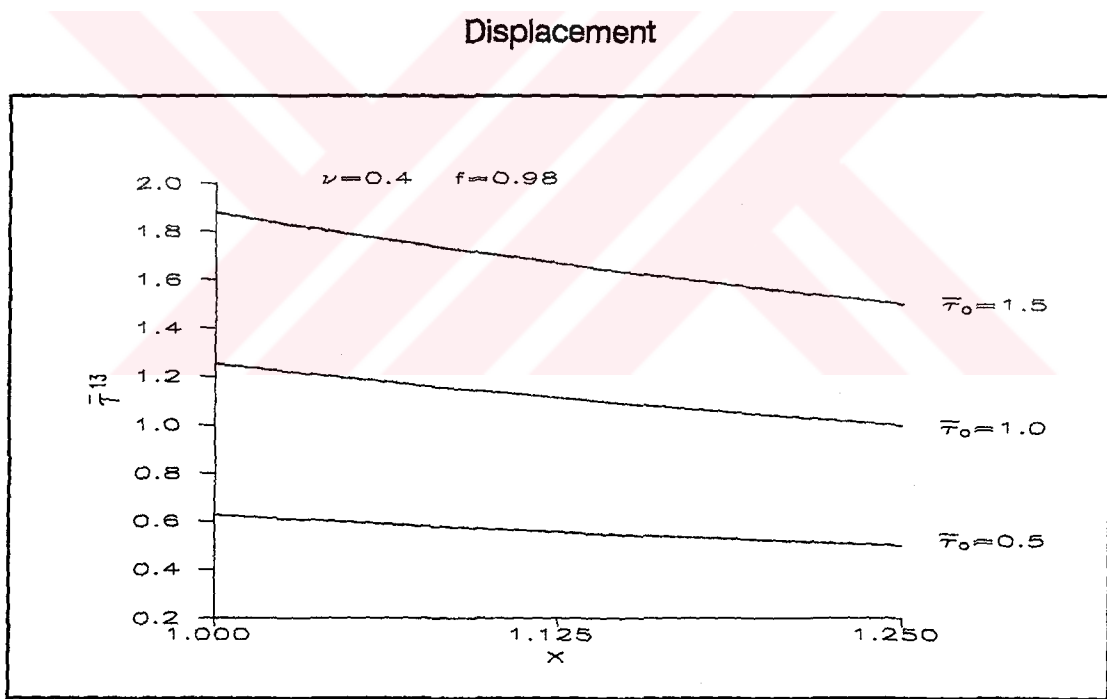


Figure 5.2. Dimensionless Radial Position vs.  $\bar{\tau}^{-13}$

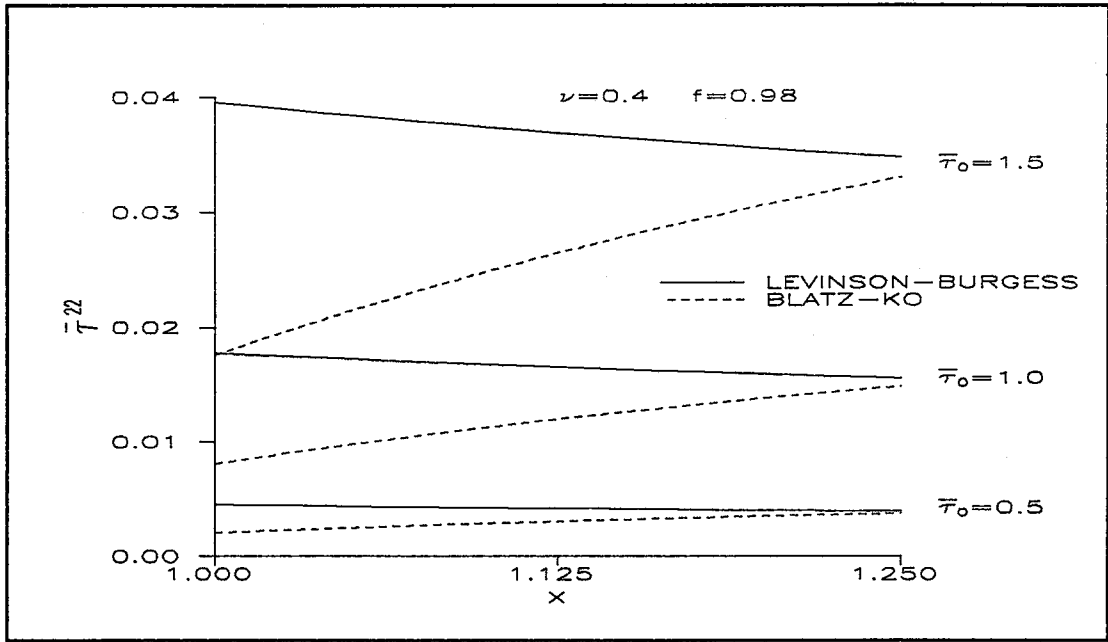


Figure 5.3. Dimensionless Radial Position vs.  $\bar{\tau}^{22}$

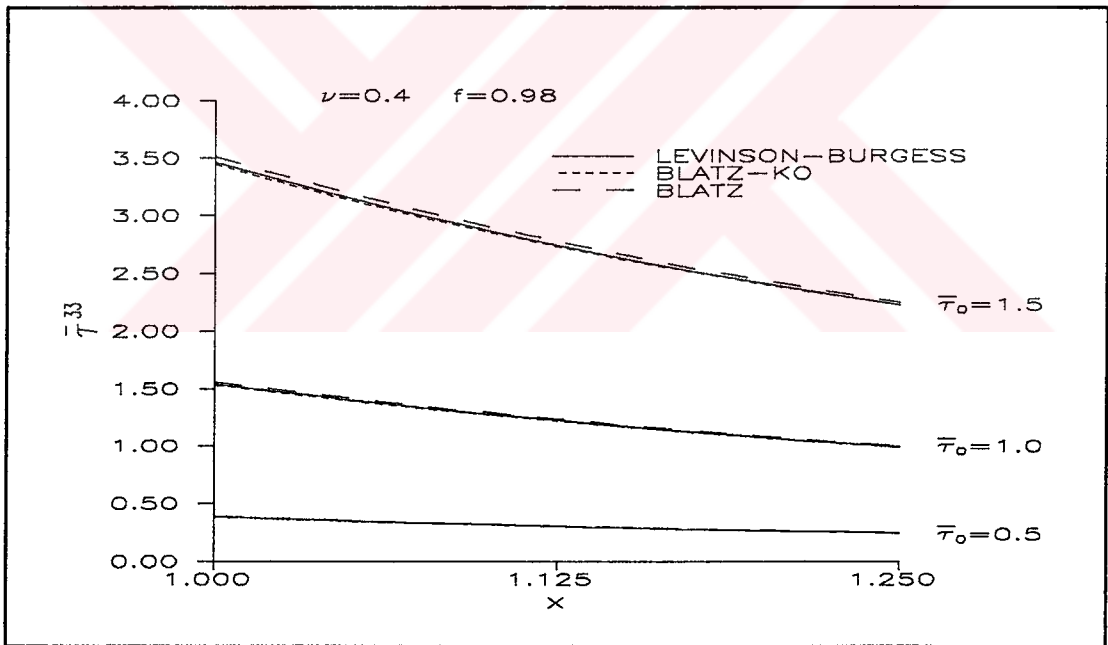


Figure 5.4. Dimensionless Radial Position vs.  $\bar{\tau}^{33}$

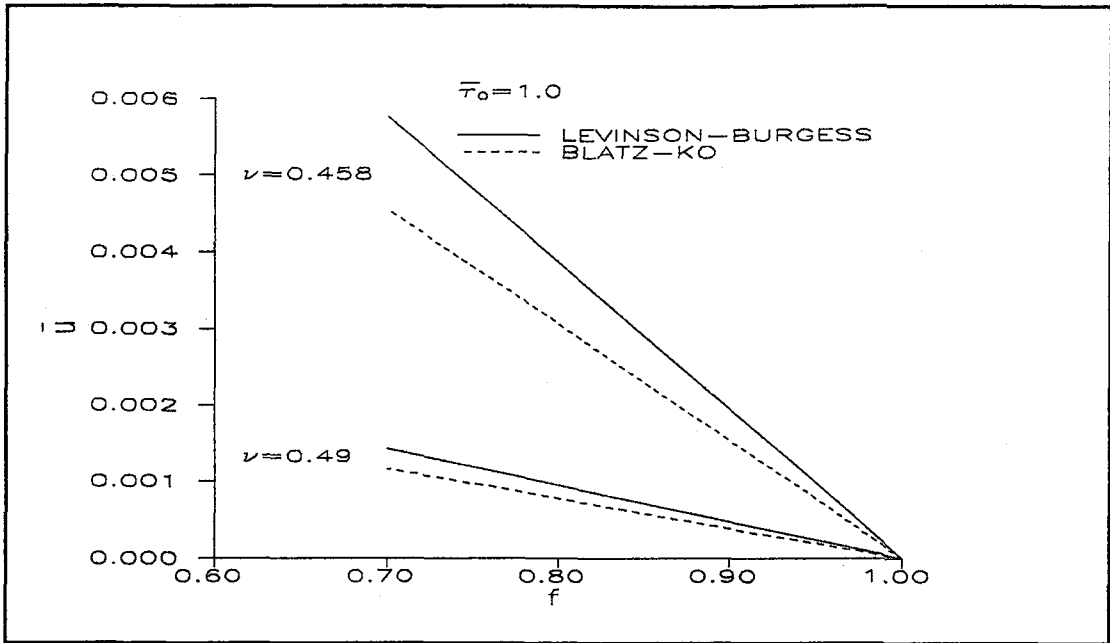


Figure 5.5.  $f$  vs. Dimensionless Radial Displacement at the Outer Boundary

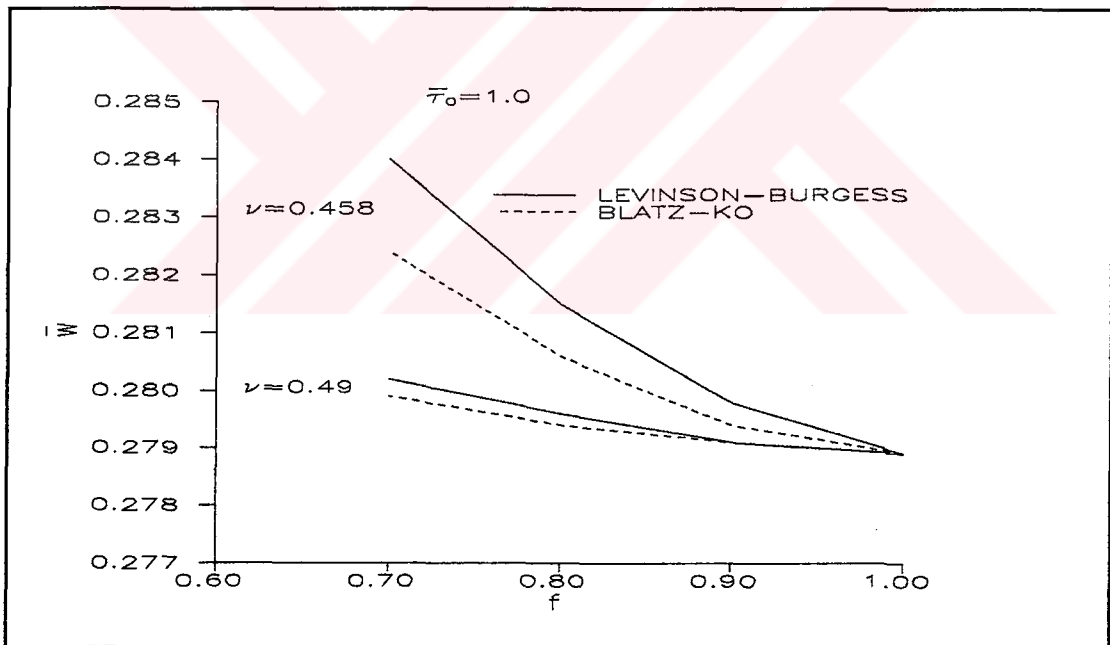


Figure 5.6.  $f$  vs. Dimensionless Axial Displacement at the Outer Boundary

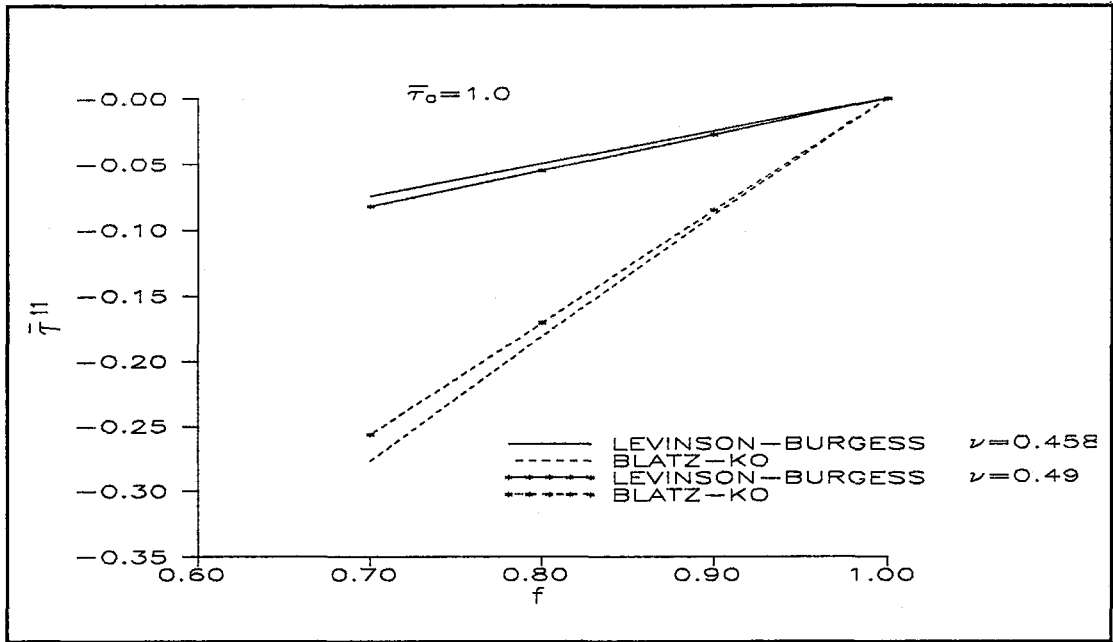


Figure 5.7.  $f$  vs.  $\bar{\tau}^{11}$  at the Inner Boundary

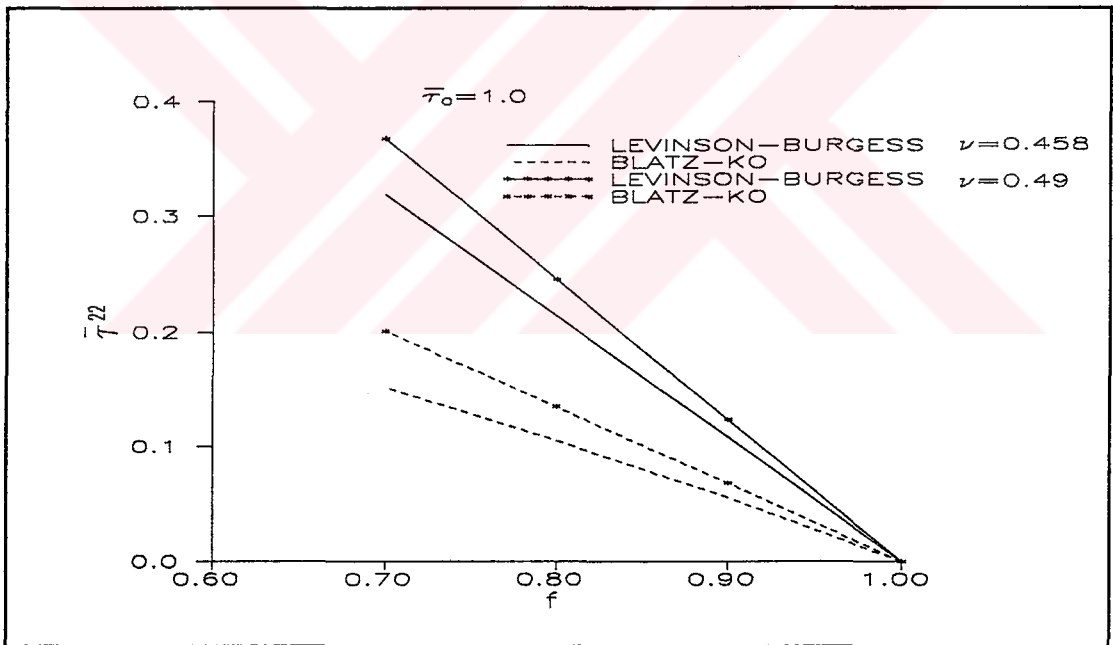


Figure 5.8.  $f$  vs.  $\bar{\tau}^{22}$  at the Inner Boundary

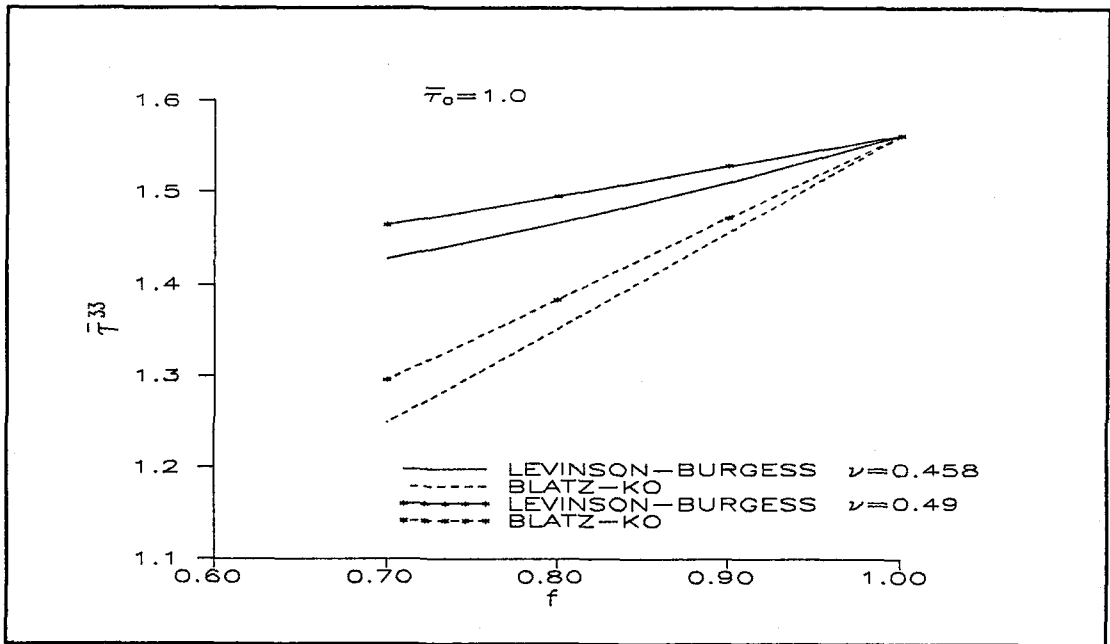


Figure 5.9  $f$  vs.  $\bar{r}^{33}$  at the Inner Boundary

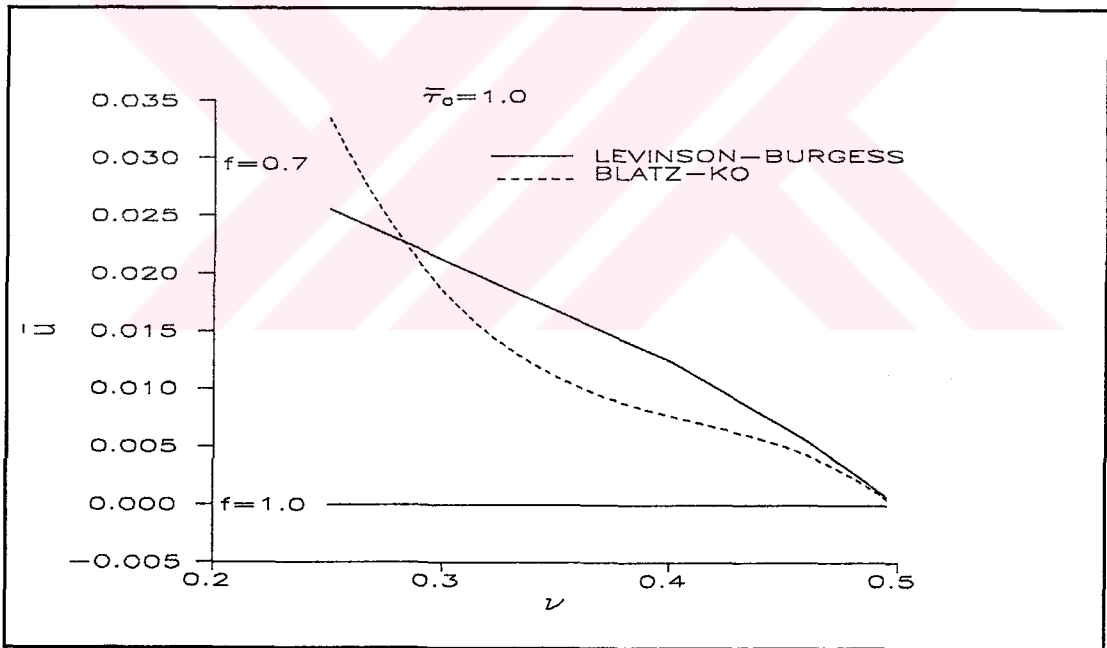


Figure 5.10.  $u$  vs. Dimensionless Radial Displacement at the Outer Boundary

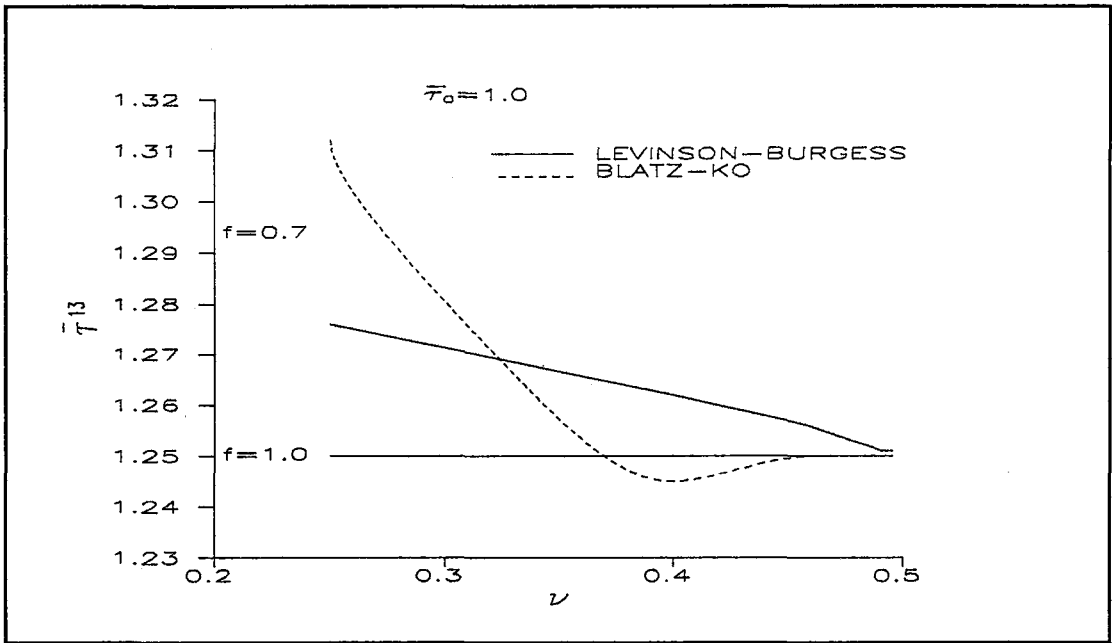


Figure 5.11.  $\nu$  vs.  $\bar{\tau}^{13}$  at the Inner Boundary

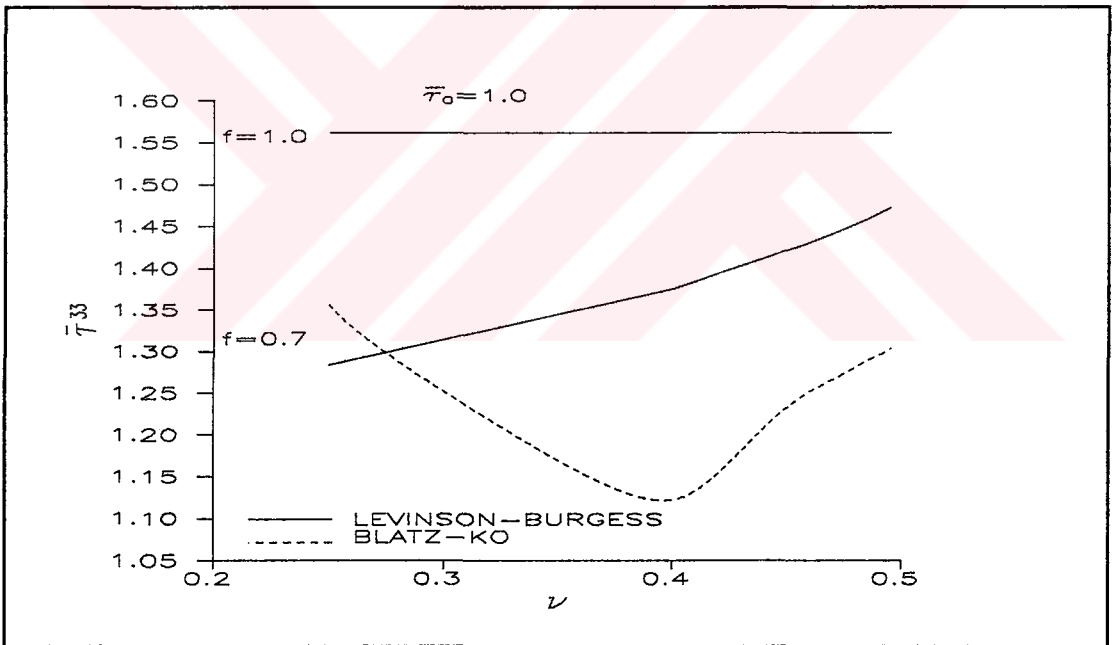


Figure 5.12.  $\nu$  vs.  $\bar{\tau}^{33}$  at the Inner Boundary

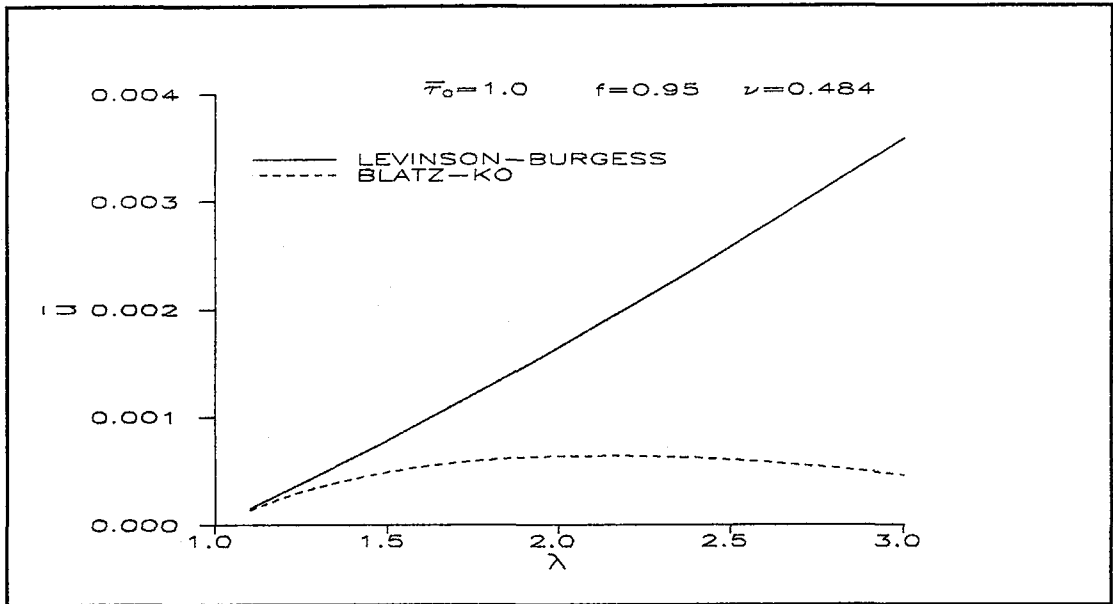


Figure 5.13.  $\lambda$  vs. Dimensionless Radial Displacement at the Outer

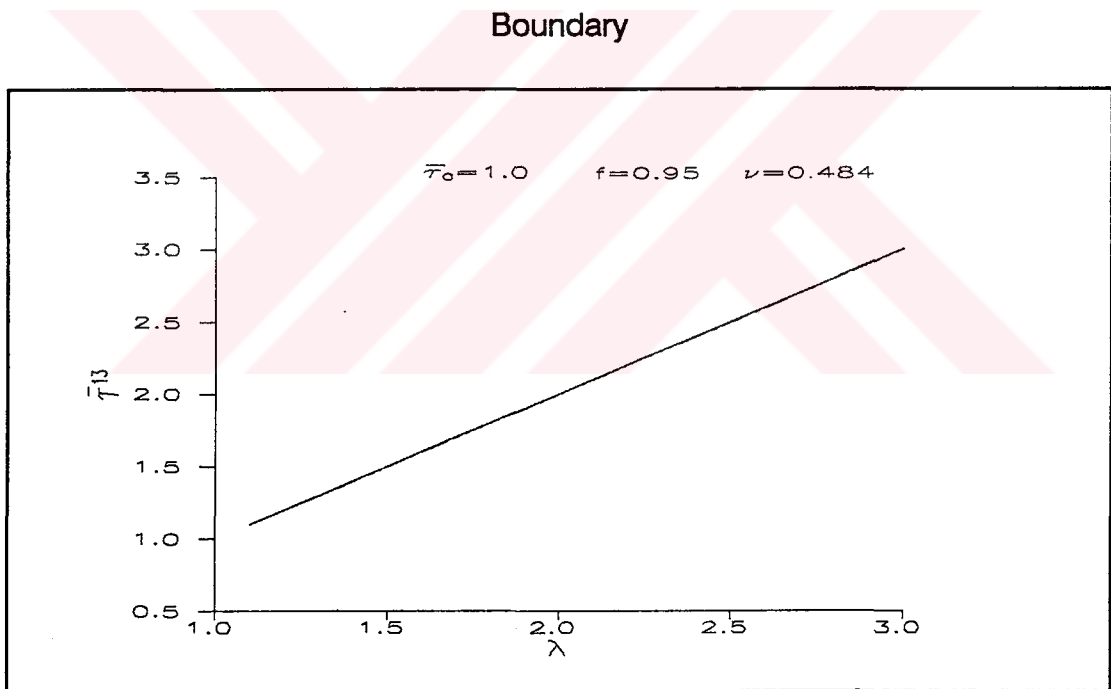


Figure 5.14.  $\lambda$  vs.  $\bar{\tau}^{-13}$  at the Inner Boundary



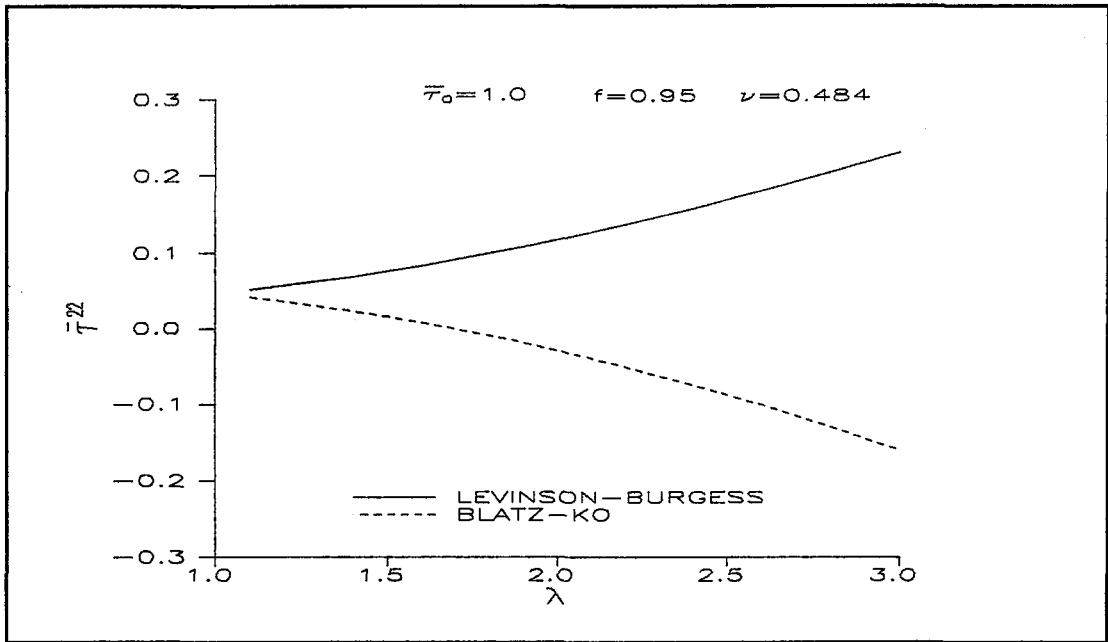


Figure 5.15.  $\lambda$  vs.  $\bar{\tau}^{22}$  at the Inner Boundary

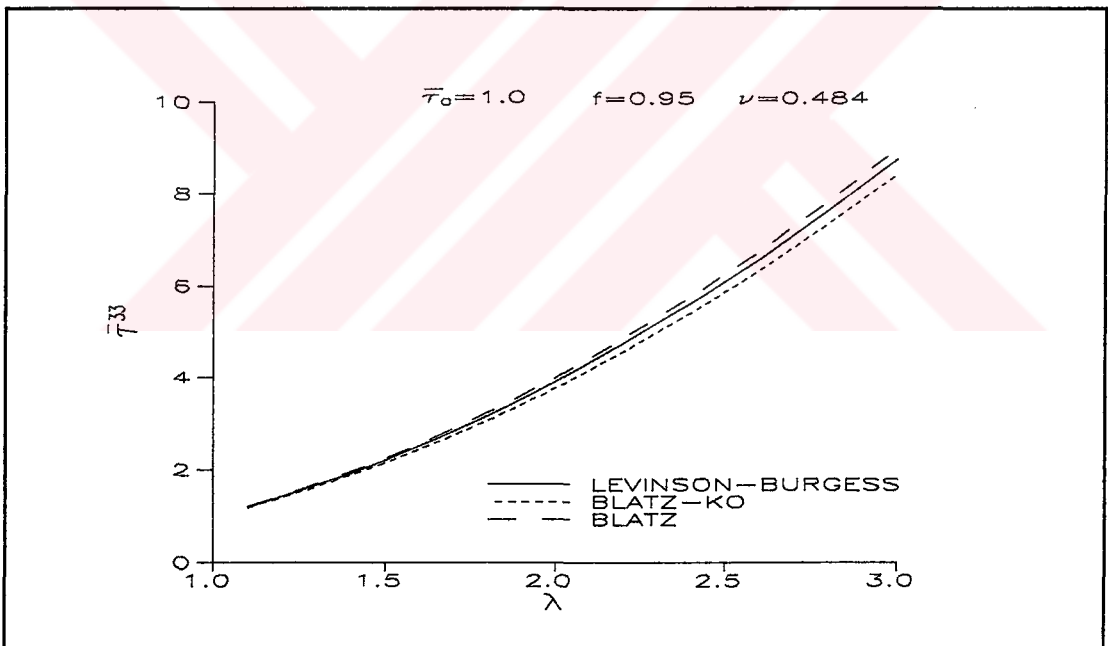


Figure 5.16.  $\lambda$  vs.  $\bar{\tau}^{33}$  at the Inner Boundary

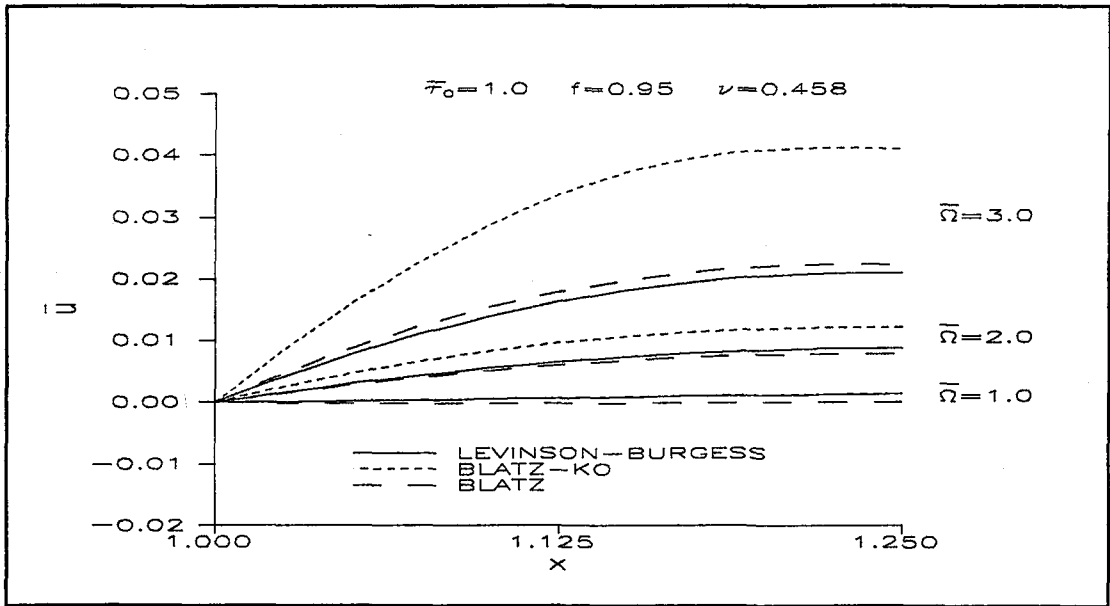


Figure 5.17. Dimensionless Radial Position vs. Dimensionless Radial Displacement

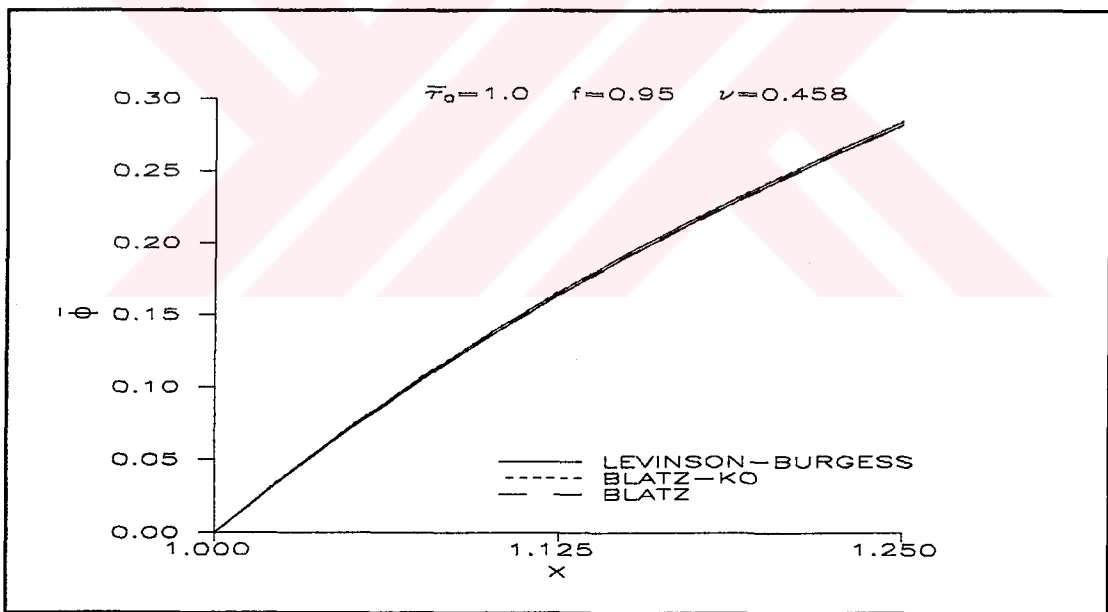


Figure 5.18. Dimensionless Radial Position vs. Dimensionless Angular Displacement

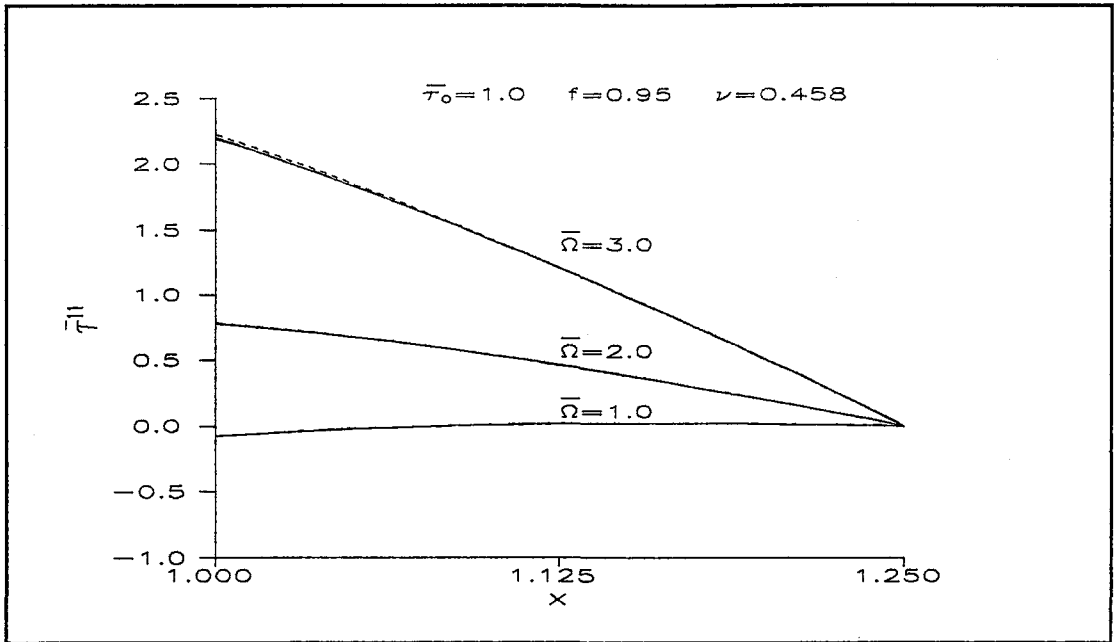


Figure 5.19. Dimensionless Radial Position vs.  $\bar{\tau}^{11}$

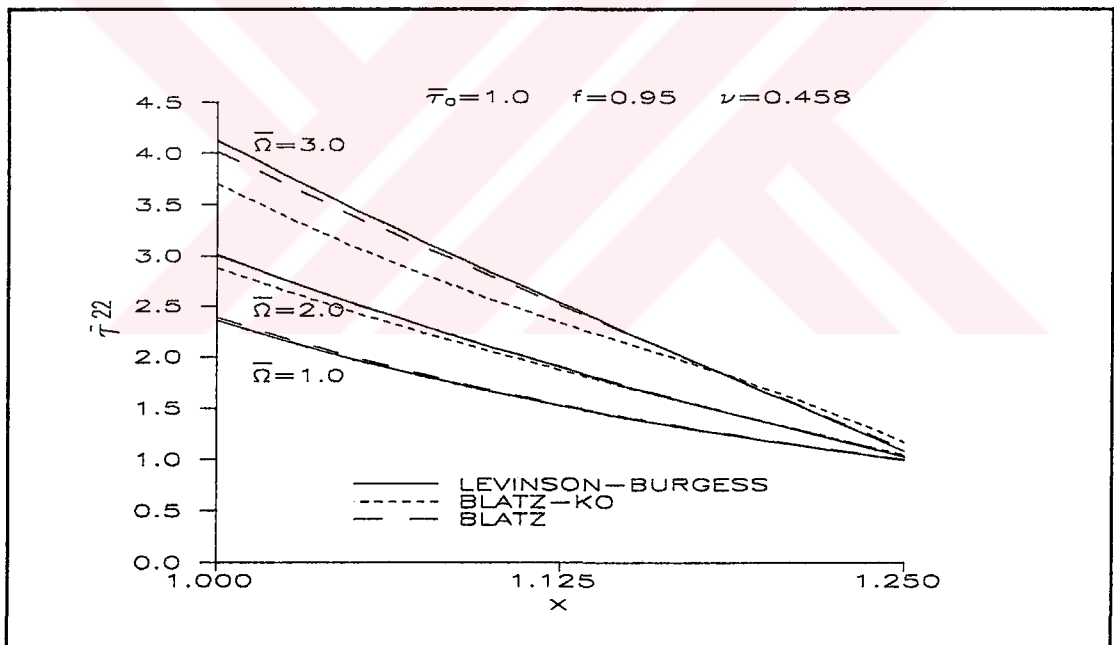


Figure 5.20. Dimensionless Radial Position vs.  $\bar{\tau}^{22}$

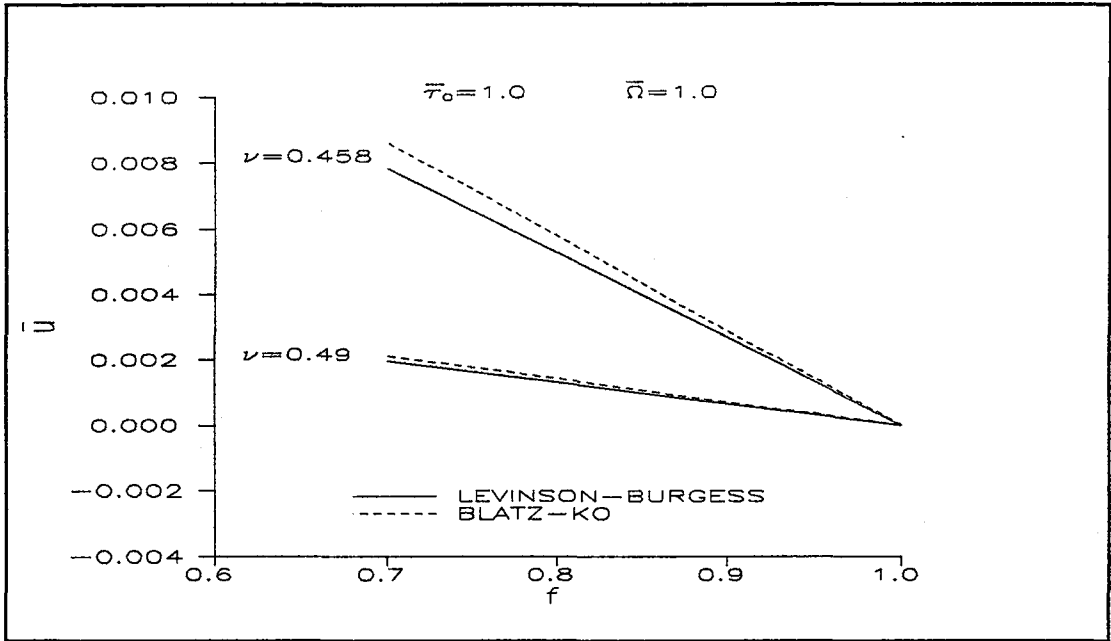


Figure 5.21.  $f$  vs. Dimensionless Radial Displacement at the Outer Bondary

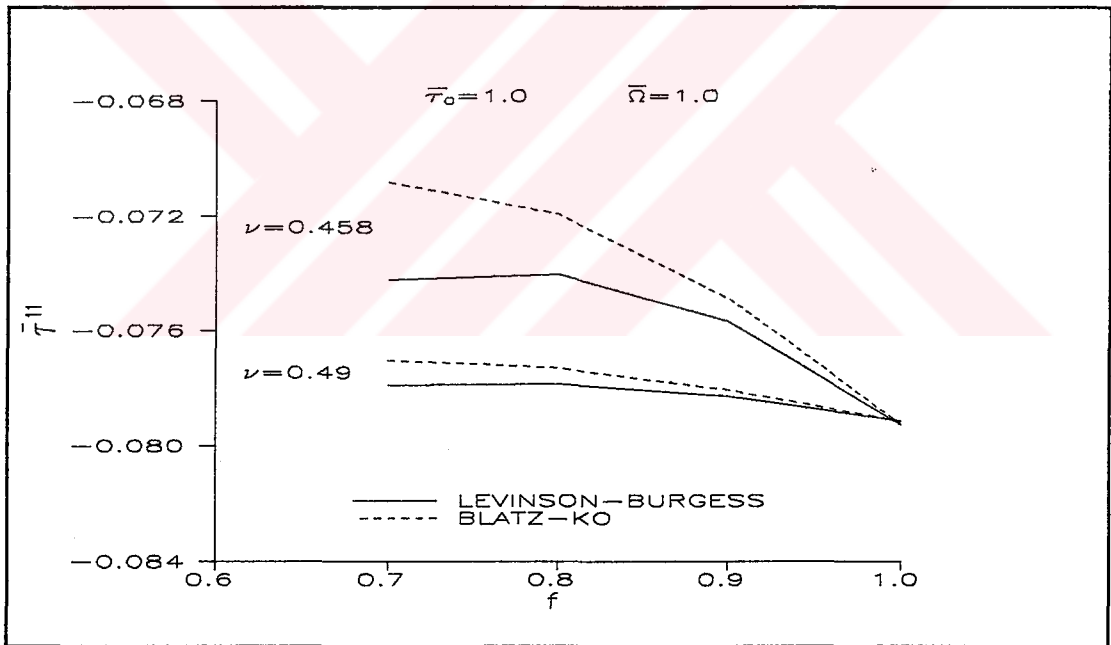


Figure 5.22.  $f$  vs.  $\bar{\tau}^{11}$  at the Inner Boundary

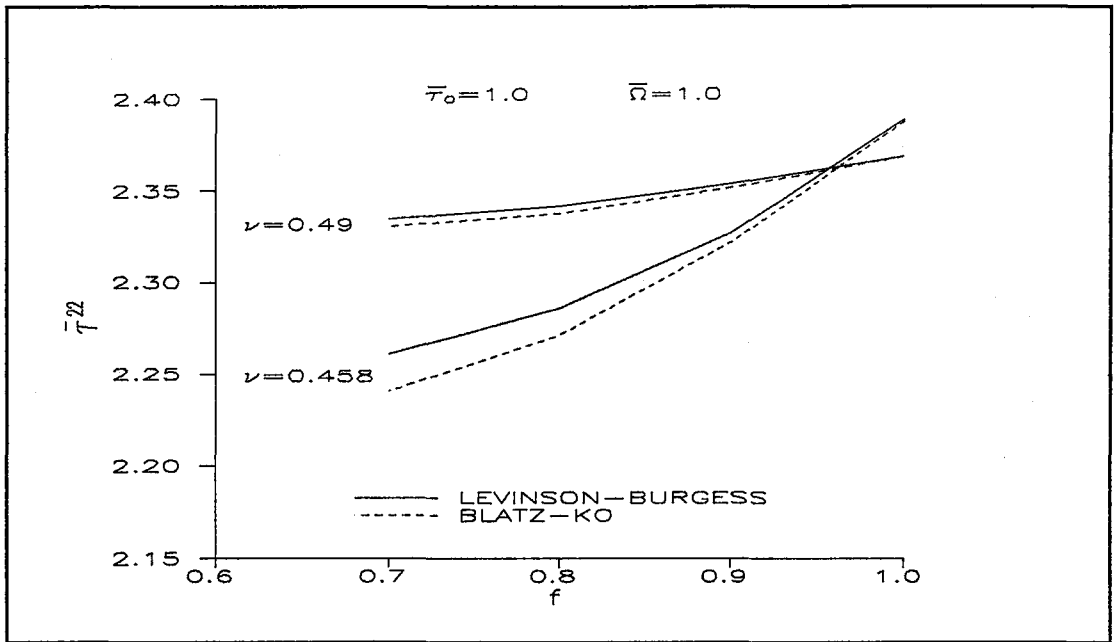


Figure 5.23.  $f$  vs.  $\bar{r}^{22}$  at the Inner Boundary

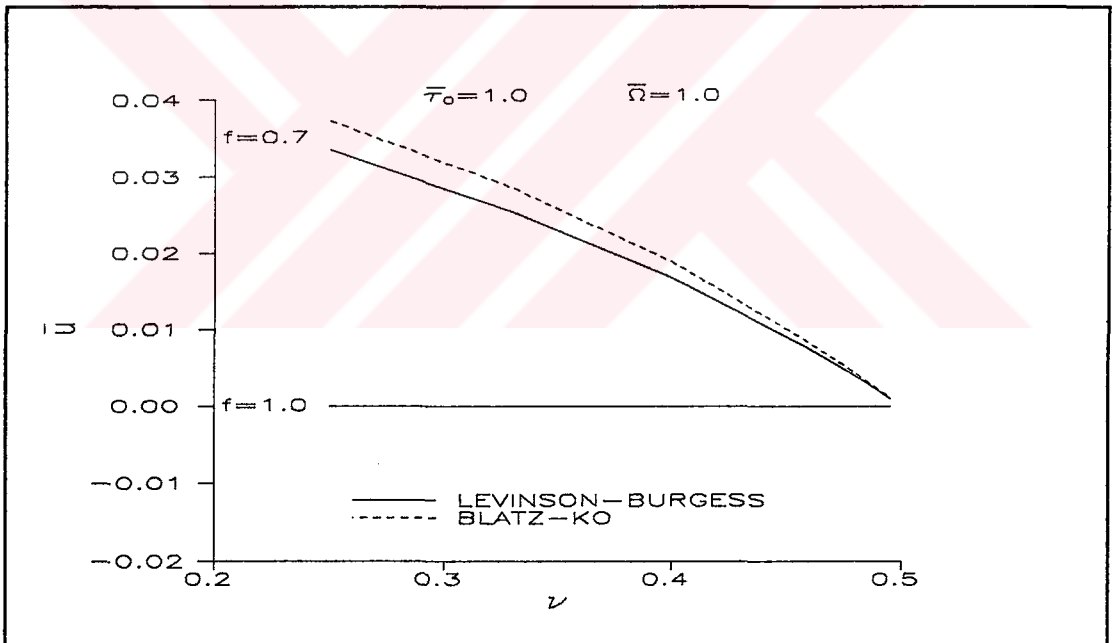


Figure 5.24.  $\nu$  vs. Dimensionless Radial Displacement at the Outer Boundary

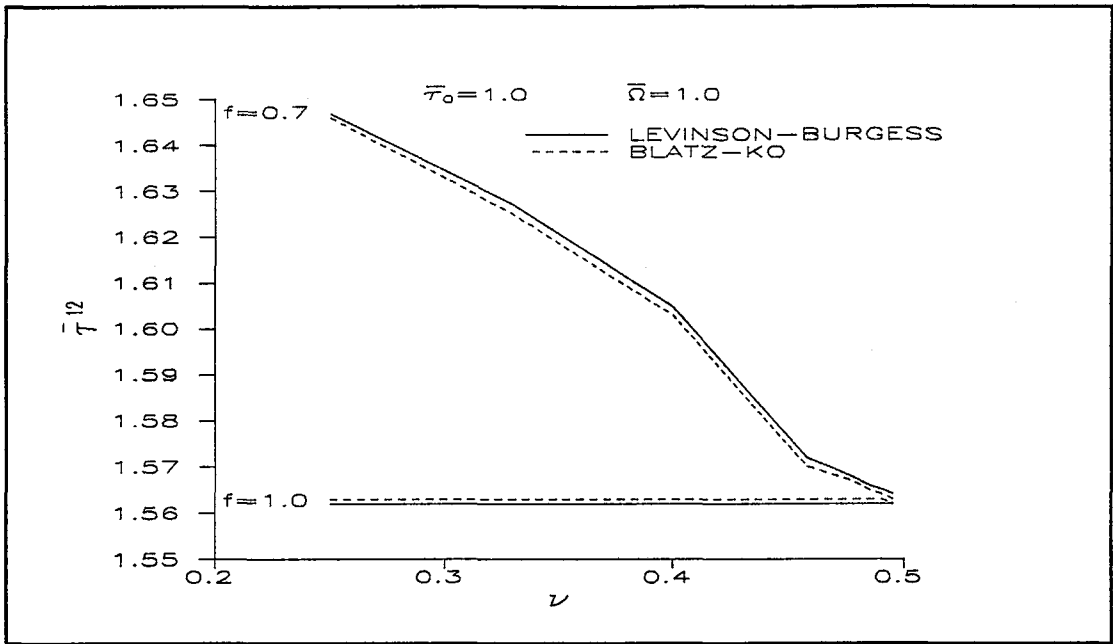


Figure 5.25.  $\nu$  vs.  $\bar{\tau}^{-12}$  at the Inner Boundary

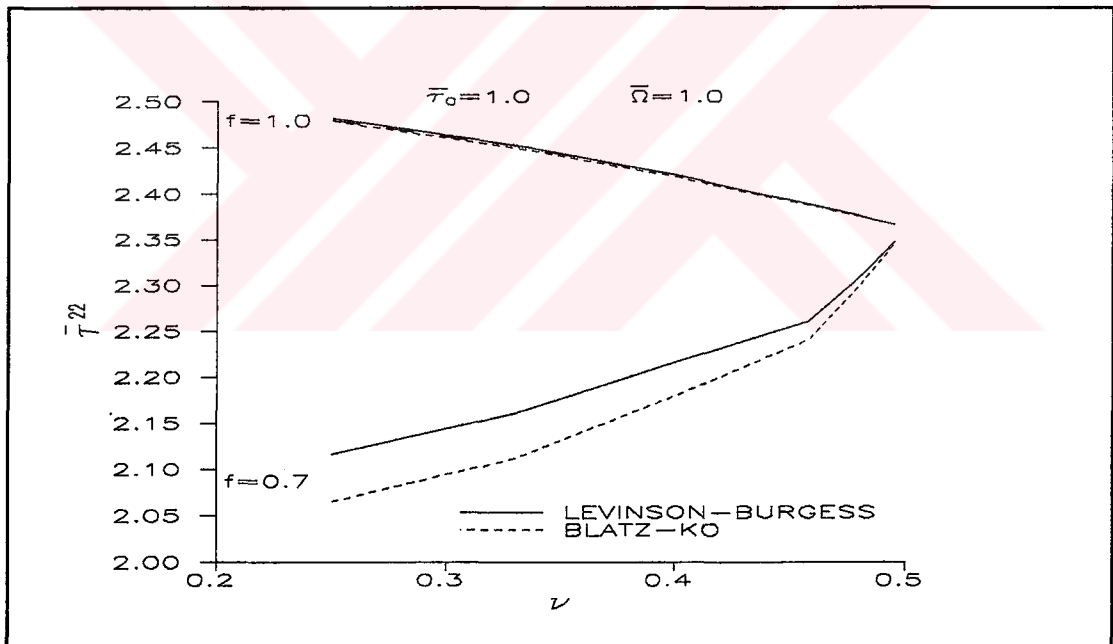


Figure 5.26.  $\nu$  vs.  $\bar{\tau}^{-22}$  at the Inner Boundary

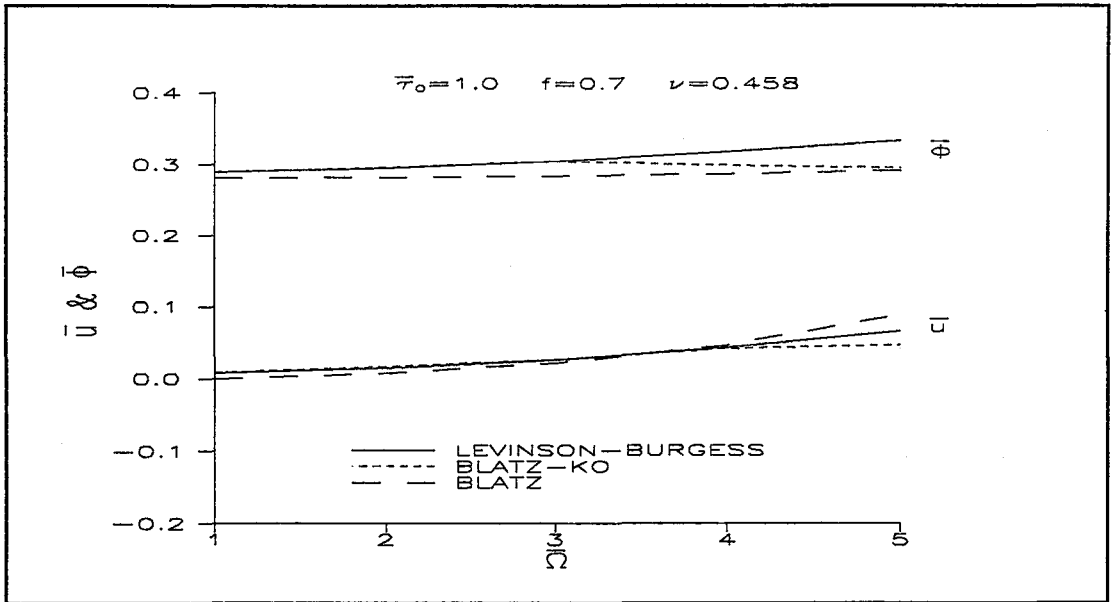


Figure 5.27. Dimensionless Spin vs. Dimensionless Radial & Angular Displacements at the Outer Boundary

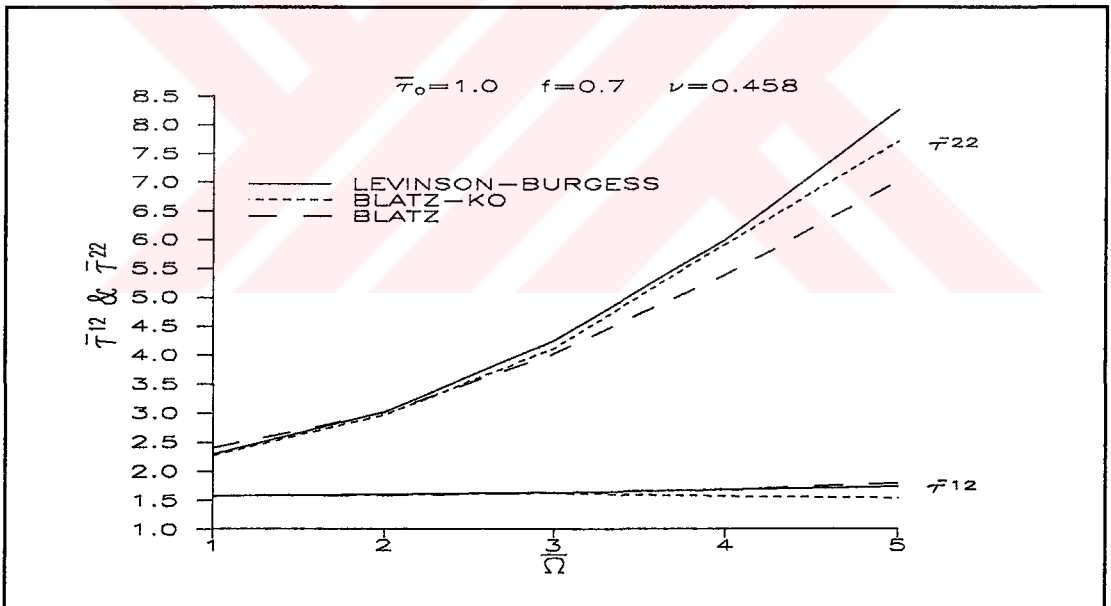


Figure 5.28. Dimensionless Spin vs.  $\bar{\tau}^{12}$  &  $\bar{\tau}^{22}$  at the Inner Boundary

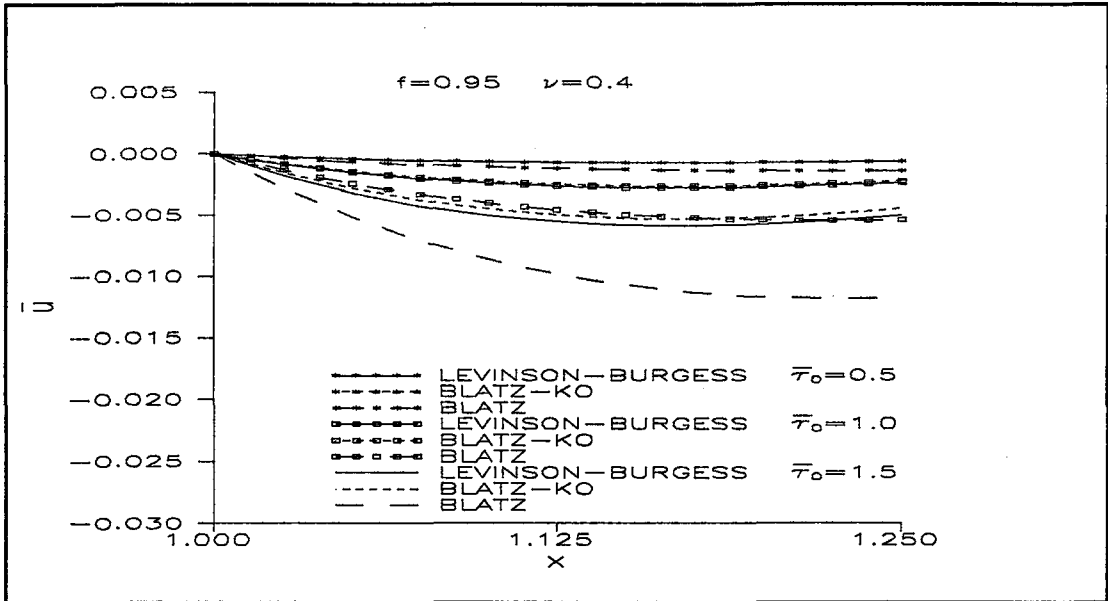


Figure 5.29. Dimensionless Radial Position vs. Dimensionless Radial

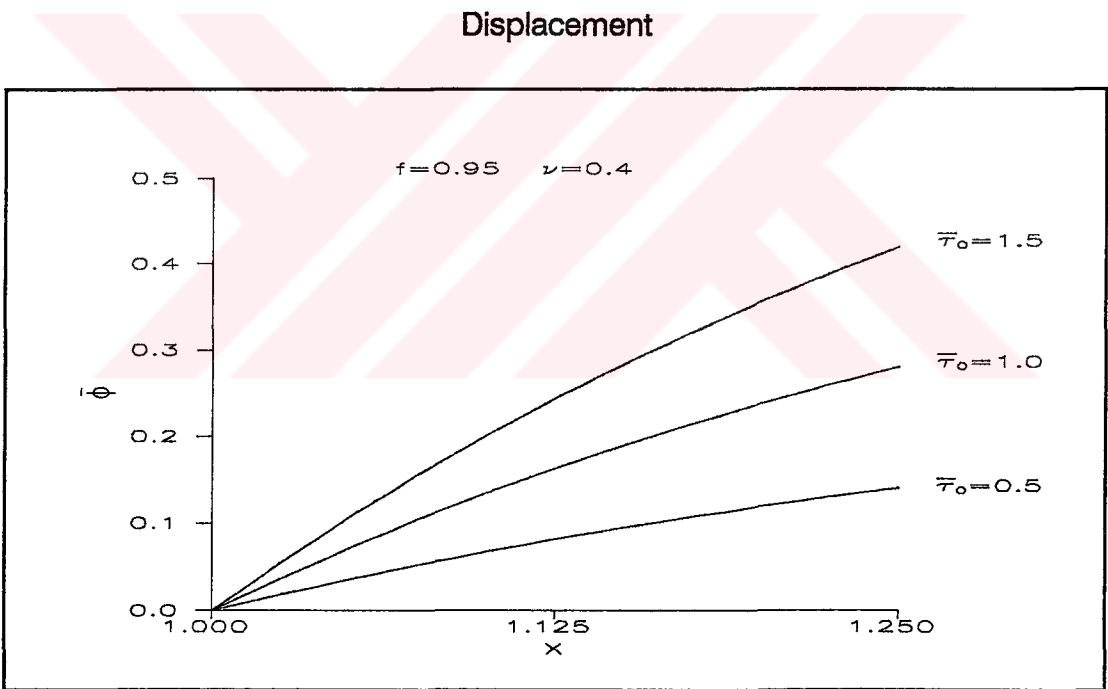


Figure 5.30. Dimensionless Radial Position vs. Dimensionless Angular

Displacement



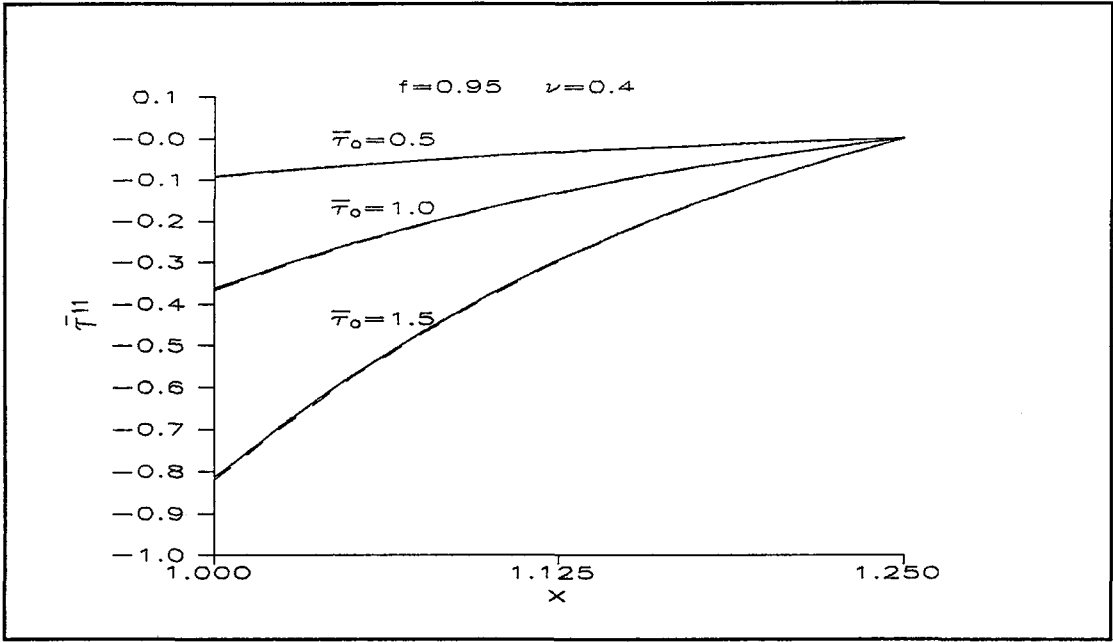


Figure 5.31. Dimensionless Radial Position vs.  $\bar{\tau}^{-11}$

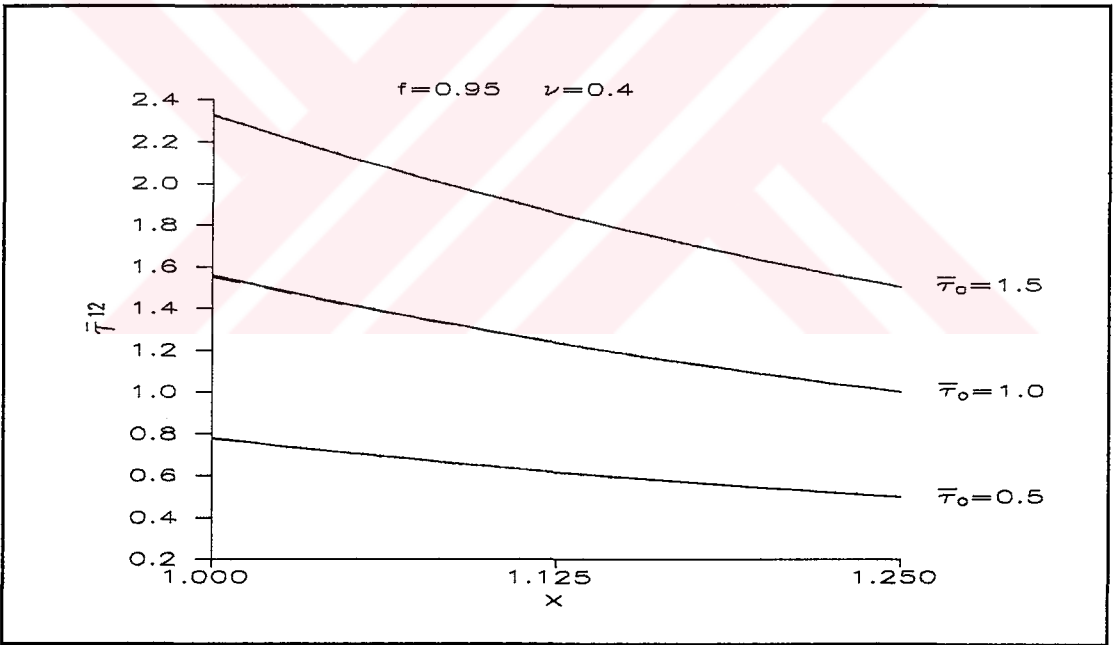


Figure 5.32. Dimensionless Radial Position vs.  $\bar{\tau}^{-12}$

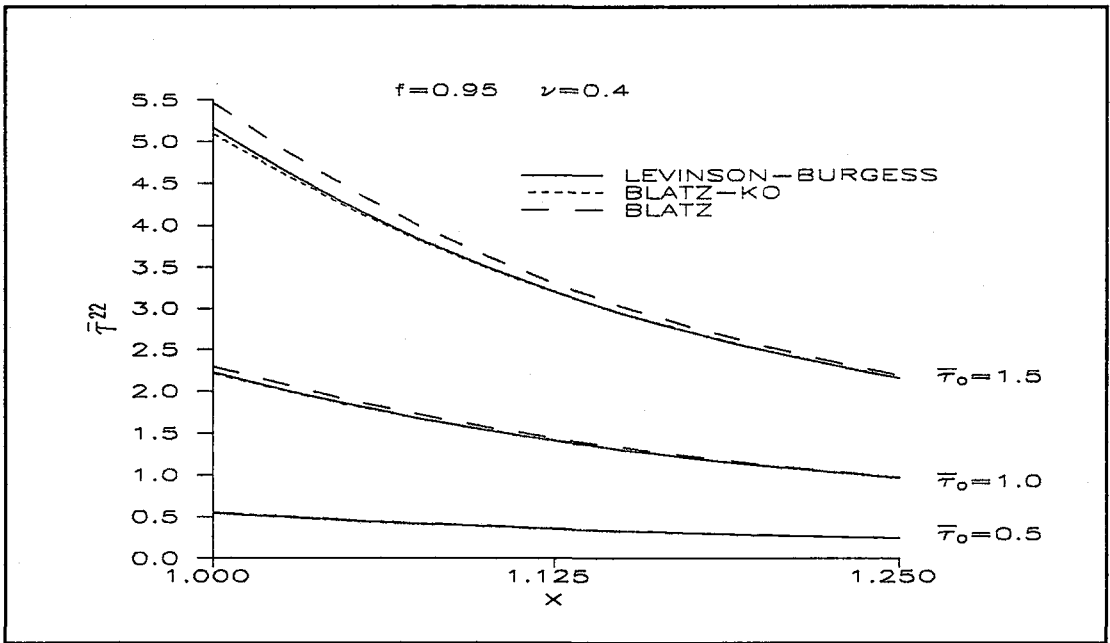


Figure 5.33. Dimensionless Radial Position vs.  $\bar{\tau}^{22}$

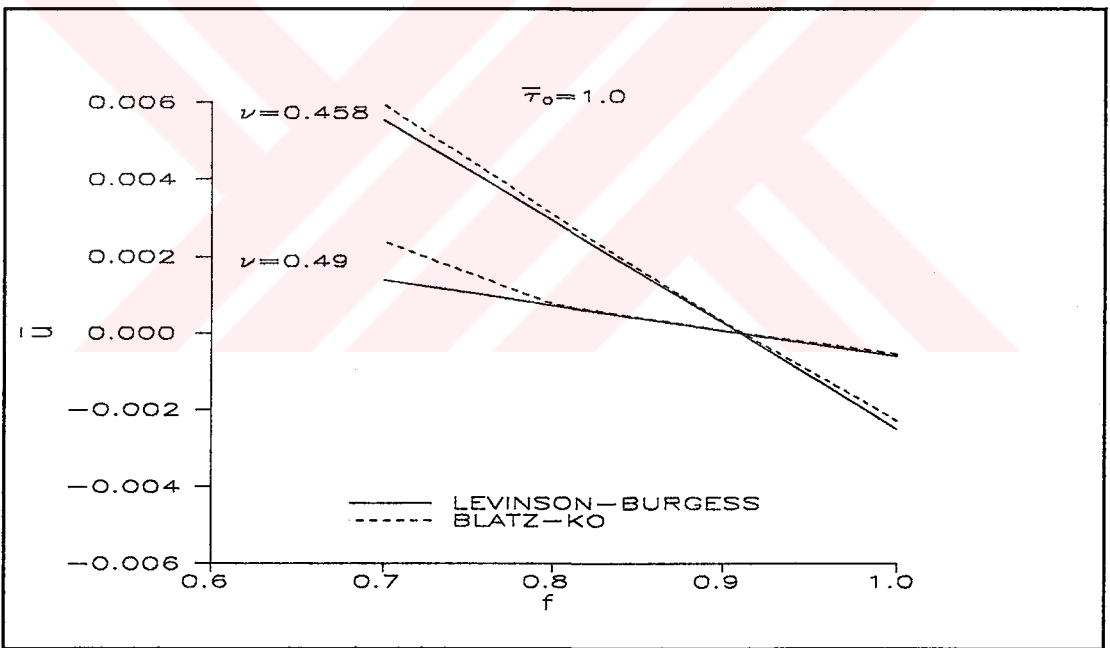


Figure 5.34.  $f$  vs. Dimensionless Radial Displacement at the Outer Boundary

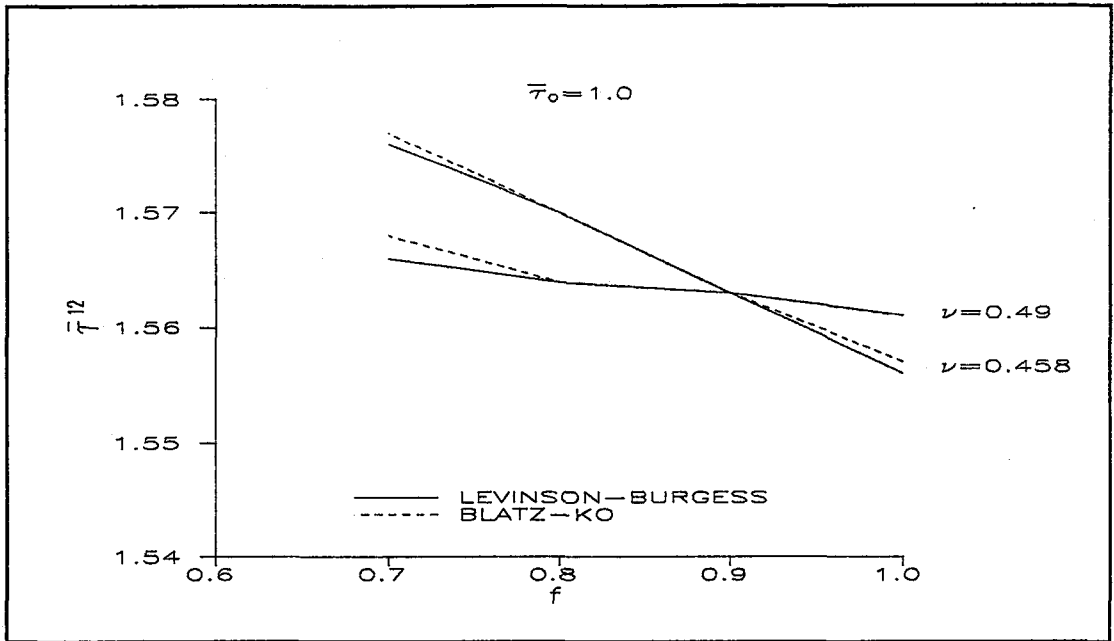


Figure 5.35.  $f$  vs.  $\bar{\tau}^{12}$  at the Inner Boundary

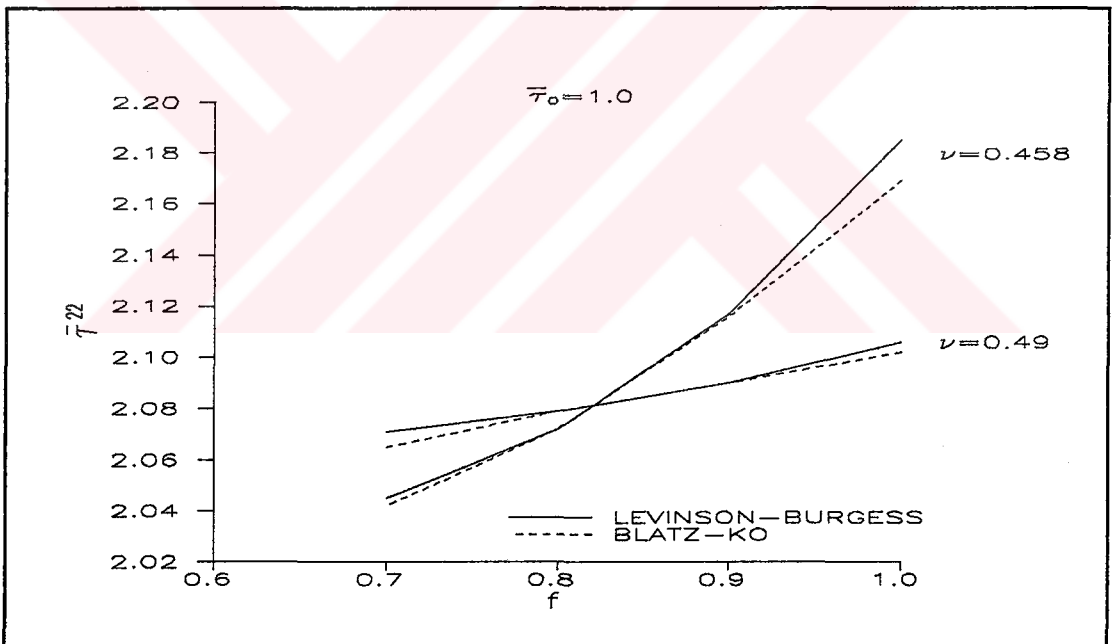


Figure 5.36.  $f$  vs.  $\bar{\tau}^{22}$  at the Inner Boundary

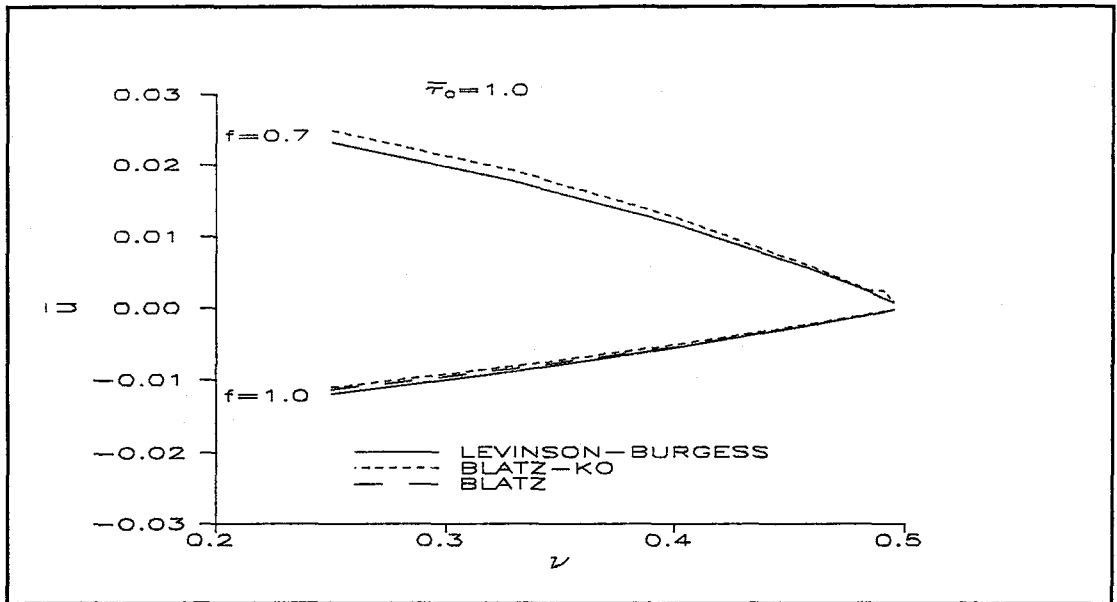


Figure 5.37.  $u$  vs. Dimensionless Radial Displacement at the Outer

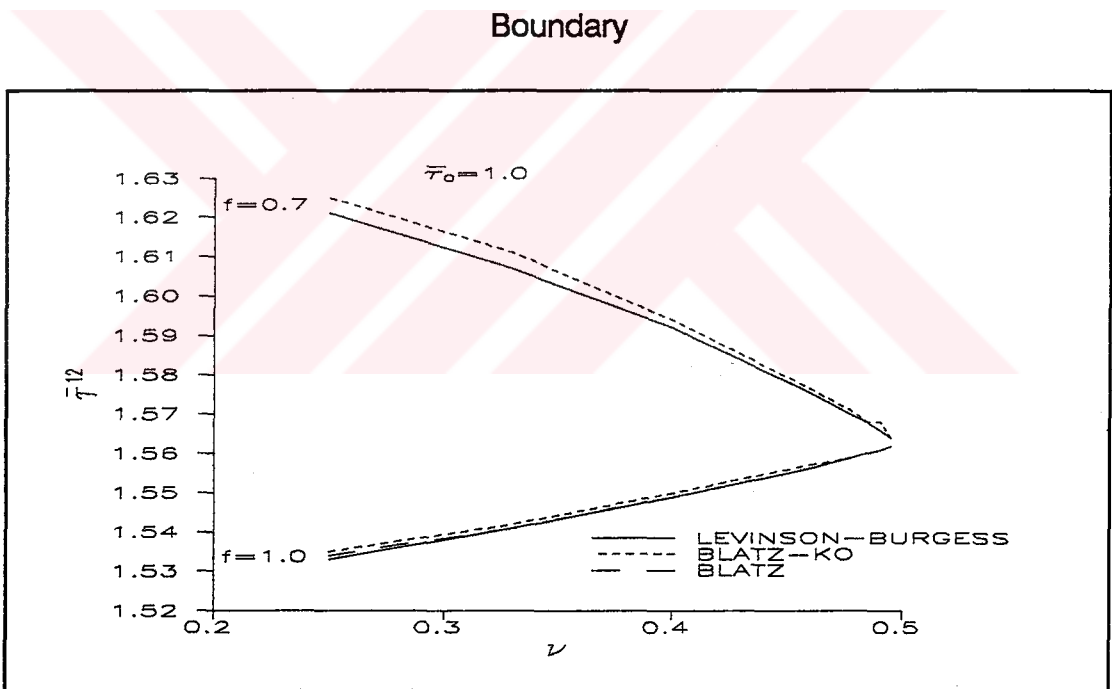


Figure 5.38  $\nu$  vs.  $\bar{\tau}^{12}$  at the Inner Boundary

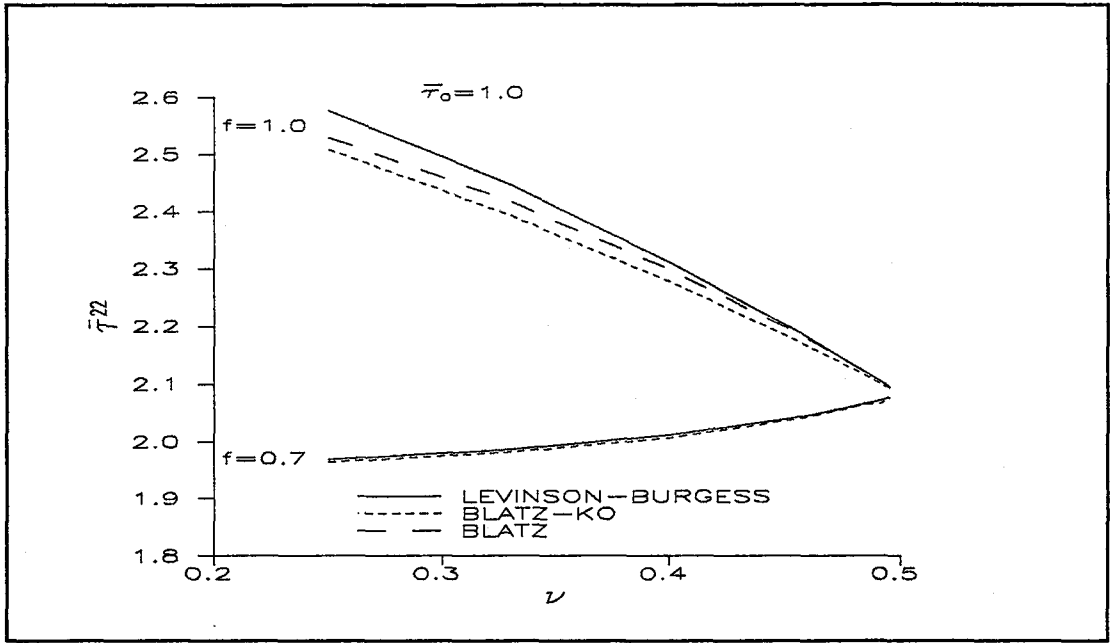


Figure 5.39.  $\nu$  vs.  $\bar{r}^{22}$  at the Inner Boundary

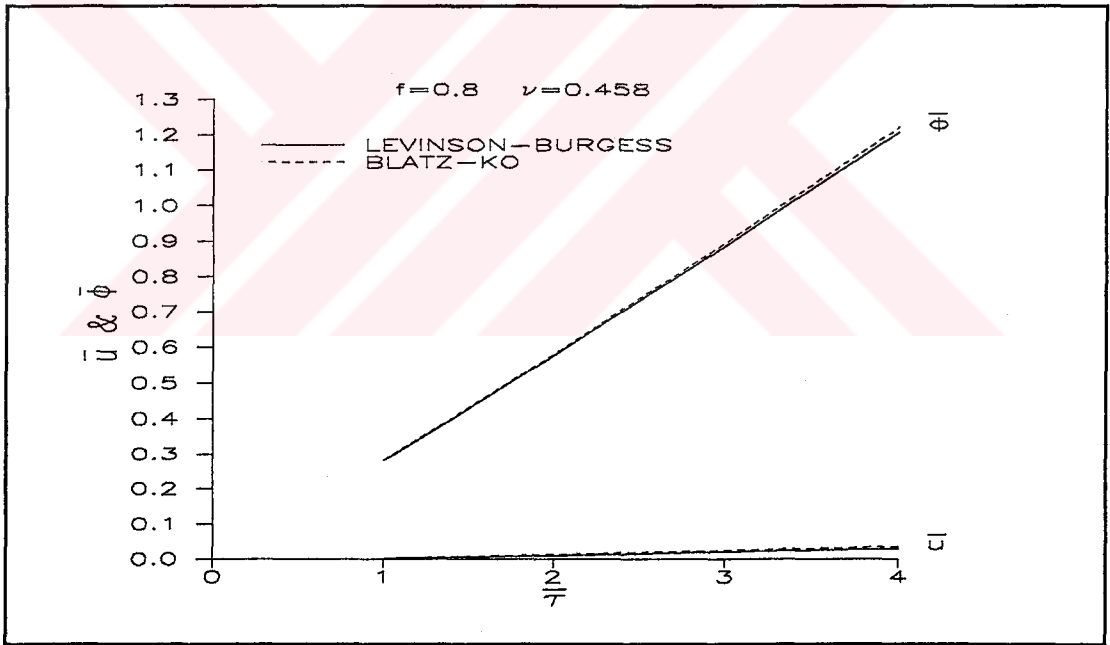


Figure 5.40. Dimensionless Surface Traction vs. Dimensionless Radial & Angular Displacements at the Outer Boundary

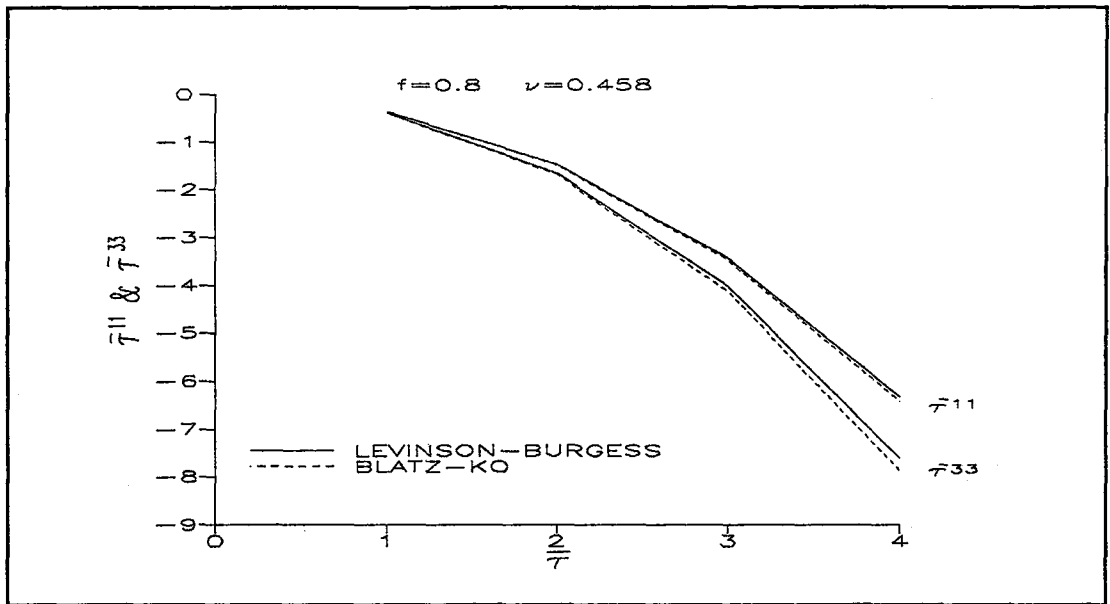


Figure 5.41. Dimensionless Surface Traction vs.  $\bar{\tau}^{11}$  &  $\bar{\tau}^{33}$  at the Inner Boundary

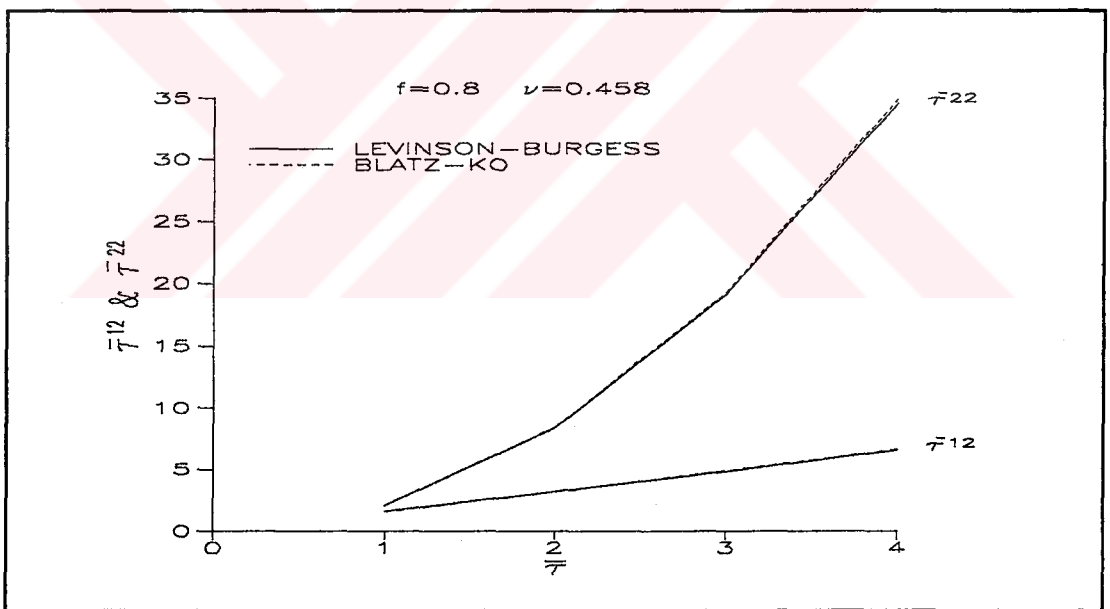


Figure 5.42. Dimensionless Surface Traction vs.  $\bar{\tau}^{12}$  &  $\bar{\tau}^{22}$  at the Inner Boundary

## CHAPTER VI

### CONCLUSIONS

The following conclusions can be stated on the bases of the numerical investigation.

In the finite anti-plane shear, for the dominant components which are axial displacement  $w$ , axial shearing stress  $\tau^{13}$ , and axial stress  $\tau^{33}$ , the three models give the same result for  $\nu$  greater than 0.458. For smaller values of  $f$  and  $\nu$ , there are significant differences between the three models. In the light of experimental findings of Blatz-Ko, it must be marked that smaller values of  $f$  and  $\nu$  belong to foam rubber for which continuum theory is no longer valid.

In the constant spin and circumferential shear, the dominant components are angular displacement  $\phi$ , circumferential shearing stress  $\tau^{12}$ , and hoop stress  $\tau^{22}$  for which there is no any significant difference between the three models. Similarly, as  $f$  and  $\nu$  decrease the differences increase.

In the uniform circumferential shear, the dominant components are angular displacement  $\phi$ , circumferential shearing stress  $\tau^{12}$ , and hoop stress  $\tau^{22}$  for which the three models give essentially the same results for bigger values of  $f$  and  $\nu$ .

In all the problems, there are differences between the three model for radial displacement  $u$  which is a second order effect for all problems.

Calculations show that the effect of material constants  $f$  and  $\nu$  on the axial displacement for anti-plane shear, and on the angular displacement for circumferential shear problems are rather insignificant.

Due to the complexity of Blatz-Ko strain energy density function, in the circumferential shear problems, it is met with computational problems. For  $f$  greater than 0.9, and applied surface traction greater than 1.6, no results can be obtained due to the overflow errors.

The initial boundary conditions are guessed in the method of adjoints. These guess values do not play an important role in the number of iteration for polynomial material model and Blatz model. However, for Blatz-Ko model the rate of convergency is dependent to the initial guess values.



The simplest strain energy density function is proposed by Blatz, in which material constant  $f$  is not considered which leads to the independency of strain energy density function from second strain invariant. Because of this simplicity the number of iteration is less for this model.

For  $f$  nearly equal to 1.0, Blatz model give the same results as the other two models. In this region, Blatz model can be used to take the results of dominant components fast.

The most suitable strain energy density function for the numerical analysis, is proposed by Levinson and Burgess which is a polynomial material model. For all values of  $f$ ,  $\nu$ ,  $R_2/R_1$ ,  $\tau_0$ , and  $\Omega$ , it gives the results in less than 50 iterations.

Although the calculations show that the material compressibility is essentially represented same in all the three models, it is proposed to use polynomial model to get the results without facing with any problem.

As a final conclusion, it is believed that the correctness of these analytical results must be checked with the experimental studies.

## REFERENCES

- [1] M. Mooney, "A Theory of Large Elastic Deformations", Journal of Applied Physics, 11, 582, (1940).
- [2] R.S. Rivlin, "Large Elastic Deformations of Isotropic Materials IV", Philosophical Transaction, A241, 379, (1948).
- [3] R.S. Rivlin, "Large Elastic Deformations of Isotropic Materials V", Proceedings of Royal Society, A195, 463, (1948).
- [4] R.S. Rivlin, "Large Elastic Deformations of Isotropic Materials VI", Philosophical Transaction, A242, 173, (1949).
- [5] A.E. Green and W. Zerna, Theoretical Elasticity, Oxford, London, (1960).
- [6] A.E. Green and R.T. Shield, "Finite Extension and Torsion of Cylinders", Philosophical Transaction, A244, 47, (1951).

[7] L.R.G. Treloar, The Physics of Rubber Elasticity, Oxford, London, (1967).

[8] H. Alexander, "A Constitutive Relation for Rubber-Like Materials", International Journal of Engineering Science, 6, 549, (1968).

[9] P.J. Blatz and W.L. Ko, "Application of Finite Elasticity Theory to the Deformation of Rubbery Materials", Transactions of the Society of Rheology, 6, 243, (1962).

[10] M. Levinson and I.W. Burgess, "A Comparison of Some Simple Constitutive Equations for Slightly Compressible Rubber-Like Materials", International Journal of Mechanical Science, 13, 563,(1971).

[11] M. Shahinpoor, "Finite Deformations of Slightly Compressible Materials on the Finite Screw Dislocation", International Journal of Engineering Science, 10, 953, (1972).

[12] F.D. Murnaghan, Finite Deformation of an Elastic Solid, Jhon Wiley, New York, (1951).

[13] A. Mioduchowski and J.B. Haddow, "Finite Telescopic Shear of a Compressible Hyperelastic Tube", International Journal of Nonlinear Mechanics, **9**, 209, (1973).

[14] J.K. Knowles, "On Finite Anti-Plane Shear for incompressible Elastic Materials", Journal of Australian Mathematical Society, **B19**, 400, (1976).

[15] J.K. Knowles, "A Note on Anti-Plane Shear for compressible Materials in Finite Elastostatics", Journal of Australian Mathematical Society, **B20**, 1, (1977).

[16] V.K. Agarwal, "On Finite Anti-Plane Shear for Compressible Elastic Circular Tube", Journal of Elasticity, **9**, 311, (1979).

[17] T. Tokdemir and A. Ertepinar, "Stability and Vibrations of Layered, Compressible Hyperelastic, Rectangular Columns", Journal of Sound and Vibration, **110**, 111, (1986).

[18] A. Ertepinar and N. Akkaş, "Stability and Vibrations of Rectangular Columns Made of a Compressible Hyperelastic Material", International Journal of Engineering Science, **24**, 953, (1986).

[19] M. M. Carroll, "Finite Strain Solutions in Compressible Isotropic Elasticity", Journal of Elasticity, 20, 65, (1988).

[20] A. Ertepinar and G. Erarslanoglu, "Finite Anti-Plane Shear of Compressible Hyperelastic Tubes", International Journal of Engineering Science, 28, 399, (1990).

[21] A. Ertepinar, "Compressible, Hyperelastic Spinning Tubes Subjected to Circumferential Shear", International Journal of Engineering Science, 29, 203, (1991).

[22] A. Ertepinar, " On the Finite Circumferential Shearing of Compressible Hyperelastic Tubes", International Journal of Engineering Science, 28, 889, (1990).

[23] S.M. Roberts and J.S. Shipman, Two-Point Boundary Value Problems: Shooting Methods, Elsevier, New York, (1972).

[24] D. Kincaid and W. Cheney, Numerical Analysis, Brooks Co., California, (1991).



**APPENDICES**

APPENDIX A  
TRANSFORMATION FORMULAS

A.1 Transformation Formulas for Defining Variables in Terms of R

In equation (3.25) radial displacement is expressed as

$$r = R + u(r) \quad (\text{A.1})$$

If equation (A.1) is differentiated with respect to  $r$ ,

$$R_r = 1 - u_r \quad (\text{A.2})$$

or applying the chain rule

$$R_r = 1 - u_R R_r \quad (\text{A.3})$$

from (A.3)

$$R_r = \frac{1}{1 + u_R} \quad (\text{A.4})$$

By inserting (A.4) into (A.2)

$$u_r = \frac{u_R}{1+u_R} \quad (\text{A.5})$$

If equation (A.1) is differentiated two times with respect to  $r$

$$R_{rr} = -u_{rr} \quad (\text{A.6})$$

that is

$$R_{rr} = -\left[\frac{u_R}{1+u_R}\right]_r \quad (\text{A.7})$$

therefore

$$R_{rr} = -\frac{u_{RR}}{(1+u_R)^3} \quad (\text{A.8})$$

and from (A.6)

$$u_{rr} = \frac{u_{RR}}{(1+u_R)^3} \quad (\text{A.9})$$

First derivative of the axial displacement  $w$  with respect to  $r$  can be expressed as

$$w_r = w_R R_r \quad (\text{A.10})$$



If (A.4) is substituted into (A.10)

$$w_r = \frac{w_R}{1+u_R} \quad (\text{A.11})$$

and if (A.11) is differentiated once more with respect to  $r$ ,

$$w_{rr} = \frac{w_{RR}}{(1+u_R)^2} - \frac{w_R u_{RR}}{(1+u)^3} \quad (\text{A.12})$$

## A.2 Formulas for the Dimensionless Terms

Dimensionless variables for radial position  $x$ , radial displacement  $u$ , axial displacement  $w$  and angular displacement  $\phi$  are defined in equations (3.46) and (3.47) as

$$x = \frac{R}{R_1} \quad (\text{A.13})$$

$$\bar{u} = \frac{u}{R_1} \quad (\text{A.14})$$

$$\bar{w} = \frac{w}{R_1} \quad (\text{A.15})$$

$$\bar{\phi} = \phi \quad (\text{A.16})$$

From (A.13)

$$dR = R_1 dx \quad (\text{A.17})$$

and

$$\frac{d}{dR} = \frac{1}{R_1} \frac{d}{dx} \quad (\text{A.18})$$

Using (A.14) and (A.18)

$$\frac{du}{dR} = \frac{d}{dR}(\bar{u}R_1) = \frac{1}{R_1} \frac{d}{dx}(\bar{u}R_1) \quad (\text{A.19})$$

and

$$\frac{du}{dR} = \frac{d\bar{u}}{dx} \quad (\text{A.20})$$

Differentiating equation (A.19) once more with respect to R,

$$\frac{d^2u}{dR^2} = \frac{d}{dR} \frac{d\bar{u}}{dx} = \frac{d}{R_1 dx} \frac{d\bar{u}}{dx} \quad (\text{A.21})$$

therefore

$$\frac{d^2 u}{dR^2} = \frac{1}{R_1} \frac{d^2 \bar{u}}{dx^2} \quad (\text{A.22})$$

Similarly, for the axial displacement

$$\frac{dw}{dR} = \frac{d\bar{w}}{dx} \quad (\text{A.23})$$

and

$$\frac{d^2 w}{dR^2} = \frac{1}{R_1} \frac{d^2 \bar{w}}{dx^2} \quad (\text{A.24})$$

Finally, for the angular displacement

$$\frac{d\phi}{dR} = \frac{1}{R_1} \frac{d\bar{\phi}}{dx} \quad (\text{A.25})$$

and

$$\frac{d^2 \phi}{dR^2} = \frac{1}{R_1^2} \frac{d^2 \bar{\phi}}{dx^2} \quad (\text{A.26})$$

APPENDIX B  
COMPUTER PROGRAM USER'S MANUAL

The general computer program is given in a 5¼ floppy disk. To run the program write "ELASTO". Then the program will ask you the problem type and the material model. After choosing the problem type and material model, the program requires the following datas:

GUESS1= Missing initial condition,  $y_3(1)$

GUESS2= Missing initial condition,  $y_4(1)$

PR= Poisson's ratio,  $\nu$

F= Material constant,  $f$  (not needed for Blatz model)

R2/R1= Thickness ratio,  $R_2/R_1$

SHEAR= Surface traction,  $\tau_0$

OMEGA= Spin speed,  $\Omega$  (only for constant spin and circumferential shear problem)

N= number of pivotal points

This a sample program which is used in the solution of constant spin and circumferential shear problem by using Blatz-Ko model

```

IMPLICIT REAL*8 (A-H,O-Z)
CHARACTER FILEN*2,OUT*12
DIMENSION Y1(100),Y2(100),Y3(100),Y4(100),X(100),F1(100),F2(100),
*F3(100),F4(100),CM(2,2)
WRITE(*,*)'INPUT GUESS1,GUESS2,F,PR,R2/R1,SHEAR,OMEGA,N'
READ(*,*)G1,G2,F,PR,RATIO,SHEAR,OMEGA,N
WRITE(1,60)F,PR,R2/R1,SHEAR,OMEGA,N
BETA=PR/(1.-2*PR)
C
C   initialize the counter on the iterative process. set k=0
C
K=0
Y10=0.
Y20=0.
C
C   for k=0 guess the missing initial conditions
C
Y30=G1
Y40=G2
D=(RATIO-1.)/(N-1.)
X1=1.
C
C   integrate the governing equations with the initial conditions
C   by using runge-kutta method. (store the profiles)
C
1 CALL RUNKUT(D,N,X1,F,OMEGA,BETA,Y10,Y20,Y30,Y40,X,Y1,Y2,Y3,Y4)
C
C   using the trial initial values and the calculated terminal values,
C   evaluate  $\delta q_i$ :  $q_3(tf), q_4(tf)$ 
C
Y1F=Y1(N)
Y2F=Y2(N)
Y3F=Y3(N)
Y4F=Y4(N)
CALL QI(F,RATIO,BETA,SHEAR,Y1F,Y3F,Y4F,Q3,Q4)
C

```

```

C   set  $\delta q_3 = -q_3(tf)$  and  $\delta q_4 = -q_4(tf)$ 
C
  DELTAQ3=-Q3
  DELTAQ4=-Q4
  DD=1.
  DK=0.

C
C   integrate the adjoint equations backward using the kronecker
C   delta. the profiles  $y_i(t)$  are used. save  $x_i(t_0)$ .
C
  CALLKUTRUN(D,N,X1,RATIO,F,OMEGA,BETA,Y10,Y20,Y30,Y40,X,F1,F2,
  *F3,F4,F31,F41,DD,DK,DK,DK)
  F311=F31
  F411=F41
  CALLKUTRUN(D,N,X1,RATIO,F,OMEGA,BETA,Y10,Y20,Y30,Y40,X,F1,F2,
  *F3,F4,F31,F41,DK,DK,DD,DK)
  F313=F31
  F413=F41
  CALLKUTRUN(D,N,X1,RATIO,F,OMEGA,BETA,Y10,Y20,Y30,Y40,X,F1,F2,
  *F3,F4,F31,F41,DK,DK,DK,DD)
  F314=F31
  F414=F41

C
C   evaluate partial derivatives
C
  CALL PD(RATIO,F,BETA,Y1F,Y3F,Y4F,Q3Y1,Q3Y3,Q3Y4,Q4Y1,
  *Q4Y3,Q4Y4,SHEAR)

C
C   form the matrix coefficients
C
  CM(1,1)=Q3Y1*F311+Q3Y3*F313+Q3Y4*F314
  CM(1,2)=Q3Y1*F411+Q3Y3*F413+Q3Y4*F414
  CM(2,1)=Q4Y1*F311+Q4Y3*F313+Q4Y4*F314
  CM(2,2)=Q4Y1*F411+Q4Y3*F413+Q4Y4*F414

C
C   solve  $\delta y_i(t_0)$   $i=1,2,\dots,n$ 
C
  DET=CM(1,1)*CM(2,2)-CM(1,2)*CM(2,1)
  DELTAY3=(CM(2,2)*DELTAQ3-CM(1,2)*DELTAQ4)/DET
  DELTAY4=(CM(1,1)*DELTAQ4-CM(2,1)*DELTAQ3)/DET
C

```

```

C   if maximum  $\delta q_i$  is less than a specified tolerance terminate the
C   calculation
C
  ACC3=ABS(DELTQA3)
  ACC4=ABS(DELTQA4)
  IF(ACC3.GT.0.000001) GOTO 2
  IF(ACC4.LT.0.000001) GOTO 3
2  Y30=DELTAY3+Y30
   Y40=DELTAY4+Y40
   K=K+1
   GOTO1
3  WRITE(1,10)
   WRITE(1,20)
   WRITE(1,30)
   DO 4 I=1,N
     J=N-I+1
     U1=Y1(I)
     U2=Y2(I)
     U3=Y3(I)
     U4=Y4(I)
     U5=X(J)
     U6=X(J)+Y1(I)
     U7=1.+Y3(I)
     U8=U5/(U6*U7)
     CALL STRESS(F,BETA,U4,U5,U6,U7,U8,S11,S12,S22,S33)
4  WRITE(1,40) X(J),Y1(I),Y2(I),S11,S12,S22,S33
   WRITE(1,50) K,DELTQA3,DELTQA4,Y3F,Y4F
10 FORMAT (4X,'RADIAL',7X,'RADIAL',6X,' ANGULAR ')
20 FORMAT (3X,'LOCATION',4X,'DISPLACEMENT',2X,'DISPLACEMENT',
  *4X,'STRESS11',6X,'STRESS12',6X,'STRESS22',6X,'STRESS33')
30 FORMAT (100(' '))
40 FORMAT (7(E11.4,3X))
50 FORMAT (3X,'NUMBER OF ITERATIONS=',I5,5X,'DELTQA3=',E15.8,5X,
  *'DELTQA4=',E15.8,/,3X,'Y3(R2)=',E15.8,5X,'Y4(R2)=',E15.8)
60 FORMAT ('F   =',F6.3,/, 'PR   =',F6.3,/, 'R2/R1='
  *,F6.3,/, 'SHEAR=',F6.3,/, 'OMEGA=',F6.3,/, 'N   =',I5,/)
  STOP
  END

```

SUBROUTINE RUNKUT(D,N,X1,F,OMEGA,BETA,Y10,Y20,Y30,Y40,X,Y1,  
\*Y2,Y3,Y4)

IMPLICIT REAL\*8 (A-H,O-Z)

C  
C  
C  
C

fourth order runge-kutta forward integration subroutine for  
governing equations

DIMENSION X(100),Y1(100),Y2(100),Y3(100),Y4(100)

X(1)=X1

Y1(1)=Y10

Y2(1)=Y20

Y3(1)=Y30

Y4(1)=Y40

DO 5 I=1,N-1

FF11=D\*DY1(Y3(I))

FF12=D\*DY2(Y4(I))

FF13=D\*DY3(F,OMEGA,BETA,X(I),Y1(I),Y3(I),Y4(I))

FF14=D\*DY4(F,OMEGA,BETA,X(I),Y1(I),Y3(I),Y4(I))

FF21=D\*DY1(Y3(I)+FF13/2.)

FF22=D\*DY2(Y4(I)+FF14/2.)

FF23=D\*DY3(F,OMEGA,BETA,(X(I)+D/2.),(Y1(I)+FF11/2.),(Y3(I)+FF13  
\*/2.),(Y4(I)+FF14/2.))

FF24=D\*DY4(F,OMEGA,BETA,(X(I)+D/2.),(Y1(I)+FF11/2.),(Y3(I)+FF13  
\*/2.),(Y4(I)+FF14/2.))

FF31=D\*DY1(Y3(I)+FF23/2.)

FF32=D\*DY2(Y4(I)+FF24/2.)

FF33=D\*DY3(F,OMEGA,BETA,(X(I)+D/2.),(Y1(I)+FF21/2.),(Y3(I)+FF23  
\*/2.),(Y4(I)+FF24/2.))

FF34=D\*DY4(F,OMEGA,BETA,(X(I)+D/2.),(Y1(I)+FF21/2.),(Y3(I)+FF23  
\*/2.),(Y4(I)+FF24/2.))

FF41=D\*DY1(Y3(I)+FF33)

FF42=D\*DY2(Y4(I)+FF34)

FF43=D\*DY3(F,OMEGA,BETA,(X(I)+D),(Y1(I)+FF31),(Y3(I)+FF33),  
\*(Y4(I)+FF34))

FF44=D\*DY4(F,OMEGA,BETA,(X(I)+D),(Y1(I)+FF31),(Y3(I)+FF33),  
\*(Y4(I)+FF34))

Y1(I+1)=Y1(I)+(FF11+2.\*FF21+2.\*FF31+FF41)/6.

Y2(I+1)=Y2(I)+(FF12+2.\*FF22+2.\*FF32+FF42)/6.

Y3(I+1)=Y3(I)+(FF13+2.\*FF23+2.\*FF33+FF43)/6.

Y4(I+1)=Y4(I)+(FF14+2.\*FF24+2.\*FF34+FF44)/6.

5 X(I+1)=X(I)+D



```

RETURN
END
C
SUBROUTINE KUTRUN(D,N,X1,RATIO,F,OMEGA,BETA,Y10,Y20,Y30,Y40,
*X,F1,F2,F3,F4,F31,F41,X10,X20,X30,X40)
IMPLICIT REAL*8 (A-H,O-Z)
C
C fourth order runge-kutta backward integration subroutine for
C
DIMENSION X(100),F1(100),F2(100),F3(100),F4(100),Y1(100),Y2(100),
*Y3(100),Y4(100)
CALL RUNKUT(D,N,X1,F,OMEGA,BETA,Y10,Y20,Y30,Y40,X,Y1,Y2,Y3,Y4)
X(1)=RATIO
F1(1)=X10
F2(1)=X20
F3(1)=X30
F4(1)=X40
DO 6 I=1,N-1
K=N-I+1
FF11=D*DG1(F,OMEGA,BETA,X(I),Y1(K),Y3(K),Y4(K),F3(I),F4(I))
FF12=D*F2(I)
FF13=D*DG3(F,OMEGA,BETA,X(I),Y1(K),Y3(K),Y4(K),F1(I),F3(I),F4(I))
FF14=D*DG4(F,OMEGA,BETA,X(I),Y1(K),Y3(K),Y4(K),F2(I),F3(I),F4(I))
FF21=D*DG1(F,OMEGA,BETA,(X(I)-D/2.),Y1(K-1),Y3(K-1),Y4(K-1),
*(F3(I)+FF13/2.), (F4(I)+FF14/2.))
FF22=D*F2(I)
FF23=D*DG3(F,OMEGA,BETA,(X(I)-D/2.),Y1(K-1),Y3(K-1),Y4(K-1),
*(F1(I)+FF11/2.), (F3(I)+FF13/2.), (F4(I)+FF14/2.))
FF24=D*DG4(F,OMEGA,BETA,(X(I)-D/2.),Y1(K-1),Y3(K-1),Y4(K-1),
*(F2(I)+FF12/2.), (F3(I)+FF13/2.), (F4(I)+FF14/2.))
FF31=D*DG1(F,OMEGA,BETA,(X(I)-D/2.),Y1(K-1),Y3(K-1),Y4(K-1),
*(F3(I)+FF23/2.), (F4(I)+FF24/2.))
FF32=D*F2(I)
FF33=D*DG3(F,OMEGA,BETA,(X(I)-D/2.),Y1(K-1),Y3(K-1),Y4(K-1),
*(F1(I)+FF21/2.), (F3(I)+FF23/2.), (F4(I)+FF24/2.))
FF34=D*DG4(F,OMEGA,BETA,(X(I)-D/2.),Y1(K-1),Y3(K-1),Y4(K-1),
*(F2(I)+FF22/2.), (F3(I)+FF23/2.), (F4(I)+FF24/2.))
FF41=D*DG1(F,OMEGA,BETA,(X(I)-D),Y1(K-1),Y3(K-1),Y4(K-1),
*(F3(I)+FF33), (F4(I)+FF34))
FF42=D*F2(I)
FF43=D*DG3(F,OMEGA,BETA,(X(I)-D),Y1(K-1),Y3(K-1),Y4(K-1),

```

```

*(F1(I)+FF31),(F3(I)+FF33),(F4(I)+FF34)
  FF44=D*DG4(F,OMEGA,BETA,(X(I)-D),Y1(K-1),Y3(K-1),Y4(K-1),
*(F2(I)+FF32),(F3(I)+FF33),(F4(I)+FF34)
  F1(I+1)=F1(I)+(FF11+2*FF21+2*FF31+FF41)/6.
  F2(I+1)=F2(I)+(FF12+2*FF22+2*FF32+FF42)/6.
  F3(I+1)=F3(I)+(FF13+2*FF23+2*FF33+FF43)/6.
  F4(I+1)=F4(I)+(FF14+2*FF24+2*FF34+FF44)/6.
6 X(I+1)=X(I)-D
  F31=F3(N)
  F41=F4(N)
  RETURN
  END

```

C

```

SUBROUTINE QI(F,RATIO,BETA,SHEAR,Y1F,Y3F,Y4F,Q3,Q4)
IMPLICIT REAL*8 (A-H,O-Z)

```

C

C boundary equations at the outer surface

C

```

E1=RATIO+Y1F
E3=1.+Y3F
EE=RATIO/(E1*E3)
Q3=F*RATIO*E3/E1-(1.-F)*RATIO*(1.+RATIO**2*Y4F**2)/(E1*E3**3)-
* F*EE**(2.*BETA+1.)+(1.-F)*EE**(1.-2.*BETA)
Q4=F*RATIO*Y4F+(1.-F)*RATIO**3*Y4F/(E1**2*E3**2)-SHEAR
RETURN
END

```

C

```

SUBROUTINE STRESS(F,BETA,U4,U5,U6,U7,U8,S11,S12,S22,S33)
IMPLICIT REAL*8 (A-H,O-Z)

```

C

C subroutine for the calculation of stresses

C

```

S11=F*U5*U7/U6-(1.-F)*(U5+U5**3*U4**2)/(U6*U7**3)-F*U8**(2.*BETA
* +1.)+(1.-F)*U8**(1.-2.*BETA)
S12=F*U5*U4+(1.-F)*U5**3*U4/(U6**2*U7**2)
S22=F*U6/(U5*U7)+F*U5*U6*U4**2/U7-(1.-F)*U5**3/(U6**3*U7)
* -F*U8**(2.*BETA+1.)+(1.-F)*U8**(1.-2.*BETA)
S33=F*(U5/(U6*U7))-(1.-F)*(U8+U8*U5**2*U4**2)-F*U8**(2.*BETA+1.)
* +(1.-F)*U8**(1.-2.*BETA)
RETURN

```

```

END
C
SUBROUTINE PD(RATIO,F,BETA,Y1F,Y3F,Y4F,Q3Y1,Q3Y3,Q3Y4,Q4Y1,
*Q4Y3,Q4Y4,SHEAR)
IMPLICIT REAL*8 (A-H,O-Z)
C
C   subroutine for the partial derivatives of boundary equations
C
E1=RATIO+Y1F
E3=1.+Y3F
EE=RATIO/(E1*E3)
Q3Y1=F*(-RATIO*E3/E1**2)+(1.-F)*RATIO*(1+RATIO**2*Y4F**2)/(E1**
* 2*E3**3)+(-F*(1.+2.*BETA)*EE**(2.*BETA)+(1.-F)*(1.-2.*BETA)*
* EE**(-2.*BETA))*(-EE/E1)
Q3Y3=F*RATIO/E1+(1.-F)*3*RATIO*(1+RATIO**2*Y4F**2)/(E1*E3**4)
* +(-F*(1.+2.*BETA)*EE**(2.*BETA)+(1.-F)*(1.-2.*BETA)*
* EE**(-2.*BETA))*(-EE/E3)
Q3Y4=- (1.-F)*2*RATIO**3*Y4F/(E1*E3**3)
Q4Y1=- (1.-F)*2*RATIO**3*Y4F/(E1**3*E3**2)
Q4Y3=- (1.-F)*2*RATIO**3*Y4F/(E1**2*E3**3)
Q4Y4=F*RATIO+(1.-F)*RATIO**3/(E1**2*E3**2)
RETURN
END
C
DOUBLE PRECISION FUNCTION DY1(Y3)
IMPLICIT REAL*8 (A-H,O-Z)
DY1=Y3
RETURN
END
C
DOUBLE PRECISION FUNCTION DY2(Y4)
IMPLICIT REAL*8 (A-H,O-Z)
DY2=Y4
RETURN
END
C
DOUBLE PRECISION FUNCTION DY3(F,OMEGA,BETA,X,Y1,Y3,Y4)
IMPLICIT REAL*8 (A-H,O-Z)
E1=X+Y1
E3=1.+Y3
BK=(1.+2.*BETA)*F*(X/(E1*E3))**(2.*BETA)-(1.-2.*BETA)*(1.-F)*

```

```

* (X/(E1*E3))**(-2.*BETA)
UST31=F**2*(-X/E1**2+1/(E1*E3)+X**2*Y4**2/(E1*E3))
* -F*(OMEGA*X)**2/(E1*E3)-(1.-F)*(OMEGA**2*X**4)/((E1*E3)**3)
UST32=F*(1.-F)*((X+X**3*Y4**2)/(E1**2*E3**4)-X**4/(E1**5*E3)-X**3
* /(E1**4*E3**2)+(X**2-3*X**4*Y4**2)/(E1**3*E3**3))
UST33=(1.-F)**2*((X**3-3*X**5*Y4**2)/(E1**4*E3**6)-X**6/(E1**7
* *E3**3))
UST34=BK*(F*(X/(E1**2*E3**2)-X**2/(E1**3*E3))+(1.-F)*(X**3/
* (E1**4*E3**4)-X**4/(E1**5*E3**3)))
ALT31=F**2*X**2/(E1**2*E3)
ALT32=F*(1.-F)*((3*X**2+3*X**4*Y4**2)/(E1**2*E3**5)+X**4/(E1**4
* *E3**3))
ALT33=(1.-F)**2*(3*X**4-X**6*Y4**2)/(E1**4*E3**7)
ALT34=BK*(F*X**2/(E1**2*E3**3)+(1.-F)*X**4/(E1**4*E3**5))
UST3=UST31+UST32+UST33+UST34
ALT3=ALT31+ALT32+ALT33+ALT34
DY3=UST3/ALT3
RETURN
END

```

C

```

DOUBLE PRECISION FUNCTION DY4(F,OMEGA,BETA,X,Y1,Y3,Y4)
IMPLICIT REAL*8 (A-H,O-Z)
E1=X+Y1
E3=1.+Y3
BK=(1.+2.*BETA)*F*(X/(E1*E3))**2*(2.*BETA)-(1.-2.*BETA)*(1.-F)*
* (X/(E1*E3))**(-2.*BETA)
UST41=F**2*(X*Y4/(E1**2*E3)+2*X**2*Y4/E1**3)
* +(1.-F)*2*OMEGA**2*X**4*Y4/(E1**3*E3**4)
UST42=F*(1.-F)*(5*X**3*Y4/(E1**4*E3**3)+(4*X**2*Y4+4*X**4*Y4**3)
* /(E1**3*E3**4)+(3*X*Y4+3*X**3*Y4**3)/(E1**2*E3**5))
UST43=(1.-F)**2*((7*X**3*Y4+3*X**5*Y4**3)/(E1**4*E3**7)+2*X**6*
* Y4/(E1**7*E3**4))
UST44=BK*(F*(X*Y4/(E1**2*E3**3)+2*X**2*Y4/(E1**3*E3**2))+(1.-F)*
* (X**3*Y4/(E1**4*E3**5)+2*X**4*Y4/(E1**5*E3**4)))
ALT41=-F**2*X**2/(E1**2*E3)
ALT42=-F*(1.-F)*((3*X**2+3*X**4*Y4**2)/(E1**2*E3**5)+X**4/(E1**4
* *E3**3))
ALT43=-F*(1.-F)**2*(3*X**4-X**6*Y4**2)/(E1**4*E3**7)
ALT44=-BK*(F*X**2/(E1**2*E3**3)+(1.-F)*X**4/(E1**4*E3**5))
UST4=UST41+UST42+UST43+UST44
ALT4=ALT41+ALT42+ALT43+ALT44

```

DY4=UST4/ALT4  
 RETURN  
 END

C

DOUBLE PRECISION FUNCTION DG1(F,OMEGA,BETA,X,Y1,Y3,Y4,F3,F4)  
 IMPLICIT REAL\*8 (A-H,O-Z)  
 E1=X+Y1  
 E3=1.+Y3  
 BK=(1.+2.\*BETA)\*F\*(X/(E1\*E3))\*\*(2.\*BETA)-(1.-2.\*BETA)\*(1.-F)\*  
 \* (X/(E1\*E3))\*\*(-2.\*BETA)  
 DBK=((1.+2.\*BETA)\*2\*BETA\*F\*(X/(E1\*E3))\*\*(2.\*BETA-1.)+(1.-2.\*BETA)  
 \* \*2\*BETA\*(1.-F)\*(X/(E1\*E3))\*\*(-2.\*BETA-1.))\*(-X/(E1\*\*2\*E3))  
 UST31=F\*\*2\*(-X/E1\*\*2+1/(E1\*E3)+X\*\*2\*Y4\*\*2/(E1\*E3))  
 \* -F\*(OMEGA\*X)\*\*2/(E1\*E3)-(1.-F)\*(OMEGA\*\*2\*X\*\*4)/((E1\*E3)\*\*3)  
 UST32=F\*(1.-F)\*(X+X\*\*3\*Y4\*\*2)/(E1\*\*2\*E3\*\*4)-X\*\*4/(E1\*\*5\*E3)-X\*\*3  
 \* /(E1\*\*4\*E3\*\*2)+(X\*\*2-3\*X\*\*4\*Y4\*\*2)/(E1\*\*3\*E3\*\*3))  
 UST33=(1.-F)\*\*2\*((X\*\*3-3\*X\*\*5\*Y4\*\*2)/(E1\*\*4\*E3\*\*6)-X\*\*6/(E1\*\*7  
 \* \*E3\*\*3))  
 UST34=BK\*(F\*(X/(E1\*\*2\*E3\*\*2)-X\*\*2/(E1\*\*3\*E3))+(1.-F)\*(X\*\*3/  
 \* (E1\*\*4\*E3\*\*4)-X\*\*4/(E1\*\*5\*E3\*\*3)))  
 ALT31=F\*\*2\*X\*\*2/(E1\*\*2\*E3)  
 ALT32=F\*(1.-F)\*((3\*X\*\*2+3\*X\*\*4\*Y4\*\*2)/(E1\*\*2\*E3\*\*5)+X\*\*4/(E1\*\*4  
 \* \*E3\*\*3))  
 ALT33=(1.-F)\*\*2\*(3\*X\*\*4-X\*\*6\*Y4\*\*2)/(E1\*\*4\*E3\*\*7)  
 ALT34=BK\*(F\*X\*\*2/(E1\*\*2\*E3\*\*3)+(1.-F)\*X\*\*4/(E1\*\*4\*E3\*\*5))  
 UST3=UST31+UST32+UST33+UST34  
 ALT3=ALT31+ALT32+ALT33+ALT34  
 UST41=F\*\*2\*(X\*Y4/(E1\*\*2\*E3)+2\*X\*\*2\*Y4/E1\*\*3)  
 \* +(1.-F)\*2\*OMEGA\*\*2\*X\*\*4\*Y4/(E1\*\*3\*E3\*\*4)  
 UST42=F\*(1.-F)\*(5\*X\*\*3\*Y4/(E1\*\*4\*E3\*\*3)+(4\*X\*\*2\*Y4+4\*X\*\*4\*Y4\*\*3)  
 \* /(E1\*\*3\*E3\*\*4)+(3\*X\*Y4+3\*X\*\*3\*Y4\*\*3)/(E1\*\*2\*E3\*\*5))  
 UST43=(1.-F)\*\*2\*((7\*X\*\*3\*Y4+3\*X\*\*5\*Y4\*\*3)/(E1\*\*4\*E3\*\*7)+2\*X\*\*6\*  
 \* Y4/(E1\*\*7\*E3\*\*4))  
 UST44=BK\*(F\*(X\*Y4/(E1\*\*2\*E3\*\*3)+2\*X\*\*2\*Y4/(E1\*\*3\*E3\*\*2))+(1.-F)\*  
 \* (X\*\*3\*Y4/(E1\*\*4\*E3\*\*5)+2\*X\*\*4\*Y4/(E1\*\*5\*E3\*\*4)))  
 UST4=UST41+UST42+UST43+UST44  
 ALT4=-ALT3  
 G3Y11=F\*\*2\*(2\*X/E1\*\*3-1/(E1\*\*2\*E3)-X\*\*2\*Y4\*\*2/(E1\*\*2\*E3))+F\*(  
 \*OMEGA\*X)\*\*2/(E1\*\*2\*E3)+(1.-F)\*3\*(OMEGA\*\*2\*X\*\*4)/(E1\*\*4\*E3\*\*3)  
 G3Y12=F\*(1.-F)\*((-2\*X-2\*X\*\*3\*Y4\*\*2)/(E1\*\*3\*E3\*\*4)+5\*X\*\*4/(E1\*\*6  
 \* \*E3)+4\*X\*\*3/(E1\*\*5\*E3\*\*2)+(-3\*X\*\*2+9\*X\*\*4\*Y4\*\*2)/(E1\*\*4

```

*      *E3**3))
G3Y13=(1.-F)**2*((-4*X**3+12*X**5*Y4**2)/(E1**5*E3**6)+
*      7*X**6/(E1**8*E3**3))
G3Y14=DBK*(F*(X/(E1**2*E3**2)-X**2/(E1**3*E3))+(1.-F)*(X**3/
*      (E1**4*E3**4)-X**4/(E1**5*E3**3)))+BK*(F*(-2*X/(E1**3*E3**2)
*      +3*X**2/(E1**4*E3))+(1.-F)*(-4*X**3/(E1**5*E3**4)+5*X**4/
*      (E1**6*E3**3)))
G3Y15=F**2*(-2*X**2/(E1**3*E3))+F*(1.-F)*((-6*X**2-6*X**4*Y4**2)
*      /(E1**3*E3**5)-4*X**4/(E1**5*E3**3)+(1.-F)**2*(-12*X**4+
*      4*X**6*Y4**2)/(E1**5*E3**7))
G3Y16=DBK*(F*X**2/(E1**2*E3**3)+(1.-F)*X**4/(E1**4*E3**5))+
*      BK*(-2*F*X**2/(E1**3*E3**3)-(1.-F)*4*X**4/(E1**5*E3**5))
G4Y11=F**2*(-2*X*Y4/(E1**3*E3)-6*X**2*Y4/E1**4)
*      -(1.-F)*6*OMEGA**2*X**4*Y4/(E1**4*E3**4)
G4Y12=F*(1.-F)*(-20*X**3*Y4/(E1**5*E3**3)-(12*X**2*Y4+12*X**4
*      *Y4**3)/(E1**4*E3**4)-(6*X*Y4+6*X**3*Y4**3)/(E1**3*E3**5))
G4Y13=(1.-F)**2*((-28*X**3*Y4-12*X**5*Y4**3)/(E1**5*E3**7)-
*      14*X**6*Y4/(E1**8*E3**4))
G4Y14=DBK*(F*(X*Y4/(E1**2*E3**3)+2*X**2*Y4/(E1**3*E3**2)))+(1.-F
*      )*(X**3*Y4/(E1**4*E3**5)+2*X**4*Y4/(E1**5*E3**4)))+BK*(F*
*      (-2*X*Y4/(E1**3*E3**3)-6*X**2*Y4/(E1**4*E3**2)))+(1.-F)*
*      (-4*X**3*Y4/(E1**5*E3**5)-10*X**4*Y4/(E1**6*E3**4)))
G3Y1=((G3Y11+G3Y12+G3Y13+G3Y14)*ALT3-(G3Y15+G3Y16)*UST3)/
*ALT3**2
G4Y1=((G4Y11+G4Y12+G4Y13+G4Y14)*ALT4+(G3Y15+G3Y16)*UST4)/
*ALT4**2
DG1=-((G3Y1*F3+G4Y1*F4)
RETURN
END

```

C

```

DOUBLEPRECISIONFUNCTIONDG3(F,OMEGA,BETA,X,Y1,Y3,Y4,F1,F3,
*F4)
IMPLICIT REAL*8 (A-H,O-Z)
E1=X+Y1
E3=1.+Y3
BK=(1.+2.*BETA)*F*(X/(E1*E3))**(2.*BETA)-(1.-2.*BETA)*(1.-F)*
* (X/(E1*E3))**(-2.*BETA)
DBK=((1.+2.*BETA)**2*BETA*F*(X/(E1*E3))**(2.*BETA-1.)+(1.-2.*BETA)
* *2*BETA*(1.-F)*(X/(E1*E3))**(-2.*BETA-1.))*(-X/(E1*E3**2))
UST31=F**2*(-X/E1**2+1/(E1*E3)+X**2*Y4**2/(E1*E3))
*      -F*(OMEGA*X)**2/(E1*E3)-(1.-F)*(OMEGA**2*X**4)/((E1*E3)**3)

```

UST32=F\*(1.-F)\*(X+X\*\*3\*Y4\*\*2)/(E1\*\*2\*E3\*\*4)-X\*\*4/(E1\*\*5\*E3)-X\*\*3  
 \* /(E1\*\*4\*E3\*\*2)+(X\*\*2-3\*X\*\*4\*Y4\*\*2)/(E1\*\*3\*E3\*\*3)  
 UST33=(1.-F)\*\*2\*(X\*\*3-3\*X\*\*5\*Y4\*\*2)/(E1\*\*4\*E3\*\*6)-X\*\*6/(E1\*\*7  
 \* \*E3\*\*3)  
 UST34=BK\*(F\*(X/(E1\*\*2\*E3\*\*2)-X\*\*2/(E1\*\*3\*E3))+(1.-F)\*(X\*\*3/  
 \* (E1\*\*4\*E3\*\*4)-X\*\*4/(E1\*\*5\*E3\*\*3)))  
 ALT31=F\*\*2\*X\*\*2/(E1\*\*2\*E3)  
 ALT32=F\*(1.-F)\*((3\*X\*\*2+3\*X\*\*4\*Y4\*\*2)/(E1\*\*2\*E3\*\*5)+X\*\*4/(E1\*\*4  
 \* \*E3\*\*3))  
 ALT33=(1.-F)\*\*2\*(3\*X\*\*4-X\*\*6\*Y4\*\*2)/(E1\*\*4\*E3\*\*7)  
 ALT34=BK\*(F\*X\*\*2/(E1\*\*2\*E3\*\*3)+(1.-F)\*X\*\*4/(E1\*\*4\*E3\*\*5))  
 UST3=UST31+UST32+UST33+UST34  
 ALT3=ALT31+ALT32+ALT33+ALT34  
 UST41=F\*\*2\*(X\*Y4/(E1\*\*2\*E3)+2\*X\*\*2\*Y4/E1\*\*3)  
 \* +(1.-F)\*2\*OMEGA\*\*2\*X\*\*4\*Y4/(E1\*\*3\*E3\*\*4)  
 UST42=F\*(1.-F)\*(5\*X\*\*3\*Y4/(E1\*\*4\*E3\*\*3)+(4\*X\*\*2\*Y4+4\*X\*\*4\*Y4\*\*3)  
 \* /(E1\*\*3\*E3\*\*4)+(3\*X\*Y4+3\*X\*\*3\*Y4\*\*3)/(E1\*\*2\*E3\*\*5))  
 UST43=(1.-F)\*\*2\*((7\*X\*\*3\*Y4+3\*X\*\*5\*Y4\*\*3)/(E1\*\*4\*E3\*\*7)+2\*X\*\*6\*  
 \* Y4/(E1\*\*7\*E3\*\*4))  
 UST44=BK\*(F\*(X\*Y4/(E1\*\*2\*E3\*\*3)+2\*X\*\*2\*Y4/(E1\*\*3\*E3\*\*2))+(1.-F)\*  
 \* (X\*\*3\*Y4/(E1\*\*4\*E3\*\*5)+2\*X\*\*4\*Y4/(E1\*\*5\*E3\*\*4)))  
 UST4=UST41+UST42+UST43+UST44  
 ALT4=-ALT3  
 G3Y31=F\*\*2\*(-1/(E1\*E3\*\*2)-X\*\*2\*Y4\*\*2/(E1\*E3\*\*2))+F\*(OMEGA\*X)\*\*  
 \* 2/(E1\*E3\*\*2)+(1.-F)\*(OMEGA\*\*2\*X\*\*4)/(E1\*\*3\*E3\*\*4)  
 G3Y32=F\*(1.-F)\*((-4\*X-4\*X\*\*3\*Y4\*\*2)/(E1\*\*2\*E3\*\*5)+X\*\*4/(E1\*\*5  
 \* \*E3\*\*2)+2\*X\*\*3/(E1\*\*4\*E3\*\*3)+(-3\*X\*\*2+9\*X\*\*4\*Y4\*\*2)/  
 \* (E1\*\*3\*E3\*\*4))  
 G3Y33=(1.-F)\*\*2\*((-6\*X\*\*3+18\*X\*\*5\*Y4\*\*2)/(E1\*\*4\*E3\*\*7)+3\*X\*\*6/  
 \* (E1\*\*7\*E3\*\*4))  
 G3Y34=DBK\*(F\*(X/(E1\*\*2\*E3\*\*2)-X\*\*2/(E1\*\*3\*E3))+(1.-F)\*(X\*\*3/  
 \* (E1\*\*4\*E3\*\*4)-X\*\*4/(E1\*\*5\*E3\*\*3)))+BK\*(F\*(-2\*X/(E1\*\*2\*E3\*\*3)  
 \* +X\*\*2/(E1\*\*3\*E3\*\*2))+(1.-F)\*(-4\*X\*\*3/(E1\*\*4\*E3\*\*5)+3\*X\*\*4/  
 \* (E1\*\*5\*E3\*\*4)))  
 G3Y35=-(F\*X/(E1\*E3))\*\*2-F\*(1.-F)\*((15\*X\*\*2+15\*X\*\*4\*Y4\*\*2)/(E1\*\*2  
 \* \*E3\*\*6)+3\*(X/(E1\*E3))\*\*4)+(1.-F)\*\*2\*(-21\*X\*\*4+7\*X\*\*6\*Y4\*\*2)  
 \* /(E1\*\*4\*E3\*\*8)  
 G3Y36=DBK\*(F\*X\*\*2/(E1\*\*2\*E3\*\*3)+(1.-F)\*X\*\*4/(E1\*\*4\*E3\*\*5))+  
 \* BK\*(-F\*3\*X\*\*2/(E1\*\*2\*E3\*\*4)-(1.-F)\*5\*X\*\*4/(E1\*\*4\*E3\*\*6))  
 G4Y31=F\*\*2\*(-X\*Y4/(E1\*\*2\*E3\*\*2))  
 \* -(1.-F)\*8\*OMEGA\*\*2\*X\*\*4\*Y4/(E1\*\*3\*E3\*\*5)



```

G4Y32=F*(1.-F)*(-15*X**3*Y4/(E1**4*E3**4)-(16*X**2*Y4+16*X**4*
*   Y4**3)/(E1**3*E3**5)-(15*X*Y4+15*X**3*Y4**3)/(E1**2*E3**6))
G4Y33=(1.-F)**2*((-49*X**3*Y4-21*X**5*Y4**3)/(E1**4*E3**8)-8*X**6
*   *Y4/(E1**7*E3**5))
G4Y34=DBK*(F*(X*Y4/(E1**2*E3**3)+2*X**2*Y4/(E1**3*E3**2))+(1.-F)
*   *(X**3*Y4/(E1**4*E3**5)+2*X**4*Y4/(E1**5*E3**4)))+BK*(F*(-3*
*   X*Y4/(E1**2*E3**4)-4*X**2*Y4/(E1**3*E3**3))+(1.-F)*
*   (-5*X**3*Y4/(E1**4*E3**6)-8*X**4*Y4/(E1**5*E3**5)))
G3Y3=((G3Y31+G3Y32+G3Y33+G3Y34)*ALT3-(G3Y35+G3Y36)*UST3)/
*ALT3**2
G4Y3=((G4Y31+G4Y32+G4Y33+G4Y34)*ALT4+(G3Y35+G3Y36)*UST4)/
*ALT4**2
DG3=-(F1+G3Y3*F3+G4Y3*F4)
RETURN
END

```

C

```

DOUBLEPRECISIONFUNCTIONDG4(F,OMEGA,BETA,X,Y1,Y3,Y4,F2,F3,
*F4)
IMPLICIT REAL*8 (A-H,O-Z)
E1=X+Y1
E3=1.+Y3
BK=(1.+2.*BETA)*F*(X/(E1*E3))**2*(2.*BETA)-(1.-2.*BETA)*(1.-F)*
* (X/(E1*E3))**(-2.*BETA)
UST31=F**2*(-X/E1**2+1/(E1*E3)+X**2*Y4**2/(E1*E3))
* -F*(OMEGA*X)**2/(E1*E3)-(1.-F)*(OMEGA**2*X**4)/((E1*E3)**3)
UST32=F*(1.-F)*(X+X**3*Y4**2)/(E1**2*E3**4)-X**4/(E1**5*E3)-X**3
* /(E1**4*E3**2)+(X**2-3*X**4*Y4**2)/(E1**3*E3**3))
UST33=(1.-F)**2*((X**3-3*X**5*Y4**2)/(E1**4*E3**6)-X**6/(E1**7
*   *E3**3))
UST34=BK*(F*(X/(E1**2*E3**2)-X**2/(E1**3*E3))+(1.-F)*(X**3/
*   (E1**4*E3**4)-X**4/(E1**5*E3**3)))
ALT31=F**2*X**2/(E1**2*E3)
ALT32=F*(1.-F)*((3*X**2+3*X**4*Y4**2)/(E1**2*E3**5)+X**4/(E1**4
*   *E3**3))
ALT33=(1.-F)**2*(3*X**4-X**6*Y4**2)/(E1**4*E3**7)
ALT34=BK*(F*X**2/(E1**2*E3**3)+(1.-F)*X**4/(E1**4*E3**5))
UST3=UST31+UST32+UST33+UST34
ALT3=ALT31+ALT32+ALT33+ALT34
UST41=F**2*(X*Y4/(E1**2*E3)+2*X**2*Y4/E1**3)
* + (1.-F)*2*OMEGA**2*X**4*Y4/(E1**3*E3**4)
UST42=F*(1.-F)*(5*X**3*Y4/(E1**4*E3**3)+(4*X**2*Y4+4*X**4*Y4**3)

```



```

*   /(E1**3*E3**4)+(3*X*Y4+3*X**3*Y4**3)/(E1**2*E3**5))
UST43=(1.-F)**2*((7*X**3*Y4+3*X**5*Y4**3)/(E1**4*E3**7)+2*X**6*
*   Y4/(E1**7*E3**4))
UST44=BK*(F*(X*Y4/(E1**2*E3**3)+2*X**2*Y4/(E1**3*E3**2))+(1.-F)*
*   (X**3*Y4/(E1**4*E3**5)+2*X**4*Y4/(E1**5*E3**4)))
UST4=UST41+UST42+UST43+UST44
ALT4=-ALT3
G3Y41=F**2*2*X**2*Y4/(E1*E3)+F*(1.-F)*(2*X**3*Y4/(E1**2*E3**4)-
*   6*X**4*Y4/(E1**3*E3**3))-(1.-F)**2*6*X**5*Y4/(E1**4*E3**6)
G3Y42=F*(1.-F)*6*X**4*Y4/(E1**2*E3**5)-(1.-F)**2*2*X**6*Y4/
*   (E1**4*E3**7)
G4Y41=F**2*(X/(E1**2*E3)+2*X**2/E1**3)
*   +(1.-F)*2*OMEGA**2*X**4/(E1**3*E3**4)
G4Y42=F*(1.-F)*(5*X**3/(E1**4*E3**3)+(4*X**2+12*X**4*Y4**2)/
*   (E1**3*E3**4)+(3*X+9*X**3*Y4**2)/(E1**2*E3**5))
G4Y43=(1.-F)**2*((7*X**3+9*X**5*Y4**2)/(E1**4*E3**7)+2*X**6/
*   (E1**7*E3**4))
G4Y44=BK*(F*(X/(E1**2*E3**3)+2*X**2/(E1**3*E3**2))+(1.-F)*
*   (X**3/(E1**4*E3**5)+2*X**4/(E1**5*E3**4)))
G3Y4=(G3Y41*ALT3-UST3*G3Y42)/ALT3**2
G4Y4=((G4Y41+G4Y42+G4Y43+G4Y44)*ALT4+G3Y42*UST4)/ALT4**2
DG4=-(F2+G3Y4*F3+G4Y4*F4)
RETURN
END

```

C